

**DIAGENESIS OF CUDI GROUP FORMATIONS
FROM DINÇER-1 AND SOUTH DINÇER-1 WELLS,
SE ANATOLIA TURKEY**

**A THESIS SUBMITTED TO
THE GRADUATE SCHOOL OF NATURAL AND APPLIED
SCIENCES
OF
MIDDLE EAST TECHNICAL UNIVERSITY**

BY

AYŞEGÜL ÖZKAN KAHRAMAN

**IN PARTIAL FULFILLMENT OF THE REQUIREMENTS
FOR
THE DEGREE OF MASTER OF SCIENCE
IN
GEOLOGICAL ENGINEERING**

DECEMBER 2010

Approval of the Thesis:

**DIAGENESIS OF CUDI GROUP FORMATIONS FROM DINÇER-1 AND
SOUTH DINÇER-1 WELLS, SE TURKEY**

Submitted by **AYŞEGÜL ÖZKAN KAHRAMAN** in partial fulfillment of the requirements for the degree of **Master of Science in Geological Engineering Department, Middle East Technical University** by,

Prof. Dr. Canan Özgen _____

Dean, Graduate School of **Natural and Applied Sciences**

Prof. Dr. Zeki Çamur _____

Head of Department, **Geological Engineering**

Prof. Dr. Asuman Günel Türkmenoğlu _____

Supervisor, **Geological Engineering, METU**

Examining Committee Members:

Prof. Dr. Vedat Toprak _____

Geological Engineering, METU

Prof. Dr. Asuman Günel Türkmenoğlu _____

Geological Engineering, METU

Asst. Prof. Dr. Zehra Karakaş _____

Geological Engineering, Ankara University

Asst. Prof. Dr. Fatma Toksoy Köksal _____

Geological Engineering, METU

Doğan Alaygut, M.Sc. _____

Turkish Petroleum Co., Research Dep.

Date: **17.12.2010**

I hereby declare that all information in this document has been obtained and presented in accordance with academic rules and ethical conduct. I also declare that, as required by these rules and conduct, I have fully cited and referenced all material and results that are not original to this work.

Name, Last name: Ayşegül Özkan Kahraman

Signature :

ABSTRACT

DIAGENESIS OF CUDI GROUP FORMATIONS FROM DINÇER-1 AND SOUTH DINÇER-1 WELLS, SE ANATOLIA TURKEY

Özkan Kahraman, Ayşegül

M.Sc., Department of Geological Engineering

Supervisor: Prof. Dr. Asuman Günel Türkmenoğlu

December 2010, 110 Pages

Dinçer-1 (1968) and South Dinçer-1 (1980) exploration wells are located at Şırnak Province of Southeast (SE) Anatolia. South Fields of SE Anatolia have received a significant attention after the completion of subjected wells and numerous studies have been implemented regarding this area. Many theories about the geological generation of these fields were put forward by people who studied this region.

Both wells have penetrated the Arabian Plate autochthonous units. The Cudi Group, of this sequence, mainly consists of dolomites and anhydrites. The samples from the cores of this referred interval and the thin sections of these cores were examined in details by X-Ray Diffraction (XRD) Analyses and petrographic microscope.

Thin sections taken from the core samples of the Cudi Group's Bakük, Çamurlu and Telhasan formations (from older to younger) stand out in the diagenetic manner. The analyses of these thin sections showed that dolomitization is the main diagenetic process along with some textural changes such as the increase in the deformation of algal structures, formation of stylolites and secondary porosity. Clay minerals, mainly illites, shows detritic behaviors rather than characters representing a diagenetic origin. Obtained results from this study showed that the dolomitization as diagenetic process plays an important role in oil and gas formations within Cudi Group. Dolomite stoichiometry studies indicated that Cudi Group formations have modern dolomites since they show poor ordering reflections. They are also younger formations which are subjected to longer periods of diagenetic effects in comparison with Uludere Formation's dolomites.

Keywords: SE Anatolia, Dinçer-1 Well, South Dinçer-1 Well, Cudi Group, Dolomitization and XRD.

ÖZ

DİNÇER-1 VE GÜNEY DİNÇER-1 KUYULARINDAKİ CUDİ GRUBU FORMASYONLARININ DİYAJENEZİNİN BELİRLENMESİ, GDA TÜRKİYE

Özkan Kahraman, Ayşegül

Yüksek Lisans, Jeoloji Mühendisliği Bölümü

Tez Yöneticisi: Prof. Dr. Asuman Günel Türkmenoğlu

Aralık 2010, 110 Sayfa

Dinçer-1 (1968) ve Güney Dinçer-1 (1980) arama kuyuları, Güneydoğu Anadolu'nun Şırnak İli sınırları içerisinde bulunmaktadır. Bu iki kuyunun tamamlanmasından sonra, GD Anadolu'nun güney sahaları önemli derecede ilgi çekmiş ve bu alanların odaklandığı bir çok çalışma gerçekleştirilmiştir. Bu sahaların jeolojik oluşumu hakkında, çalışan araştırmacılar tarafından birçok teori öne sürülmüştür.

Bu iki kuyu, bilinen Otokton Arap Plakası birimlerini kesmektedir. Bu istifte bulunan Cudi Grubu, çoğunlukla dolomit ve anhidritlerden oluşmaktadır. Cudi Grubu'nun formasyonlarına ait karot ve ince

kesitleri, X-Işını Kırınım difraktometresi (XRD) ve petrografik mikroskop ile detaylı olarak incelenmiştir.

Dinçer-1 ve Güney Dinçer-1 kuyularında kesilen Cudi Grubu'na ait ve diyajenez açısından öne çıkan Bakük, Çamurlu ve Telhasan (yaşlıdan gence doğru) formasyonlarına ait karot örneklerinden ince kesitler alınmıştır. İncelenen ince kesitlerde ana diyajenez ürünü olarak başlıca dolomitleşme görülmüştür. Ayrıca, algal yapıların bozulması, stilolitlerin varlığı ve ikincil porozitenin gelişmesi diyajenetik evrimi işaret etmektedir. Yapılan çalışmalar sonucunda petrol ve gaz oluşumu açısından dolomitleşme, Cudi Grubu'nda ikincil gözenekliliği arttırdığından önemli bir rol oynamaktadır. Kil mineralleri, özellikle illit, ise detrital kökenli olup, diyajenetik karaktere sahip değildir. Dolomit stokyometresi çalışmaları, Cudi Grubu dolomitlerinin zayıf derecede kristal yapılara sahip olan modern dolomitler olduğunu göstermiştir. Bu oluşumlar, Uludere Formasyonu dolomitlerine kıyasla daha uzun süreli bir diyajenezin etkisiyle gelişmişlerdir.

Anahtar Sözcükler: GD Anadolu, Dinçer-1 Kuyusu, Güney Dinçer-1 Kuyusu, Cudi Grubu, Dolomitleşme ve XRD.

ACKNOWLEDGEMENTS

I would like to express my heartfelt gratitude to my supervisor Prof. Dr. Asuman Günel Türkmenođlu for her guidance, suggestions and precious time throughout this study.

I am very grateful for the helps and advices of Mr. Dođan Alaygut and guidance of Prof. Dr. Vedat Toprak.

I also would like to state my sincere thankfulness to TPAO management for permitting me to use the necessary data.

I wish to show my deepest gratefulness and appreciation to my father Prof. Dr. Hüsnü Özkan for his encouragements, intellectual guidance and inspiration from the beginning to the end of this master study, my mother Mrs. Nurten Özkan for her tremendous support, understanding and tenderness throughout the working and my husband Mr. Ömer Kahraman for his endless support, motivation and vital effort in completing this thesis. This study would not have been possible without their lovingly cheers.

TABLE OF CONTENTS

ABSTRACT	iv
ÖZ	vi
ACKNOWLEDGEMENTS	viii
TABLE OF CONTENTS	ix
LIST OF TABLES	xi
TABLE OF FIGURES	xii
CHAPTERS	
1 INTRODUCTION	1
1.1 Purpose and Scope	1
1.2 Geological Setting of the Study Area	4
1.3 Literature Survey	7
1.3.1 Geology of SE Anatolia and Study Area	7
1.3.2 Diagenesis of Carbonate Rocks: Dolomitization	16
1.4 Methods of Study	28
1.4.1 Sampling	28
1.4.2 Laboratory Work	35
1.4.2.1 Petrographic Analyses	35

1.4.2.2 X-Ray Powder Diffraction Analyses	36
2 RESULTS OF THE STUDY	40
2.1 Results of the Petrographic Analyses.....	40
2.2 Results of X-Ray Powder Diffraction Analyses	52
2.2.1 Qualitative Analyses of the Whole Rock Samples	52
2.2.2 Quantitative Analyses of the Whole Rock Samples ...	71
2.3 Results of Clay Fraction Analyses by XRD	77
2.4 Dolomite Stoichiometry	82
3 DISCUSSION OF THE RESULTS	90
3.1 Depositional Environment of Cudi Group Sequence as Indicated by their Petrographic and Mineralogical Characteristics	90
3.2 Dolomite Stoichiometry and Dolomitization	94
4 CONCLUSIONS	96
REFERENCES	100

LIST OF TABLES

TABLES

Table 1. General properties of dolomites.	23
Table 2. Dinger-1 Exploration Well's detailed core data.	31
Table 3. South Dinger-1 Exploration Well's detailed core data.	34
Table 4. Mineral facies for Dinger-1 Exploration Well.....	70
Table 5. Mineral facies for South Dinger-1 Exploration Well.	70
Table 6. Whole rock mineral composition after XRD analyses for Dinger-1 Exploration Well.....	72
Table 7. Whole rock mineral composition after XRD analyses for South Dinger-1 Exploration Well.	75
Table 8. X-ray diffraction data of studied samples for Dinger-1 Exploration Well.....	85
Table 9. X-Ray Diffraction data of studied samples for South Dinger-1 Exploration Well.....	87

TABLE OF FIGURES

FIGURES

Figure 1. Location map of the study area located at SE Anatolia, Turkey indicating Petroleum District X (green rectangle).	2
Figure 2. Geological map of the study area. Location of the studied wells are shown with blue arrows (modified from TPAO-Exploration Department's Directorate of Interpretation Systems).	5
Figure 3. Generalized stratigraphic section of the Cudi Group prepared from the wells located at Gaziantep and Nusaybin-Cizre fields (modified from Yılmaz and Duran, 1997).	14
Figure 4. Generalized stratigraphic section of the Cudi Group at Şırnak and Hakkari region (modified from Yılmaz and Duran, 1997).	15
Figure 5. Dınçer-1 Well's vertical section with core information. ..	30
Figure 6. South Dınçer-1 Well's vertical section with core information.	33
Figure 7. Photomicrograph of thin section no: 257587 belonging to South Dınçer-1 Well's Telhasan Formation (anh: anhydrite and sty: stylolite), a) Cross nicols, b) Single nicol.	42
Figure 8. Photomicrograph of thin section no: 257598 belonging to South Dınçer-1 Well's Çamurlu Formation (anh: anhydrite, dol: dolomite, sty: stylolite and alg: algal structures), a) Cross nicols, b) Single nicol.	43

Figure 9. Photomicrograph of thin section no: 257609 belonging to South Dınçer-1 Well's Çamurlu Formation (dol: dolomite, anh: anhydrite and sty: stylolite), a) Cross nicols, b) Single nicol.	44
Figure 10. Photomicrograph of thin section no: 257616 belonging to South Dınçer-1 Well's Çamurlu Formation (dol: dolomite, anh: anhydrite and sty: stylolite), a) Cross nicols, b) Single nicol.	45
Figure 11. Photomicrograph of thin section no: 257618 belonging to South Dınçer-1 Well's Çamurlu Formation (anh: anhydrite and f. f.: fossil fragment), a) Cross nicols, b) Single nicol.....	46
Figure 12. Photomicrograph of thin section no: 257624 belonging to South Dınçer-1 Well's Bakük Formation (dol: dolomite, anh: anhydrite and sty: stylolite), a) Cross nicols, b) Single nicol.	47
Figure 13. Photomicrograph of thin section no: 257639 belonging to South Dınçer-1 Well's Bakük Formation (dol: dolomite and anh: anhydrite), a) Cross nicols, b) Single nicol.	48
Figure 14. Photomicrograph of thin section no: 43440 belonging to Dınçer-1 Well's Bakük Formation (cal: calcite, dol: dolomite, anh: anhydrite, alg: algal structures and s. f.:shell fragment), a) Cross nicols, b) Single nicol.	49
Figure 15. Photomicrograph of thin section no: 43443 belonging to Dınçer-1 Well's Bakük Formation (qtz: quartz, dol: dolomite, anh: anhydrite and sty: stylolite), a) Cross nicols, b) Single nicol.	50
Figure 16. XRD diffractogram of bulk sample D-AK-1 belonging to Cudi Group's Telhasan Formation.	53
Figure 17. XRD diffractogram of bulk sample D-AK-2 belonging to Cudi Group's Telhasan Formation.	54

Figure 18. XRD diffractogram of bulk sample D-AK-3 belonging to Cudi Group's Telhasan Formation.....	54
Figure 19. XRD diffractogram of bulk sample D-AK-4 belonging to Cudi Group's Telhasan Formation.....	55
Figure 20. XRD diffractogram of bulk sample D-AK-5 belonging to Cudi Group's Telhasan Formation.....	56
Figure 21. XRD diffractogram of bulk sample D-AK-6 belonging to Cudi Group's Telhasan Formation.....	56
Figure 22. XRD diffractogram of bulk sample GD-AK-1 belonging to Cudi Group's Telhasan Formation.....	57
Figure 23. XRD diffractogram of bulk sample GD-AK-2 belonging to Cudi Group's Telhasan Formation.....	58
Figure 24. XRD diffractogram of bulk sample GD-AK-3 belonging to Cudi Group's Telhasan Formation.....	58
Figure 25. XRD diffractogram of bulk sample GD-AK-4 belonging to Cudi Group's Telhasan Formation.....	59
Figure 26. XRD diffractogram of bulk sample GD-AK-5 belonging to Cudi Group's Telhasan Formation.....	60
Figure 27. XRD diffractogram of bulk sample GD-AK-6 belonging to Cudi Group's Telhasan Formation.....	60
Figure 28. XRD diffractogram of bulk sample GD-AK-7 belonging to Cudi Group's Çamurlu Formation.....	61
Figure 29. XRD diffractogram of bulk sample GD-AK-8 belonging to Cudi Group's Çamurlu Formation.....	62

Figure 30. XRD diffractogram of bulk sample GD-AK-9 belonging to Cudi Group's Çamurlu Formation.....	62
Figure 31. XRD diffractogram of bulk sample D-AK-7 belonging to Cudi Group's Bakük Formation.....	63
Figure 32. XRD diffractogram of bulk sample D-AK-8 belonging to Cudi Group's Bakük Formation.....	64
Figure 33. XRD diffractogram of bulk sample D-AK-9 belonging to Cudi Group's Bakük Formation.....	64
Figure 34. XRD diffractogram of bulk sample GD-AK-10 belonging to Cudi Group's Bakük Formation.	65
Figure 35. XRD diffractogram of bulk sample GD-AK-11 belonging to Cudi Group's Bakük Formation.	66
Figure 36. XRD diffractogram of bulk sample GD-AK-12 belonging to Cudi Group's Bakük Formation.	66
Figure 37. XRD diffractogram of bulk sample D-AK-10 belonging to Çiğli Group's Uludere Formation.....	68
Figure 38. XRD diffractogram of bulk sample GD-AK-13 belonging to Çiğli Group's Uludere Formation.	68
Figure 39. XRD diffractogram of bulk sample GD-AK-14 belonging to Çiğli Group's Uludere Formation.	69
Figure 40. X-ray diffractograms of clay minerals belonging to Dinçer-1 Well's D-AK-9 numbered XRD sample (ill: illite, kln: kaolinite, qtz: quartz and fsp: K-feldspar minerals).	79

Figure 41. X-ray diffractograms of clay minerals belonging to South Dincer-1 Well' GD-AK-7 numbered XRD sample (ill: illite, qtz: quartz and fsp: K-feldspar minerals). 81

Figure 42. Dincer-1 Exploration Well scattergram showing the relation of ordering ratio with CaCO₃% (Hardy and Tucker,1988) 86

Figure 43. South Dincer-1 Exploration Well scattergram showing the relation of ordering ratio in with CaCO₃% (Hardy and Tucker, 1988). 88

CHAPTER 1

INTRODUCTION

1.1 Purpose and Scope

The aim of this study is to examine the petrography and diagenesis of the Triassic-Jurassic aged Cudi Group units, especially the Triassic aged Bakük, Çamurlu and Telhasan formations, within Dinger-1 and South Dinger-1 exploration wells located at the Petroleum District X of SE Anatolia, Turkey (Figure 1). The location of the wells is at the northern side of the Arabian plate between Nusaybin County of Mardin Province and İdil County of Şırnak Province, although both wells reside in the borders of Şırnak Province. Additionally, the distance between the two wells is 1.6 kilometers.

The main reasons for studying the Cudi Group is the good reservoir properties of its units around the studied fields (Nusaybin-Cizre Fields) and to understand the diagenetic processes of Triassic-Jurassic age interval within the two important exploration wells in addition to the previous studies.

Factors affecting the selection of Dinger-1 and South Dinger-1 Exploration Wells can be listed as follows:

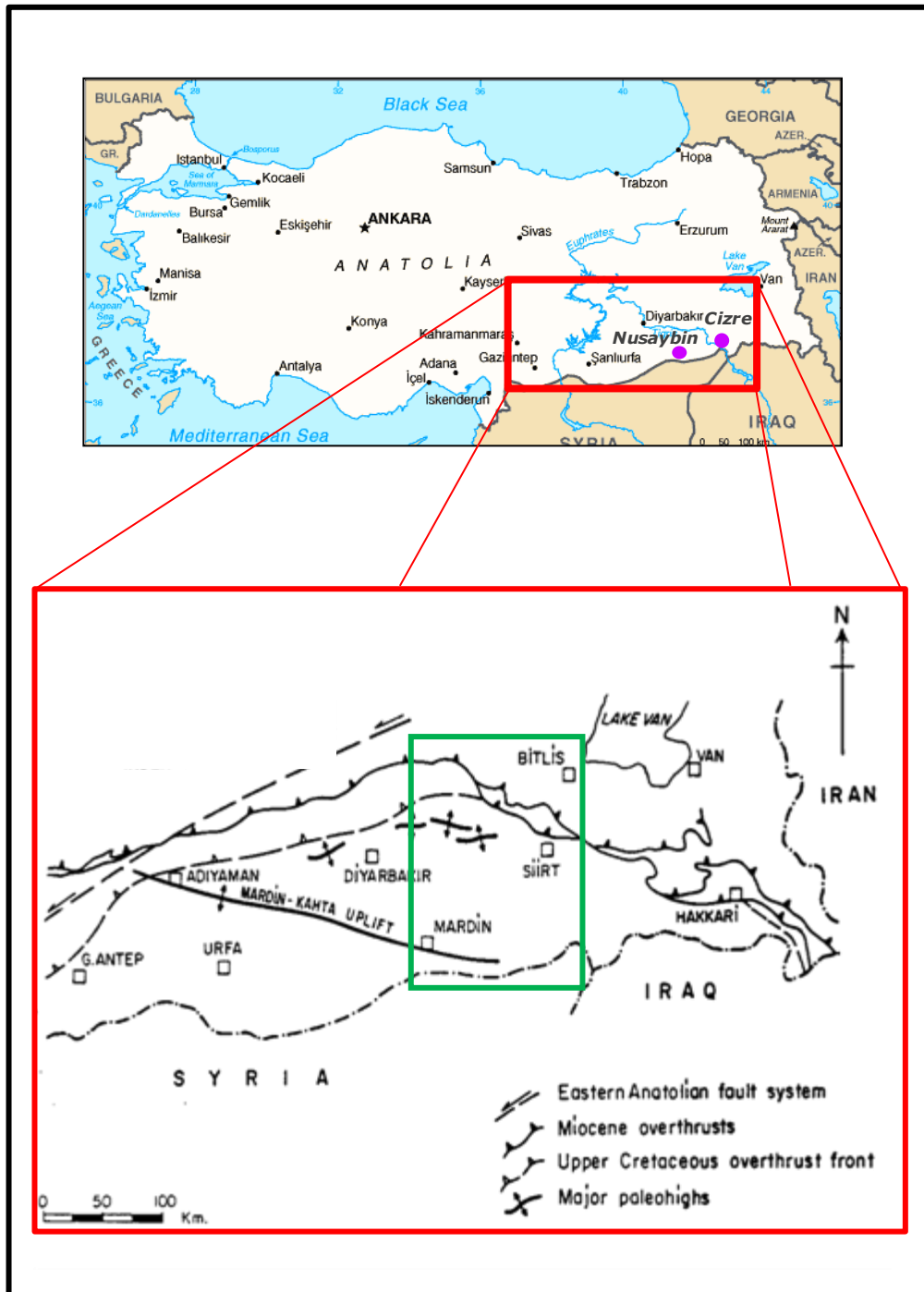


Figure 1. Location map of the study area located at SE Anatolia, Turkey indicating Petroleum District X (green rectangle).

Dinçer-1 Exploration Well is regarded to be the first well drilled at the subject field. After observing oil and gas show from the well in 1968, the interest towards the surrounding fields increased and today's known discoveries were made. South Dinçer Field is one of the most important production fields located in Turkey, discovered and operated by TPAO, and South Dinçer-1 Well is the very first discovery well of this major field.

At the time of drilling and operation, selected wells remained in the provincial boundary of Şırnak Province's Cizre District (before and around 1980's). However, Dinçer-1 and South Dinçer-1 Wells currently reside in Şırnak's İdil District as mentioned before.

In this study, clay mineral diagenesis and dolomitization processes of the Cudi Group units were underscored and some clues about the relationship between these processes with the oil and gas generation by the help of porosity, permeability and the diagenesis stages were gained.

Total of 22 thin sections from Dinçer-1 and 28 thin sections from South Dinçer-1 Exploration Well were examined at TPAO's and METU's laboratories. All of these thin sections, belonging to Cudi Group (a couple of them to Mardin and Çığlı Group) formations, were also studied regarding their XRD analyses.

1.2 Geological Setting of the Study Area

The whole area, where these two wells are located, are covered with basalts of Quaternary age (Figure 2). Both at the northern and southern parts of the Dincer structure, the alignment of the basalt groups in one line points out an existence of a fault. The topography of the field is uplifted in NE-SW direction. Likely to be more significant at the Miocene age, the structure was covered with basaltic flows thereafter and gained its current form (Açıkbaş and Akalın, 1968).

The current tectonic position of Southeast Anatolia has been formed at the Alpine Orogenesis. During this formation period, the region has mostly been exposed to compressive forces and now is an epicontinental basin which is in between the Arabian uplift and Alpine orogenesis field. The basins northern side border is the southeastern part of the Toros Mountains located at the drift zone and the southern side is the Arabian uplift (Eroğlu, 1984). Gondwana Plate, in the south hemisphere, covered the Arabian Plate in Paleozoic period of time and Arabian Plate got closer to the equator by moving towards the North Pole (Burke and Dewy, 1973; Bambach et al., 1980).

A tectonic evolution with two phases is seen at the South Dincer Field. At the first phase, a graben has occurred as a result of the tension forces and at the second phase, as a result of the compressional forces coming from north, strike-slip faults have been formed.

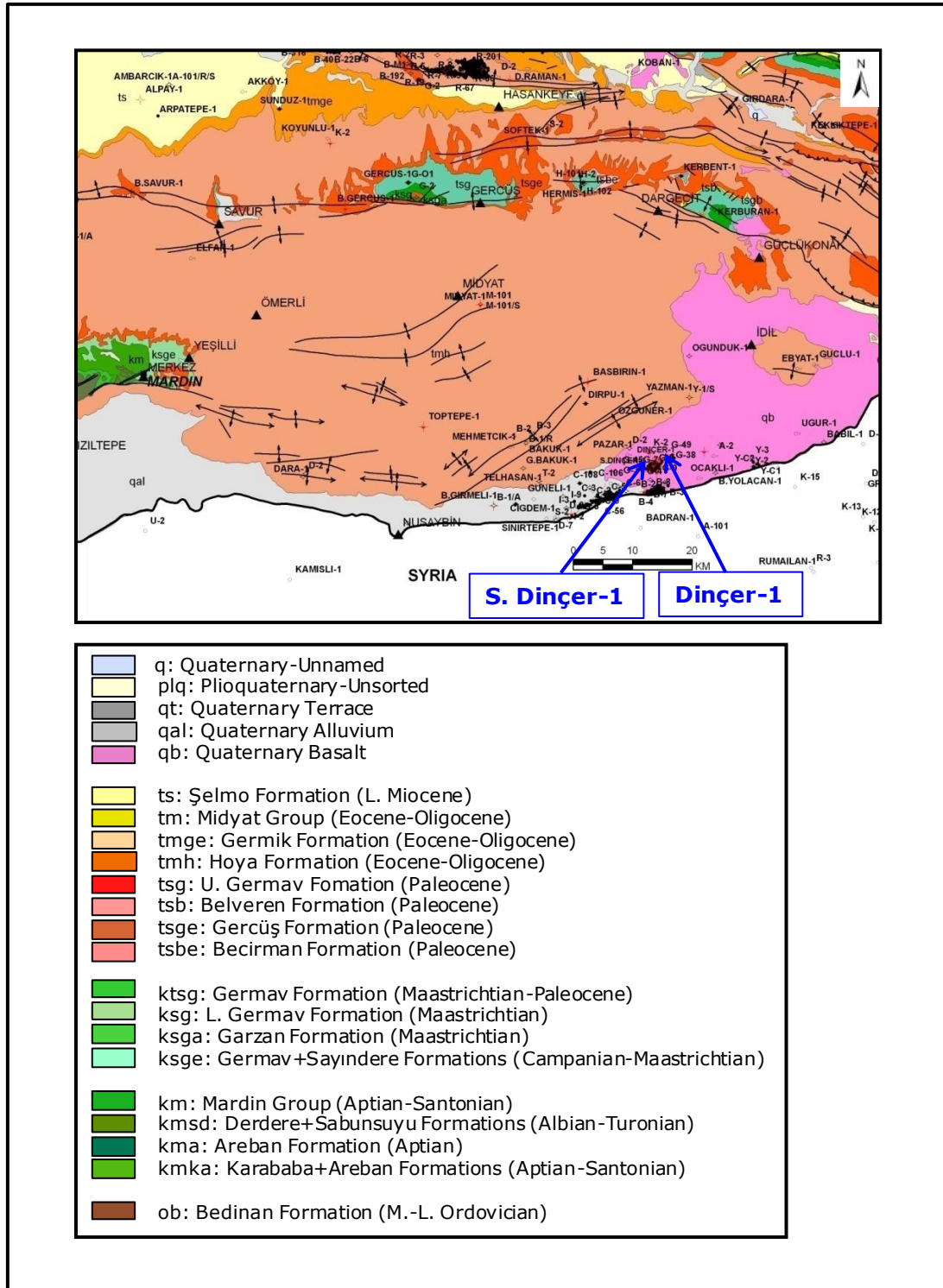


Figure 2. Geological map of the study area. Locations of the studied wells are shown with blue arrows (modified from TPAO-Exploration Department’s Directorate of Interpretation Systems).

The field where the two studied wells located is mostly affected by the Mardin-Kahta High (Figure 1). This structure was defined as a high for the first time in 1964 by Rigo and Cortesini, with east-northwest direction and southeast subduction zone (Bozdoğan and Erten, 1991). The outcrops through this uplift can be considered as the main key structure to understand the formations of this area.

The Mardin-Kahta High is efficient beginning from the Early Ordovician age but the Ordovician depositions were not able to pass the high over. The sedimentation was regulated until the Cretaceous age. One can say that the high separates the platform into two basins as the Diyarbakır basin in the east-northeast and the Akçakale basin in the west-southwest directions. Additionally, the Mardin part of the uplift was exceeded by the Late Ordovician Sea whereas the Kahta part maintained its positive area structure until the Cretaceous age (Bozdoğan and Erten, 1990).

Cudi Group's name was given after the Cudi Mountains located at Şırnak Province, in 1952, by Altınlı. The group mainly consists of light-dark gray, black, white, pinkish beige colored dolomites, anhydrites and limestones along with shale fragments. The age interval within this group is in between Middle-Late Triassic and Early Cretaceous. The maximum thickness of this group is approximately 2000 meters. This relatively thick sequence has shallow marine environment. The group's relationship with its bottom neighbor Çığlı Group is conformable whereas the relationship with its upper neighbor Mardin Group is discordance.

1.3 Literature Survey

1.3.1 Geology of SE Anatolia and Study Area

Turkey was affected by both Paleotethys and Neotethys orogenesis. At the Anatolian region, Tethys which opened at the beginning of Triassic, started to close at Cretaceous. At the Late Cretaceous, the oceanic crust of Tethys has been submerged at the subduction zone that is in front of the North Anatolian Mountains and reached the African subduction zone. The oceanic materials were spread out to the south from this zone through all of the Anatolia (Sungurlu and Arpat, 1978).

Various geological periods should be studied to understand the evolution of the regions geology. During these periods, the major factor affecting the development of the areas stratigraphy is the relation of Anatolian plate at the north and Arabian plate at the south.

The main factor that generates the evolution of SE Anatolia Turkey is the closure of the Neotethys (Perinçek et al., 1992).

The collision of the Arabian and the Anatolian plates has developed the present tectonic features of this region. The location of SE Anatolia is on the northern margin of the Arabian-African shelf platform and the regional stratigraphic rock units were deposited from Early Cambrian to Late Miocene ages (SE Anatolia District Geologists of TPAO, 1979).

The oldest autochthonous sequence unit is known to be the Precambrian aged Telbesmi Formation. This unit consists of volcanics, volcanoclastics, sandstones and shales (Güven et al., 1991). At most cases, Telbesmi Formation is overlain by Derik Group and this group which is Cambrian aged is characterized by continental to transitional type clastics at the bottom, shelf carbonates in the middle and shallow marine shale and sandstone alternations at the top (Perinçek et al., 1992). At the top of this group, Ordovician aged Habur Group's shallow marine deposits are graded. After this period, at the Late Silurian age section (Diyarbakır Group's Dadaş Formation only), a sedimentological break has occurred at the rest of the area. Afterwards; Late Silurian-Devonian aged Diyarbakır Group, Late Devonian-Early Carboniferous aged, coastal to shallow marine Zap Group and Permian aged Tanin Group, composed of carbonates and clastics, have been deposited at SE Anatolia. As we can understand from these Permian aged formations (Kaş and Gomanibrik), the region is surfaced with the Tethys Sea at the first periods of Mesozoic.

The complete period of this phase relatively passed calm. Until the end of Mesozoic; some parts of the region were as deep marine facies. At Triassic and Jurassic ages; these facies, especially towards the south fields, are characterized as shallow marine or even tidal environments.

The duration of the depositional sequences of shallow water carbonate platforms range from 1 to 10 m. y. and these sequences reflect long term changes in accommodation linked to third order

global eustatic cycles on cratons and passive margins (Read and Horbury, 1993). In a region, where we observe shallow-water carbonate sedimentation, physical, chemical and biological processes are in consequently changing relationships. These processes are mainly photosynthesis, respiration, precipitation of CaCO_3 , evaporation, rainfall and fresh water run-off from the coasts. The partial pressure of CO_2 in the water fluctuates due to these activities (Bathurst, 1976).

Early Triassic aged Çiğlı Group, representing the lowermost unit of the Mesozoic sequence, contains carbonates separated by a red bed sequence. The Arabian Platform had undergone an extensional tectonics up to the Late Jurassic (Ulu and Karahanoğlu, 1998; Sungurlu, 1974; Ala and Moss, 1979; Sass and Bein, 1980 and Lang and Mimran, 1985). Additionally; during the Middle-Late Triassic, on the Arabian Platform's NE edge, a shallow water carbonate shoal elongated through NW-SE direction was located.

The circulation of water between the epicontinental sea that extended over the Arabian Platform and South Tethys was obstructed by this shoal. Oxygen destituted facies with low energy were deposited within the subsiding Mesopotamian Depression (Bordenave and Hegre, 2010, James and Wynd, 1965). At the bottom of hypersaline waters during the sea-level falls, thick evaporites were accumulated, whereas anoxic episodes were corresponded to highstand periods (Bordenave and Hegre, 2010).

A rifting created a block faulted terrain with topographic highs and lows during Late Jurassic to Early Cretaceous age (Ulu and Karahanoğlu, 1998). SE Anatolia was an east-western trending topographic high within this age section (Ulu and Karahanoğlu, 1998, Temple and Perry 1962). During the Aptian and Santonian age periods, Mardin Group's carbonates were deposited following a transgression flooding this high. Consequently, SE Anatolia was considered to be a part of the most important platform created on the Arabian shelf (Görür et al., 1991). At the top of Çığlı Group, Middle Triassic-Early Cretaceous aged Cudi Group exists. Cudi Group, located at the mid-southern parts of SE Anatolia, is represented by a carbonate-evaporate sequence of tidal flat origin.

At the Laramien phase, which occurs after Late Cretaceous age, the region was uplifted and folded. Following the compressional characters, the Savien phase occurs after the Oligocene age. As a result of this period, occurring especially at the Mardin and Diyarbakır fields, Midyat carbonates were formed. At the Rodanien phase, arising after the Miocene stage, thrusting towards south occurs and as a result thrusts are seen in patches. Also, at the Caledonian Orogenetic phase, folds in patches and faults are formed after this tectonic process.

Organic evolution stages, oceanographic factors, sea-level fluctuation, and tectonic activity patterns as well as the subsidence rates controls the carbonate facies but all of these factors maintains their efficiencies by existing all together (Wilson, 1990).

South Dincer Field, located at the southern side of SE Anatolia, is in the form of a structure lying through southeast–northwest direction and this structure's northern margin leans on a graben. This main structure was exposed to some various small scaled tectonics with faults in patches. The main graben has separated the North and South Dincer Fields into two different blocks.

A graben surrounds the north of the South Dincer Field like a set and forms a barrier. This barrier controls the oil–water contact in this field until the elevation of approximately -985 meters and enables an oil production up to this elevation value. This value decreases approximately to -1020 meters at the block which shows a different structure and where the 22 numbered well is located. As a result, one can say that the South Dincer Field is in the form of structural trap because it has gained its current structure as a result of tectonic movements.

Mardin-Kahta High, the main tectonic unit affecting the paleogeography of the studied area, has briefly begun at Early Ordovician age and has maintained its function through time.

The uplift has enabled relatively thick sediments to be deposited at the eastern side of the area. This fact has occurred due to the fault systems of the uplift's horst-graben structure.

Mardin-Kahta Uplift separates SE Anatolia into two basins in the Ordovician age. These two basins which are mainly Akçakale basin at the west and Diyarbakır basin at the east are related with the

uplift's southern edge where the subduction occurs. These basins show similar depositions within the Ordovician age period but entirely different stratigraphic structures after this age section.

After the Ordovician age, sedimentation has not occurred through Triassic age at the south and Cretaceous age at the north within Akçakale basin. So, large erosions are seen at the Ordovician deposits. However, it can be said that Early Silurian aged sediments and Carboniferous aged deposits of Syria could have deposited at this basin and eroded afterwards. Nevertheless, a thick Ordovician, Silurian-Devonian age deposits as well as Permian, Triassic and Jurassic sediments have filled Diyarbakır basin (Bozdoğan and Erten, 1991).

South Dincer Field was explored with South Dincer-1 well and the initial date of the oil production within this field is recorded as March 29, 1981. Dincer-1 well is also located very near to this oil production field. The total area within this field with oil is 3.8 km² and the oil production is ongoing with total of six wells. The field's monthly oil production is determined as 1.745 barrels with a 9 bbl/hr flow rate and the cumulative oil production is observed as 7.294.896 barrels. The total amount of remaining productive oil of this production field is approximately 760.104 barrels.

The Cudi Group, age interval mainly in between Triassic and Early Cretaceous ages, has been divided into 2 separate formations which are Çanaklı Formation at the bottom and Latdağı Formation at the top (Figure 3). Çanaklı Formation has 7 different sub-

formations which are from bottom to top, Bakük, Girmeli, Çamurlu, Telhasan, Dinçer, Kozluca and Yolaçan formations (Figure 4). Meanwhile, the passage from Triassic to Jurassic is represented by unconformity.

Accounts of the disconformities at the top of this group on the regarded field were expressed by various investigators throughout 60 years. This major break is well documented at this district in surface sections on the Mardin-Kahta Uplift and in numerous oil and gas targeted wells (Schmidt, 1964).

Cudi Group comprises predominantly of dolomite and anhydrite. The dolomite of this group can be classified as finely and coarsely crystalline dolomite. The most important type of the first group dolomite is dolomicrite and the second group contains ghosts of fossil fragments, pellets, intraclasts and oolites. Cudi Group secondarily consists of micritic argillaceous limestone and shale. These limestones were also reported to have fossil fragments, intraclasts and pellets where shales were defined to be derived from outside the basin and afterwards redistributed by circulating currents. We can see the dolomites very frequently throughout the sequence but anhydrites are generally located at the Bakük, Girmeli, Telhasan and Kozluca formations. On the other hand shales are mostly found in relatively thicker sequences or in intervals with high intensive and periodic evaporates (Salem, 1984).

AGE	GROUP	FORMATION	THICKNESS (m)	LITHOLOGY	DEFINITIONS
APTIAN-ALBIAN	MARDIN	AREBAN			LIMESTONE-SHALE-SILTSTONE
MIDDLE/? LATE TRIASSIC - EARLY CRETACEOUS	I D U	LATDAĞI	219		DOLOSTONE:Black colored, thick layered. LIMESTONE:Dark dun colored, thick layered. DOLOSTONE:Dun, black colored, middle to thick layered, black colored, laminated with black colored shale. DOLOSTONE:Dun, brownish black colored, thin to middle layered.
		ÇANAKLI	807	1026	DOLOSTONE:Dun, blackish dun colored, solid. DOLOSTONE:Dark dun colored, middle to thick layered. DOLOSTONE:Light dun colored, middle to thick layered, solid. DOLOSTONE:Dun colored, middle to thick layered and uncertain layered in patches. LIMESTONE:Dark dun colored, thin layered. DOLOSTONE:Light dun colored, middle to thick layered, solid. LIMESTONE:Dun, cloudy yellow colored, solid.
					DOLOSTONE:Blackish dun, dun colored, middle to thick layered, solid. LIMESTONE:Dun, white colored, solid. DOLOSTONE:Dun colored, solid. DOLOMITIC LIMESTONE: Dun colored, solid. DOLOSTONE:Dun, white colored, solid. LIMESTONE:Light dun colored, solid. DOLOSTONE:Dun, colored, middle to thick layered.
EARLY TRIASSIC	ÇIĞLI	UZUN-GEÇİT			LIMESTONE:Blackish dun, dun colored, thin to middle thick layered, with lumps in patches. SHALE CLAYEY LIMESTONE

Figure 3. Generalized stratigraphic section of the Cudi Group prepared from the wells located at Gaziantep and Nusaybin-Cizre fields (modified from Yılmaz and Duran, 1997).

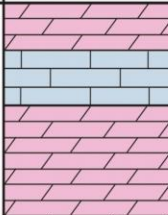
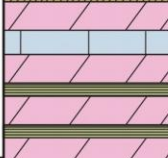
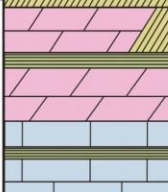
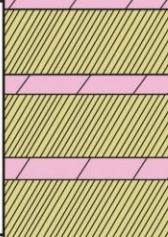
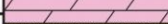

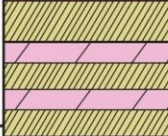
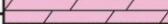
AGE	GROUP	FORMATION	THICKNESS (m)	LITHOLOGY	DEFINITIONS
UPPER TRIASSIC- LOWER JURASSIC	I	YOLAÇAN	21-525		DOLOSTONE: Cream, gray, white colored. LIMESTONE: Cream, white, dark gray colored in patches. DOLOSTONE: White, cream, beige colored, laminated with thin shale.
		ÇAMURLU	125-208		LIMESTONE: Gray, cream colored. DOLOSTONE: Gray, white, beige, cream, brown colored, intercalated with shale.
M I D D L E - U P P E R T R I A S S I C	U	BAKÜK	105-472		DOLOSTONE: Beige, gray, cream, brown, blakish gray colored, intercalated with thin shale and evaporite. LIMESTONE: Gray, beige, brown colored, intercalated with thin shale.
		GIRMELI	42-511		EVAPORITE: Light gray, white colored, with dolostone laminated with alg and intercalated with shale.
		TELHASAN DİNÇER KOZLUCA	52-63		DOLOSTONE: Light gray, greenish gray, cream, beige colored.
		TELHASAN DİNÇER KOZLUCA	15-59		EVAPORITE: White, beige colored.
		TELHASAN DİNÇER KOZLUCA	18-121		DOLOSTONE: Cloudy white, white, beige, cream, greenish gray, gray colored, with shale intercalates and lenses. EVAPORITE: Gray, white colored shale, marl, limestone and dolostone intercalation.
		TELHASAN DİNÇER KOZLUCA	52-63		DOLOSTONE: Cloudy white, white, beige, cream, greenish gray, gray colored, with shale intercalates and lenses.

Figure 4. Generalized stratigraphic section of the Cudi Group at Şırnak and Hakkari region (modified from Yılmaz and Duran, 1997).

The formation of Cudi Group has begun with a general subsidence which was defined as a transgressive sequence of carbonates and shales. Before this activity, the area was traversed by normal fault blocks and ridges from the former tectonics. Secondly, tectonic sequence periods occurred and basins were filled despite the predominated open marine conditions. Thereafter, shallow water carbonates and dolomites and finally evaporates were deposited. Cudi Group formations were developed after the repetition of this whole process.

Small amounts of primary porosity as well as secondary porosity consisting intercrystalline and vuggy typed porosities can be preserved at this group rocks. At the first porosity type, partial or complete reduction can be frequently observed either by compaction and/or cementation. The intercrystalline porosity of the second type was formed between dolomite crystals of different sizes and the vuggy porosity occurred by leaching and dissolution of allochems or matrix. At the general formation of the Cudi Group, removal of the material during dolomitization and diagenesis increased the porosity of the secondary type porosity (Salem, 1984).

1.3.2 Diagenesis of Carbonate Rocks: Dolomitization

The resemblances between carbonates and sandstones or shale end at the time of deposition, for processes of solution, cementation, re-crystallization, replacement, and the introduction

of internal sediment form complex and different changes in highly soluble carbonate rocks (Ham and Pray, 1961). Before defining the factors related to these diagenetic changes, the term diagenesis can be defined as follows; several characteristic and compositional changes of the sediments which occurs starting from the deposition, through the moving of the resulting rocks to the place of metamorphism or the sustaining of these rocks to the effects of atmospheric weathering (Larsen and Chilingar, 1979). This alteration can also be defined as the reaction of a sedimentary rock to its physicochemical environment.

In the formation of the above diagenetic changes, the following factors play a major role; the higher solubility of the carbonate minerals as compared to the sedimentary minerals of sandstones and shales, the different solubility's and stability relationships of aragonite, magnesium calcite and dolomite, different rates of solution and re-crystallization caused by the variety of carbonate mineral's crystal size within the initial sediment, and the access of solutions of compositions different from those in which the sediments were deposited caused by the relatively high porosities and permeabilities of carbonate sediments. The equilibrium of carbonate minerals can be disturbed very easily by slight changes in physical and chemical conditions, and similar variations can form reversals of diagenetic process. The interpretation, description and classification of the carbonate rocks can be influenced by the final effects of diagenesis. In contrast, they can bring some questions to mind like does the sparry calcite of carbonate rocks stand for cementation in original void space or does it represent re-

crystallization of the initial lime mud (Ham and Pray, 1961). A rich inventory of primary sedimentary structures and early diagenetic features exists in modern shallow marine carbonate environments such as; thin bedding, stromatolites, evaporate minerals, and so on (Demicco and Hardie, 1994).

The factors effecting diagenesis are pressure, temperature, the environment's Eh and pH, the concentration of various anions and cations (Larsen and Chilingar, 1979). There are also some additional factors which affects the diagenesis of carbonate sediments. Some of these factors are; geographic, geochemical and physicochemical factors, geotectonism, geomorphologic position, sediment's initial composition and purity, grain size, the accessibility of limestone frameworks to the surface, the existence of interstitial fluids and gases and their properties (Chilingar et al., 1979a). On the other hand; physicochemical, biochemical-organic and physical processes can be defined as the actual processes that lead to these subject alterations and modifications of limestones.

In addition to the factors defined above; during diagenetic, syngenetic and epigenetic stages, some certain processes can alter limestones. The first two examples of these processes can be given as corrasion and corrosion which forms diagenetic micro-karst structures. These can give some information about the paleogeographic conditions as well as details of porosity and permeability. Diagenesis can be affected by corrasion and corrosion in an important manner. They can form micro-karst structures and internal cavities can be observed numerously. Depressions and

irregularities, ranging from a few millimeters up to a few feet, can be formed by pitting of algal encrusted limestone surfaces. Patches, lenses, laminae and beds of marls or clay can be observed as a result of corrosion, solution and leaching of argillaceous limestone after the limestone's deposition. By solution, the calcareous skeletons are removed, leaving the internal cast in case the organisms are filled with less soluble material (Chilingar et al., 1979a).

Considerable corrosion, solution and disintegration of calcareous sediments can be observed as a result of both direct and indirect organic processes, such as the bacterial processes. After the organisms die and are buried, the bacteria decompose the soft parts of those organisms. While this decomposition occurs, shells lost 10-24% of their calcium carbonate within one to two months and insoluble chitinous material traces are left over following the removal of the carbonate (Chilingar et al., 1979a).

Rock's diagenetic alteration patterns are the summation of all the varied pore fluid effects that have flowed through the rocks during burial, in combination with the physical and geochemical conditions involved.

Within the studied Cudi Group's thin section samples, an important proportion of Algae were observed. The growth of these Algae is dominantly controlled by a dynamic relation between living and algal-mat forming blue-green Algae and the entrapment and precipitation of CaCO_3 (Bathurst, 1976). The algal images can be

very important regarding the shallow-water diagenesis, specifically limestone genesis. The lime precipitates of algae can occur as crusts and they are counted as of syngenetic origin. Respiration processes lead to the precipitation of calcium carbonate (CaCO_3) by Algae and the alternation of corrosion as well as precipitation at night and day light respectively are the key factors of this process.

Corrosion takes place at night by Algae giving off CO_2 into the environment. In contrast, precipitation of CaCO_3 and pelagosite by alkaline conditions caused by the utilization of CO_2 during photosynthesis occurs in daylight. There can also be some other possible causes of algal cementation. As an example, dissolving surface layers chemically by boring Algae can precipitate calcium carbonate within the sediments (Emery et al., 1954). Another example can be given as detritus-binding Algae (Chilingar et al., 1979a).

Also, precipitation carbonate on surfaces or by absorbing CO_2 from the water medium internally can be done by some genera. A thin section of these kinds of biogenic carbonates shows a dense cryptocrystalline character (Chilingar et al., 1979a).

Diagenesis has enormous effects in oil and gas production field. Porosity and permeability are related to the original fabric and composition of sediments as well as the diagenetic processes (Horbury and Robinson, 1993). One of the factors effecting the partial replacement of anhydrite by calcite is noted to be the sulfate-reducing bacteria. In marine waters, sulfate reduction can

only be limited by the organic matter amount. Anaerobic bacterial processes, the product of which should accumulate, lead to the oxidization of organic matter (Chilingar et al., 1979a).

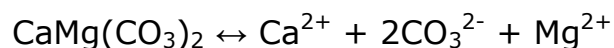
Diagenesis, in general, helps to answer some important questions regarding cementation, re-crystallization, the type and the origin of porosity and permeability, the reasons that in some cases, non-reef limestones gaining good reservoir qualities whereas in similar environments showing cap rock characteristics and the properties that makes shallow-water limestones good or poor source rocks (Chilingar et al., 1979a).

The mineral dolomite was described for the first time by French naturalist and geologist Deodat de Dolomieu in 1791, in *Journal de Physique*. The geologist's discovery of dolomite was from a field trip to the Alps of Tyrol (today part of Italy) and he discovered a calcareous rock which did not effervesce in weak acid like limestone. After this discovery, the rock was named Dolomieu the next year. Moreover, both the rock and its mineral carry the name Dolomieu, Dolomite, as well as the mountain range in northwestern Italy, where the mentioned geologist first identified the rock. Later on, in 1914, Van Tuyl wrote the first review paper about dolomite and dolomitization. The first hydrocarbon reservoirs in dolomitized carbonates were discovered in the 1920's. Giant oil fields were produced following the oil discoveries from dolostone reservoir rocks which have high porosities and permeabilities in Canada and United States of America (Machel, 2004). These discoveries

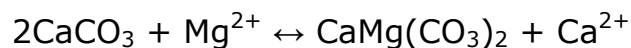
increased the studies regarding the dolomites in 1950's and the following researches proceeded incrementally throughout the years.

Dolomite is a sedimentary carbonate rock and a mineral, both composed of calcium magnesium carbonate found in crystals. The term "dolostone" is commonly used to define the rock dolomite.

Dolomite is the iron rich member of the dolomite-ankerite $\text{Ca}(\text{Mg,Fe})(\text{CO}_3)_2$ mineral series. In dolomites, Fe can replace Mg and when the Mg amount is smaller than that of the Fe amount, the mineral becomes ankerite (Gribble and Hall, 1992). Ideal, ordered dolomite has a formula of $\text{CaMg}(\text{CO}_3)_2$ and consists of alternating layers of $\text{Ca}^{2+}-\text{CO}_3^{2-}-\text{Mg}^{2+}-\text{CO}_3^{2-}-\text{Ca}^{2+}$, etc., perpendicular to the crystallographic c-axis. Dolomite rock (dolostone) is composed predominantly of the mineral dolomite. This mineral crystallizes in the trigonal-rhombohedral system and forms white, gray to pink, commonly curved crystals. The chemical reaction from which a dolomite is precipitated is as follows;



Also, the evaluation equation of this reaction in which calcite is replaced by dolomite can be seen below;



The physical properties of it can be mistaken for the mineral calcite. The main difference of these two minerals is that, unless it is scratched or found in powdered form, dolomite does not dissolve or fizz in dilute hydrochloric acid. Usually, in thin section studies, staining with Alizarin Red S technique is used for distinguishing dolomite from calcite and it is observed that calcite turns into pink color when stained whereas dolomites stays unaffected. Mainly sand sized or larger dolomite crystals contain concentric, alternating zones of iron-rich (red colored) and iron-poor (clear) dolomite, indicating stages of growth of the rhomb. They can have some amounts of ferrous iron in their structure as a substitute for magnesium. Calcium is never apparently zoned since iron cannot substitute for calcium and the iron-enriched zones of the former dolomite are maintained by the calcitized dolomite. To gain a visible form, ferrous iron must be oxidized to the ferric form (Blatt, 1982). Some of the properties of a dolomite are listed in Table 1.

Table 1. General properties of dolomites.

Chemical Formula	CaMg(CO ₃) ₂
Color	White, Gray, Reddish white, Brownish white
Cleavage	{1011}Perfect, {1011}Perfect, {1011}Perfect
Molecular Weight	184.40 gm
Density	2.8-2.9 gm/cc (Average=2.84 gm/cc)
Fracture	Brittle - Conchoidal
Hardness	3.5-4
Crystal System	Trigonal-Rhombohedral
X Ray Diffraction (I/0)	2.883(1), 1.785(0.6), 2.191(0.5)
Luminescence	Non-fluorescent
Luster	Vitreous (Glassy)

Dolomite is stoichiometric ideally but in natural environment it cannot be seen as such. Because of this form of dolomite, its depositional environment's geochemistry can be solved. The ordering ratios of dolomites are also important by means of being the primary precipitation products or not. Naturally, they are ordered to an extent with most modern dolomites showing poor ordering related reflections (Süzen and Türkmenoğlu, 2000).

Dolomites resemble limestones in several ways. For example, they occur on the shallow shelves of low-lying continents, far from the nearest convergent plate margin. Additionally, like limestones, they are basically mono-mineralic resulting varied observations in textures and structures. One can say that dolomites form as replacement of limestones. In ancient reef environments, the seaward front of the reef is observed as limestone whereas the landward, back of the reef part has been replaced by dolomite. With the help of stratigraphic relationships and the fossil existences, the bulk of dolomites, like of limestones, are observed to be marine. Although the fossil amounts within the dolomites are considerably less. The majority of them are found as distinct beds or formations interlayered with other sedimentary rocks which are nondetrital and have similar thicknesses (Blatt, 1982).

Also, a dolomite bed may grade laterally into another rock type, usually a limestone or evaporate and in most cases, this evaporate is gypsum or anhydrite. The intervals where limestones form are mainly intertidal and shallow subtidal areas on the shallow seafloor.

On the other hand, evaporates requires large-scale saline water evaporation forming by subaerial exposure or in an isolated arm of the sea (Blatt, 1982).

There are three main categories of dolomites accepted by most of the researchers. The first among this classification are the "primary dolomites", these occur within the sediment-water interface by direct precipitation from the solution. The second types are the "diagenetic dolomites" which are formed by the replacement of calcium carbonate sediments in the post-depositional phase. The third types are named as "epigenetic or catagenetic dolomites", these are formed by the replacement of lithified calcium carbonate sediments (Chilingar et al., 1979b).

In addition to the above types of dolomite, there are also ancient and modern dolomites. Additionally, all present dolomite occurrences are believed to be formed by the fresh water-seawater mixing in the shallow subsurface under a carbonate shoreline or by a chemical process in which the evaporate formation takes place above mean high tide of a carbonate basin, within a narrow zone. Meanwhile, dolomite can be found parallel and adjacent to fault surfaces; this condition states that the origin of the water in which the regarded dolomite crystallizes is below the dolomites' accommodation. They can also be formed in modern salt lakes or during relatively deep limestone diagenesis. In ancient record, main hypotheses about the origin of the dolomites can be accepted as follows; During the Precambrian and Paleozoic ages, the composition of the seawater was different than of today's.

Especially, magnesium was more abundant (Blatt, 1982). It has been observed from the field studies carried out through the past century that dolomite occurs in rocks of all ages, especially in older rocks. It is noted that, it forms less than 5% of the carbonate rocks of Tertiary age, 10% of those of Mesozoic age, 35% of those of Paleozoic age, and more than two-thirds of Precambrian age (Blatt, 1982; Garrels and Meckenzie, 1971).

Dolomitization processes can be clearly come down to post-depositional or diagenetic. There are economic importances of dolomites and dolomitization processes, in means of oil and gas production since porosity changes occurs during diagenesis. An important amount of oil and gas can be stored in cavities of local dolomitization porosities and new oil fields have been discovered within these dolomites in past centuries. In contrast, a discovery of a locally dolomitized limestone does not always guarantee an oil or gas exploration. Local dolomites can be non-porous or non-productive by being situated in a condition that no suitable trap for oil accumulation can be present (Landes, 1946).

Dolomitization is the replacement of CaCO_3 by $\text{CaMg}(\text{CO}_3)_2$. Large scale dolomite bodies must result from replacement reactions with fluids importing Mg and removing Ca (Whitaker et al., 2004; Land, 1985; Machel and Mountjoy, 1986 and Hardie, 1987). In a situation where a carbonate sequence is composed of both dolomite and limestone, the dolomitization intensity increases in the direction of the craton. In natural systems the time available for dolomitization is commonly considerable and geochemical acceleration of the

process may not be necessary (Whitaker et al., 2004). There are some critical factors affecting this dolomitization process. For example, Ca-rich waters become dolomitizing fluids at temperatures above 60°C and these fluids makes most natural subsurface waters capable of dolomitization. Time may be the key element at low temperature conditions, so that seawater will become a major dolomitizing fluid only where stable circulation systems can drive seawater through carbonate platforms for many years ranging from thousands to millions (Hardie, 1987).

At the first stage dolomitization, a transformation from calcitic to dolomitic form of rock occurs and fine to medium size crystals (4-30 microns) develops. The following stage results in purer dolomite crystals of about 20 microns to 70 microns. At the third and the final stage, which is considered to be cementation, overgrowth of the enlarged dolomite crystals occurs and a new dolomite layer is being added on to the dolomite crystals. This stage can be associated with deposition of dolomite cement crystals in the inter-granular and inter-crystalline pore spaces, in original cavities or in vugs. This dolomite cement includes large crystals of dolomite and some of these dolomites are limpid crystals which are fresh or brackish water solution indicators (Salem, 1984).

At the Dincer-1 and South Dincer-1 Well cores, the dolomites of the Cudi Group can be observed as very fine, coarser grained and limpid typed. The first group occurs as intraclasts and mainly associates with anhydrite crystals. Because of this association as well as the lack of any indication of fresh water, one can say that

these dolomites probably formed on a hyper-saline tidal flat. The size of these fine dolomites can be noted between 1-16 microns. The second type of Cudi Group's dolomites appears to be the main lithology of this group. The size of these coarser dolomites ranges from 16 to 125 microns (fine to medium crystalline) and are formed as a result of replacement of calcites. The reflux of hyper-saline water or the passage of fresh/salt water mixing zone through the sediments and the dolomitization of lithified carbonates by buried water can be considered at the origin of these types of replacement dolomites. As a result, the regarded dolomites can be formed by the elevation of temperature and geothermal gradient. The limpid dolomite was primarily defined by Folk, Roberts, Moore and Siedlecka (1973, 1974) and later on described by Folk and Land (1975). These are extraordinarily transparent gem-like crystals and are considered to be the products of fresh to brackish water. Here, in dilute solutions, these dolomites are formed very quietly and it is possible to identify them in cores by the help of acid, rather than observing them in thin sections (Salem, 1984).

1.4 Methods of Study

1.4.1 Sampling

The cores of Dınçer-1 and South Dınçer-1 exploration wells were examined and the ones belonging to the Cudi Group sequence, in addition to its uppermost unit Mardin Group and lowermost unit Çığlı Group sequence were selected and dissected.

The thin sections of these selected cores were studied depending on some possible diagenesis and dolomitization mechanisms, brief descriptions of them were made and their photomicrographs were taken.

From Dinger-1 Well, total of 14 cores were taken throughout the penetration. These cores, belonging to Midyat Group's Hoya Formation, Şırnak Group's Bozova Formation, Beloka Formation (without a specified group), Mardin Group's Derdere and Sabunsuyu formations, Cudi Group's Telhasan, Girmeli and Bakük formations and Çiğli Group's Uludere Formation (Figure 5) were checked thoroughly and the ones belonging to the Cudi and Çiğli group formations were further studied in details. From top to bottom, two cores from Telhasan (core numbers 9 and 10), one core from Bakük (core number 13) and one core from Uludere (core number 14) formations were selected as some of the key factors of this study (Table 2). 22 thin sections of these 4 cores, regarding the Triassic and Jurassic age interval of SE Anatolia, were undertaken for the regarded scope.

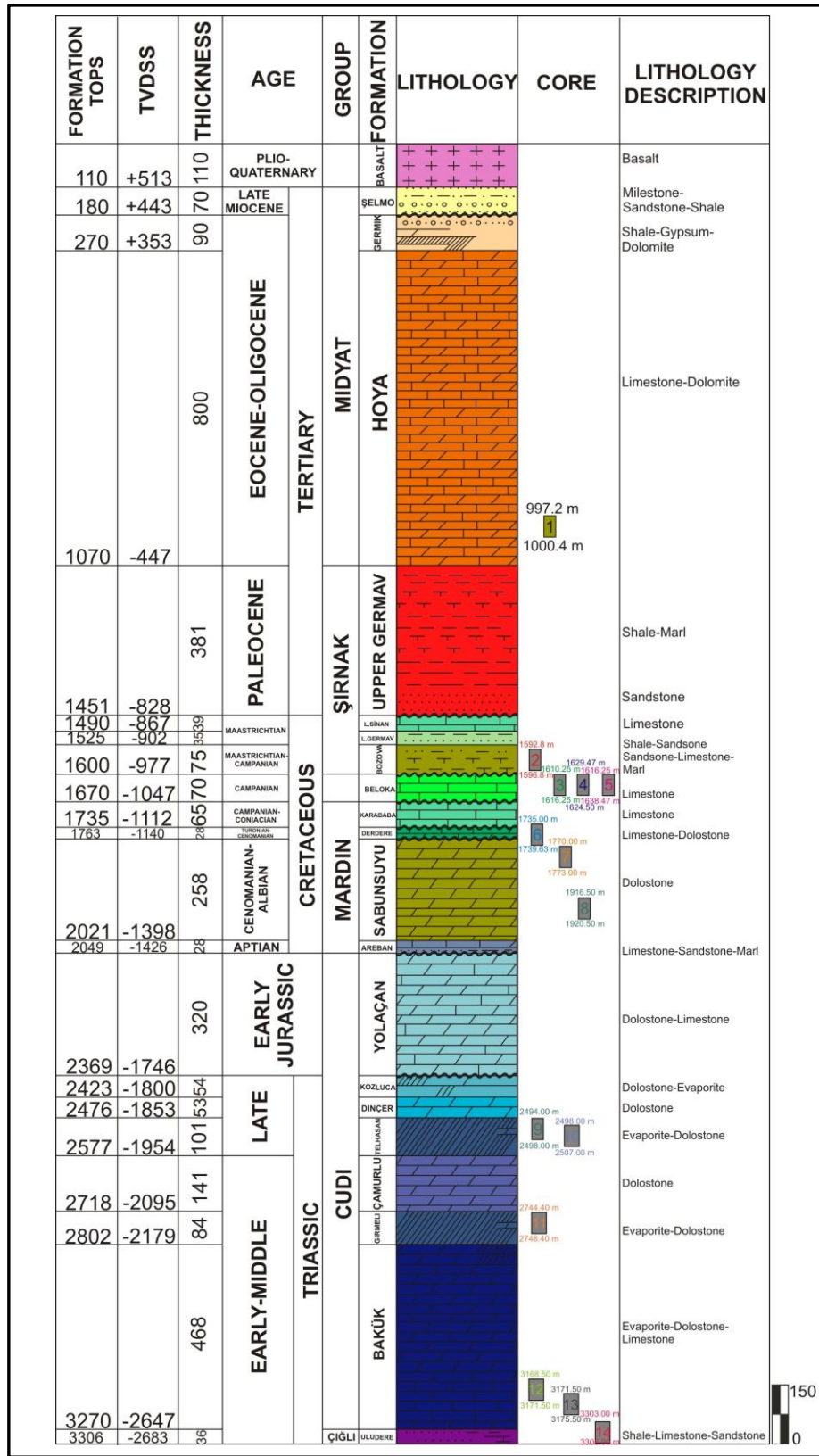


Figure 5. Dinçer-1 Well's vertical section with core information.

Table 2. Dinger-1 Exploration Well's detailed core data.

List No	Thin Section No	Core No	Box No	Depth Interval (m)	Recovered Core Thickness (m)	Total Core Recovery (%)	Formation	Selected for XRD (Y/N)	Exact XRD Sample Depth (m)
1	40940	9	3494	2494.00-2498.00	4.00	100	Telhasan	Y	2495.97
2	40941	9	3495	2494.00-2498.00	4.00	100	Telhasan	N	-
3	40942	9	3496	2494.00-2498.00	4.00	100	Telhasan	N	-
4	40943	10	3499	2498.00-2507.00	9.00	100	Telhasan	Y	2498.29
5	40944	10	3500	2498.00-2507.00	9.00	100	Telhasan	N	-
6	40945	10	3500	2498.00-2507.00	9.00	100	Telhasan	Y	2502.00
7	40946	10	3502	2498.00-2507.00	9.00	100	Telhasan	Y	2502.30
8	40947	10	3505	2498.00-2507.00	9.00	100	Telhasan	Y	2505.50
9	40948	10	3507	2498.00-2507.00	9.00	100	Telhasan	Y	2505.80
10	43439	13	3515	3171.50-3175.50	2.92	73	Bakük	Y	3171.95
11	43440	13	3516	3171.50-3175.50	2.92	73	Bakük	Y	3172.95
12	43441	13	3516	3171.50-3175.50	2.92	73	Bakük	N	-
13	43442	13	3517	3171.50-3175.50	2.92	73	Bakük	N	-
14	43443	13	3517	3171.50-3175.50	2.92	73	Bakük	Y	3174.00
15	43444	13	3517	3171.50-3175.50	2.92	73	Bakük	N	-
16	43445	14	3517	3303.00-3306.00	1.50	50	Uludere	N	-
17	43446	14	3518	3303.00-3306.00	1.50	50	Uludere	Y	3303.15
18	43447	14	3518	3303.00-3306.00	1.50	50	Uludere	N	-
19	43448	14	3518	3303.00-3306.00	1.50	50	Uludere	N	-
20	43449	14	3518	3303.00-3306.00	1.50	50	Uludere	N	-
21	43450	14	3518	3303.00-3306.00	1.50	50	Uludere	N	-
22	43451	14	3518	3303.00-3306.00	1.50	50	Uludere	N	-

As in Dinger-1 Exploration Well's studies, total of 19 cores were taken throughout the penetration of South Dinger-1 Exploration Well. These cores, belonging to Beloka Formation (without a specified group), Mardin Group's Karababa, Sabunsuyu and Areban formations, Cudi Group's Dinger, Telhasan, Çamurlu and Bakük formations and Çiğli Group's Uludere Formation (Figure 6) were overviewed. In addition to Dinger-1 Well's selected core samples, 1-4, 6, 8 and 10-19 numbered cores, belonging to Beloka Formation, Mardin Group, studied Cudi and Çiğli group formations were examined. These cores were briefly from Beloka Formation (without a main group; core numbers 1-4, 6), Mardin Group's Karababa Formation (core number 8), Cudi Group's Dinger Formation (core number 10), Telhasan Formation (core numbers 11-14), Çamurlu Formation (core number 15 and 16), Bakük Formation (core numbers 17-18) and Çiğli Group's Uludere Formation (core number 19). To sum up, 28 thin sections belonging to these 16 cores were underscored at the studies carried out for South Dinger-1 Exploration Well (Table 3).

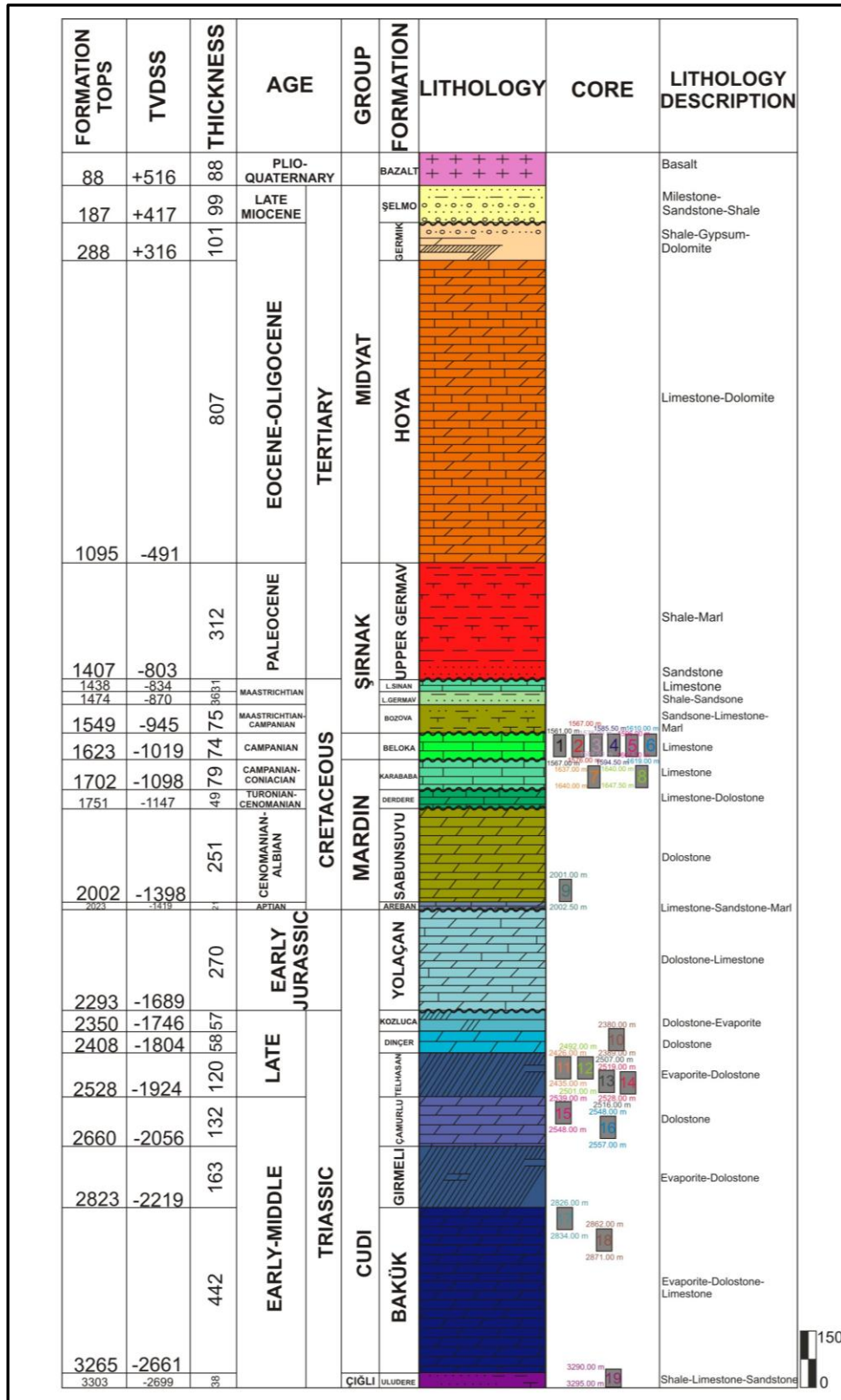


Figure 6. South Dinger-1 Well's vertical section with core information.

Table 3. South Dincer-1 Exploration Well's detailed core data.

List No	Thin Section No	Core No	Box No	Depth Interval (m)	Recovered Core Thickness (m)	Total Core Recovery (%)	Formation	Selected for XRD (Y/N)	Exact XRD Sample Depth (m)
1	134823	1/2	8794	1561.00-1567.00	3.96	66	Beloka	N	-
2	134826	2/1	8797	1567.00-1576.00	5.85	65	Beloka	N	-
3	134832	3/3	8805	1576.00-1584.50	5.04	63	Beloka	N	-
4	134836	4/2	8809	1585.50-1594.50	4.50	50	Beloka	N	-
5	135193	6/3	8818	1610.00-1619.00	7.74	86	Beloka	N	-
6	135200	8/2	8825	1640.00-1647.50	1.72	23	Karababa	N	-
7	257554	10/1	9023	2380.00-2389.00	4.05	45	Dinçer	N	-
8	257558	11/2	9028	2426.00-2435.00	7.20	80	Telhasan	N	-
9	257560	11/4	9030	2426.00-2435.00	7.20	80	Telhasan	N	-
10	257563	11/7	9033	2426.00-2435.00	7.20	80	Telhasan	Y	2430.80
11	257571	12/3	9037	2492.00-2501.00	8.10	90	Telhasan	N	-
12	257582	13/1	9043	2507.00-2516.00	7.29	81	Telhasan	Y	2507.45
13	257587	13/6	9043	2507.00-2516.00	7.29	81	Telhasan	Y	2510.05
14	257595	14/1	9048	2519.00-2528.00	8.55	95	Çamurlu	N	-
15	257596	14/2	9052	2519.00-2528.00	8.55	95	Çamurlu	Y	2520.30
16	257598	14/4	9052	2519.00-2528.00	8.55	95	Çamurlu	Y	2522.65
17	257602	14/8	9054	2519.00-2528.00	8.55	95	Çamurlu	Y	2525.10
18	257609	15/1	9058	2539.00-2548.00	2.25	25	Çamurlu	Y	2539.00
19	257614	16/1	9060	2548.00-2557.00	4.41	49	Çamurlu	N	-
20	257616	16/3	9064	2548.00-2557.00	4.41	49	Çamurlu	Y	2549.65
21	257618	16/5	9064	2548.00-2557.00	4.41	49	Çamurlu	Y	2550.15
22	257624	17/1	9066	2826.00-2834.00	7.60	95	Bakük	Y	2826.25
23	257626	17/3	9067	2826.00-2834.00	7.60	95	Bakük	N	-
24	257628	17/5	9071	2826.00-2834.00	7.60	95	Bakük	Y	2827.75
25	257630	17/7	9071	2826.00-2834.00	7.60	95	Bakük	N	-
26	257637	18/1	9073	2862.00-2871.00	5.13	57	Bakük	N	-
27	257639	18/3	9073	2862.00-2871.00	5.13	57	Bakük	Y	2862.90
28	257641	18/5	9077	2862.00-2871.00	5.13	57	Bakük	N	-
29	-	19/1	9080	3290.00-3295.00	3.65	73	Uludere	Y	3290.00
30	-	19/2	9081	3290.00-3295.00	3.65	73	Uludere	N	-
31	-	19/3	9082	3290.00-3295.00	3.65	73	Uludere	Y	3291.00
32	-	19/4	9083	3290.00-3295.00	3.65	73	Uludere	N	-

1.4.2 Laboratory Work

The mineralogical and petrographical properties of the rock samples were studied by means of optical microscopy and X-ray powder diffraction techniques. Thin sections of the studied core samples were borrowed from TPAO by the permission of the General Directorate of Petroleum Affairs and General Management of TPAO.

1.4.2.1 Petrographic Analyses

All of the thin sections of the two wells, belonging to the Cudi Group, were examined and studied in details. These thin sections were studied in the laboratories of METU and TPAO. Their micrographs were taken at the Research Center Laboratories of TPAO. For examining the studied thin sections and having the images of the relevant parts which most resembles the whole rock, Zeiss Axio Imager-A2m model polarization microscope and AxioVision Release 4.7 computer software were used.

As mentioned above, from Dincer-1 Exploration Well, 22 thin sections belonging to the Cudi Group (Telhasan and Bakük formations) and Çiğlı Group (Uludere Formation), as well as 28 thin sections from South Dincer-1 Exploration Well, regarding Beloka Formation (unspecified group), Mardin Group (Karababa, Sabunsuyu and Areban formations), Cudi Group (Telhasan, Çamurlu and Bakük formations) and Çiğlı Group (Uludere Formation) were studied.

Data of these thin sections correlated with their core numbers, depth intervals and related formation names can be seen at Tables 2 and 3. The micrographs of some of these thin sections are provided in section 2.1.

1.4.2.2 X-Ray Powder Diffraction Analyses

Following the examination of the referred cores and thin sections, the most important ones in relation with this study were selected and X-ray powder diffraction analyses were implemented at TPAO's Research Center Laboratories.

The chosen core samples were powdered and sieved with a 0,062 mm mesh with ASTM number 230 for the whole rock analyses.

Rigaku D/Max-2200 Ultima⁺/PC generator is used for the XRD analyses with 40 kV, 20 mA and Cu tube along with a wave length of ($K\alpha_1$) 1.54 Angstrom (\AA) and 1-2 °/min scan speed.

For the evaluation of the X-ray diffractograms, Jade-7.0 software which is in control of a computer directly linked to diffractometer was used in addition to Inorganic Crystal Structure Database (ICSD) of International Center for Diffraction Data (ICDD). XRD analysis outputs were utilized by Jade-7.0 software's "profile-based matching" and Easy Quant software's "reference intensity ratios (RIR)". As a result, studied sample's whole rock minerals which are in the range of the device's detection limits (4% by volume) were determined as type and relative abundance.

After the interpretation of the X-ray powder diffraction analyses which are performed at TPAO's laboratories for the whole rock analyses, three samples were chosen for further XRD clay mineral analyses, related to the clay mineral percentages of their structures. These samples are D-AK-9 (Bakük Formation), GD-AK-5 (Çamurlu Formation) and GD-AK-7 (Çamurlu Formation) (detailed information at Tables 2 and 3). Following the selection of the samples, XRD analyses were carried out in the laboratories of METU's Geological Engineering Department in order to identify the clay minerals within the selected core samples.

For this study, the samples were grounded and digested for the needed powder form in order to complete the analyses. After being powdered, 10 gram of each sample was put inside a 1 liter beaker and 10% HCl acid was applied. Formed solution stirred continuously for two hours and then kept in a refrigerator, for a cool acid treatment, for one night. The reason for this acid treatment is to ease the separation of carbonate minerals from the clay minerals and so to further dissolve them including dolomite. Before the separation of clay fraction less than 2 µm by sedimentation and centrifugation according to Stokes' Law, applied acid is washed with distilled water.

Stokes's Law (1845), with the formula given below, is used to determine the rate of sedimentation;

$$V_g = g d^2 (\rho_s - \rho_f) / 18\mu$$

where;

V_g : Sedimentation Velocity	d : Particle Diameter (cm)
ρ_s : Particle Density	ρ_f : Fluid Density
g : Gravitational Acceleration (cm/s ²)	μ : Fluid Viscosity (cm ² /s)

This law is often simplified to;

$$V = CD^2 \text{ (cm/s)}$$

where; C is a constant equaling $(\rho_s - \rho_f) g / 18 \mu$ and D is the diameter of particles (spheres) in centimeters. For a range of common laboratory temperatures, C values have been calculated thus, sedimentation (settling) velocity (V) can be determined easily for a known particle diameter (D) (Boggs, 1995).

According to this law, a particle moving through viscous liquid gains a constant velocity or sedimentation rate. For particles whose density is close to that of the liquid, whose diameter is small or where the viscosity is high, the mentioned rate can be very slow. Faster sedimentation can be attained by replacing gravitational acceleration with the acceleration generated by a rotating centrifuge. Centrifugal acceleration can be thousands of times greater than that of gravity, so the centrifugal sedimentation rate is thousands of times greater.

Each 10 gram samples which were added a small quantity of sodium polyphosphate ($\text{Na}_5\text{P}_3\text{O}_{10}$) to form the suspension of clay,

were held 8 hours in order to aid dispersion. After the waiting period, top 10 cm of solution (mostly water) in the beaker was siphoned and removed. The remaining solution was put in a centrifuge with 6000 rpm for 10 minutes. Remaining water in the beaker was removed after this centrifugation process and the remaining clay paste at the bottom was smeared on special glass plates which are "AD (air dried)", "EG (ethylene-glycol)" and "heated (350-550°C)". The plates left to dry for one full day before the X-ray diffraction analysis.

For this study Rigaku MiniFlex II Desktop X-ray Diffractometer was used by operating with Cu tube.

CHAPTER 2

RESULTS OF THE STUDY

2.1 Results of the Petrographic Analyses

From Cudi Group formations, a total of 15 thin sections pertaining to Dinger-1 and 21 thin sections belonging to South Dinger-1 exploration wells were examined regarding their petrographic studies. Examining of these thin sections was carried out at TPAO's Research Center Laboratories.

Thin section photographs of Telhasan, Çamurlu and Bakük formations encountered in both wells (Dinger-1 and South Dinger-1) are prepared in order to describe these formations in an increasing depth.

Around the study area, Telhasan Formation consists of anhydrites in general. 257587 numbered thin section, from 2510.05 metered depth (XRD sample no: GD-AK-3) within this formation, is invaded with anhydrite and also contains stylolites from place to place (Figure 7). Stylolites are irregular discontinuities or non-structural fractures formed as a result of diagenesis and usually filled with hydrocarbons around investigated fields.

On the other hand, Çamurlu Formation of the Cudi Group is mainly composed of dolomicrite with anhydrite inclusions. Within the thin section number 257598 (XRD sample no: GD-AK-5) of South Dinger-1 Well, from 2522.65 metered interval, anhydrite takes place with dolomite as the dominant mineral (Figure 8).

Çamurlu Formation is also encountered in thin section number 257609 (XRD sample no: GD-AK-7), 257616 (XRD sample no: GD-AK-8) and 257618 (XRD sample no: GD-AK-9) from depths 2539, 2549.65 and 2550.15 meters respectively (Figures 9, 10 and 11). As in the other thin section depths representing this formation, the dominant mineral is dolomite followed with anhydrite. Trace amounts of stylolite (in thin section no: 257616) and fossil fragments (in thin section no: 257618) are also observed.

The Bakük Formation is mainly composed of pelloidal and laminated dolomicrite in the study area. South Dinger-1 Well's Bakük Formation is mainly composed of dolomite as the dominant mineral in addition to anhydrite in thin sections 257624 (XRD sample no: GD-AK-10) and 257639 (XRD sample no: GD-AK-12) (Figure 12 and 13) from 2826.25 and 2862.90 metered depths respectively. Stylolites are also detectable in thin section number 257624.

Dolomicrites in Bakük Formation belonging to Dinger-1 Well consists of calcite as well as dolomite in thin section number 43440 (XRD sample no: D-AK-8) and quartz in addition to dolomite in thin section number 43443 (XRD sample no: D-AK-9). Both thin sections contain trace amounts of anhydrite, algal structures and shell fragments as shown in Figure 14 and 15 respectively.

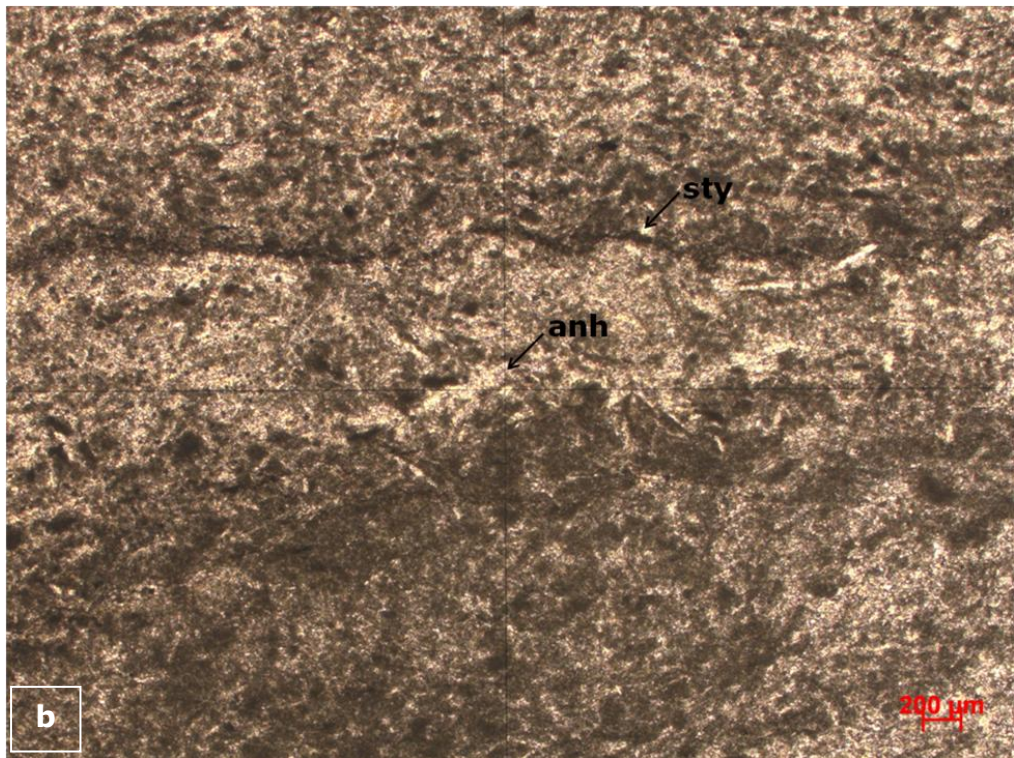
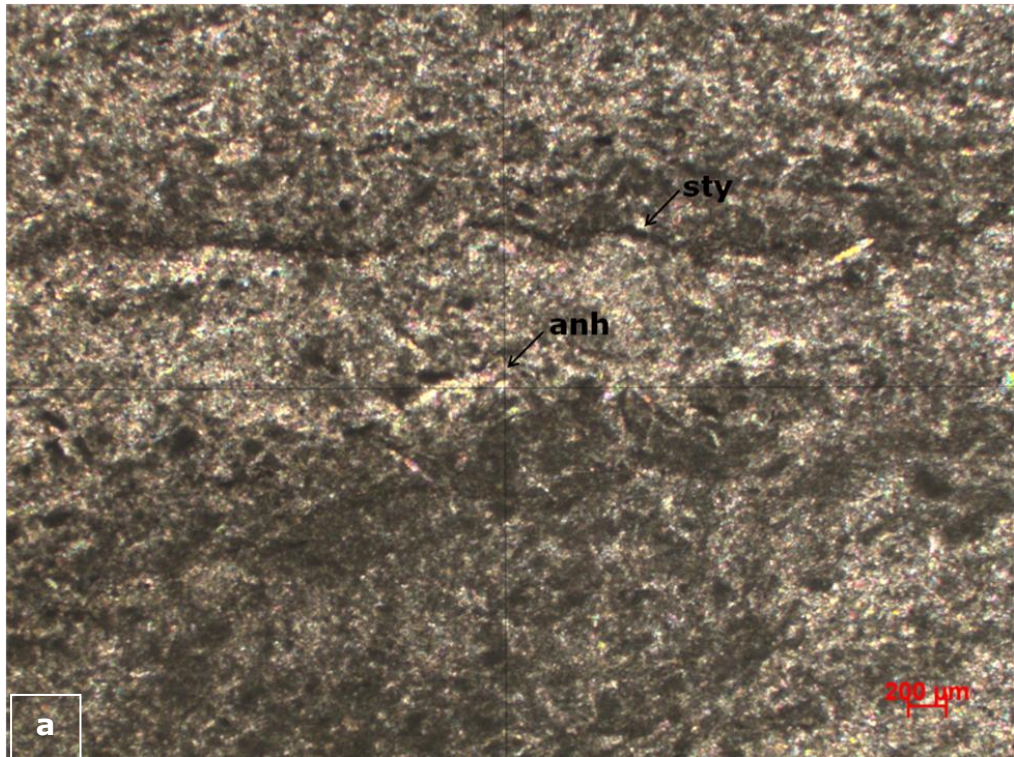


Figure 7. Photomicrograph of thin section no: 257587 belonging to South Dincer-1 Well's Telhasan Formation (anh: anhydrite and sty: stylolite), a) Cross nicols, b) Single nicol.

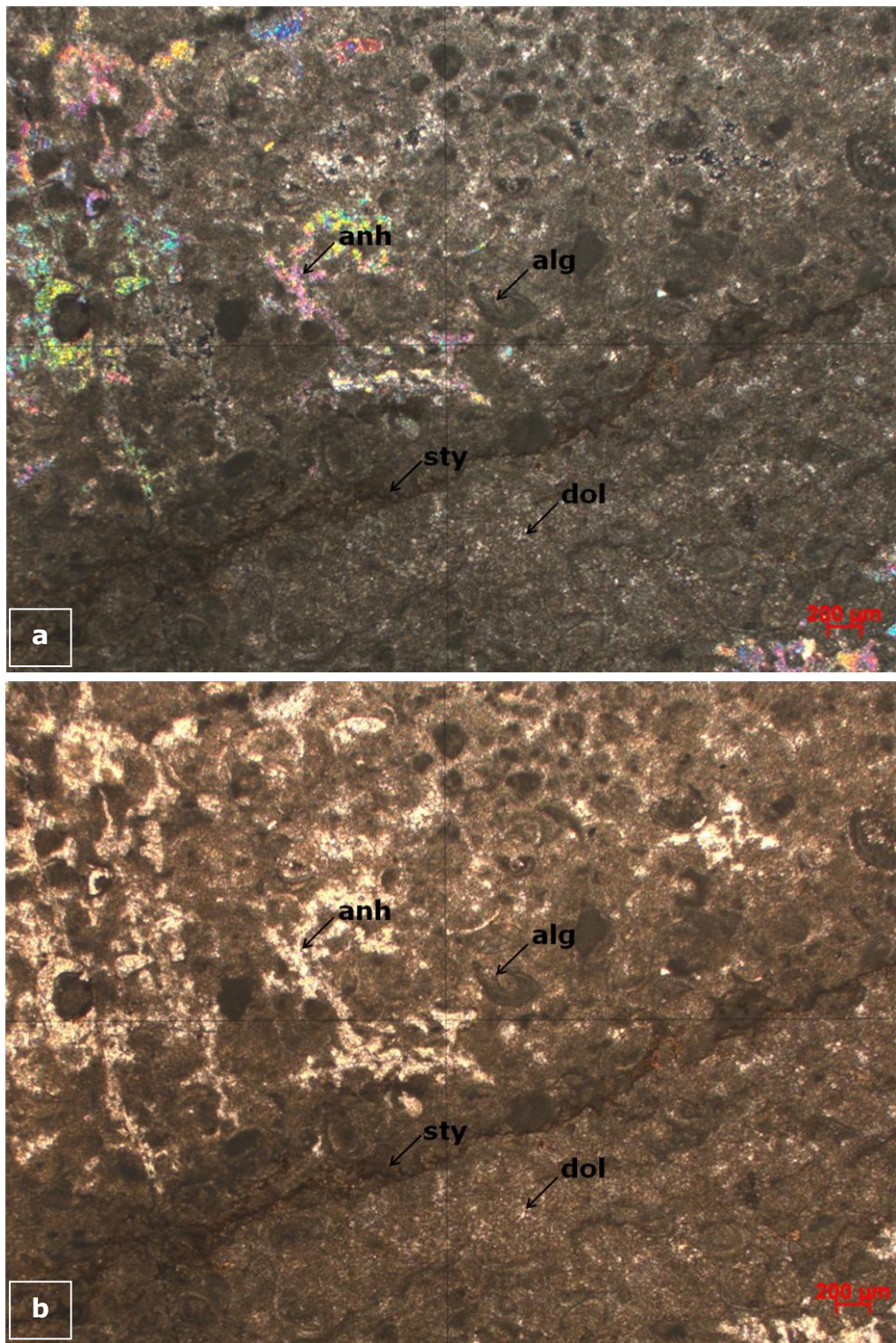


Figure 8. Photomicrograph of thin section no: 257598 belonging to South Dincer-1 Well's Çamurlu Formation (anh: anhydrite, dol: dolomite, sty: stylolite and alg: algal structures), a) Cross nicols, b) Single nicol.

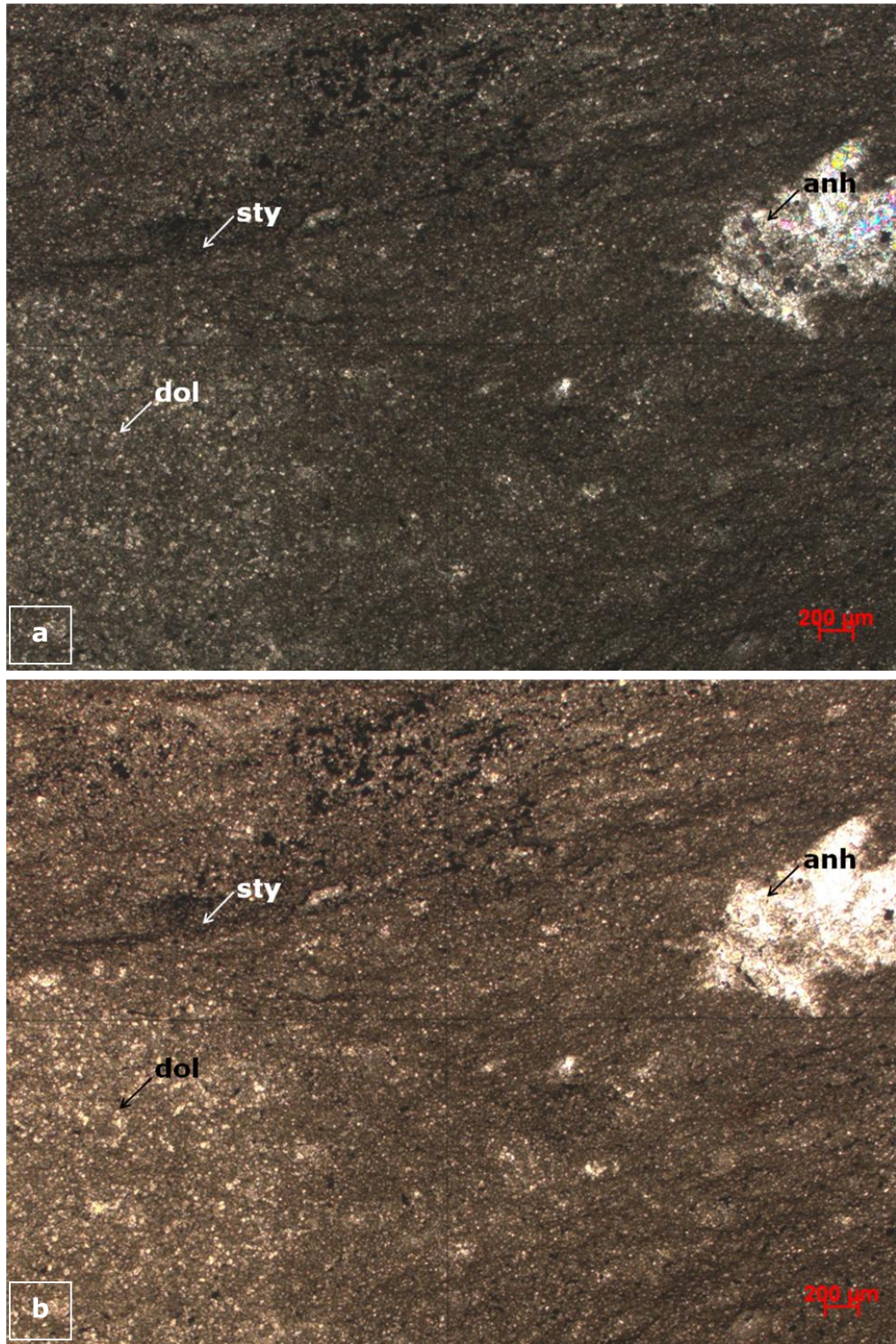


Figure 9. Photomicrograph of thin section no: 257609 belonging to South Dincer-1 Well's Çamurlu Formation (dol: dolomite, anh: anhydrite and sty: stylolite), a) Cross nicols, b) Single nicol.

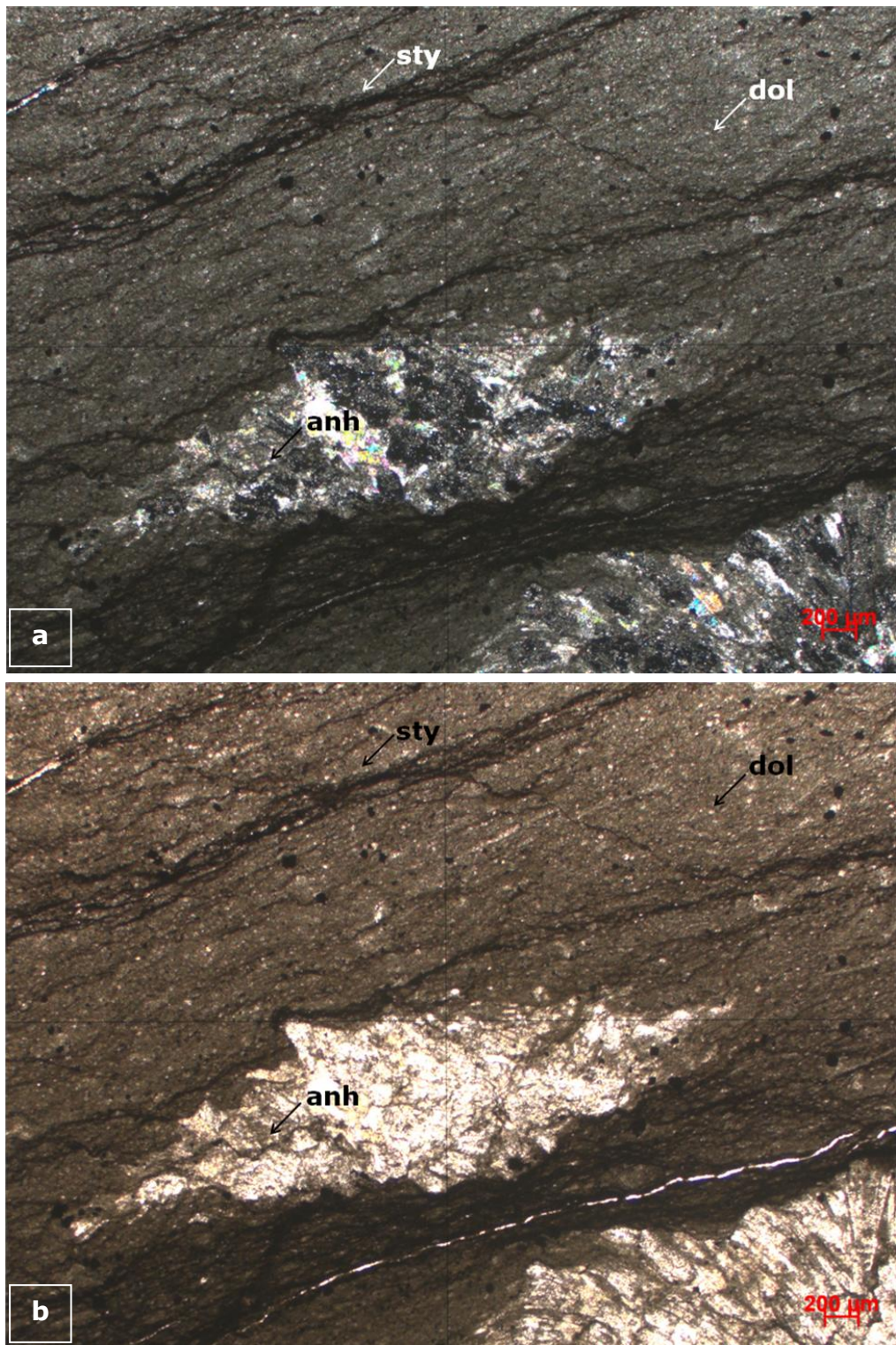


Figure 10. Photomicrograph of thin section no: 257616 belonging to South Dincer-1 Well's Çamurlu Formation (dol: dolomite, anh: anhydrite and sty: stylolite), a) Cross nicols, b) Single nicol.

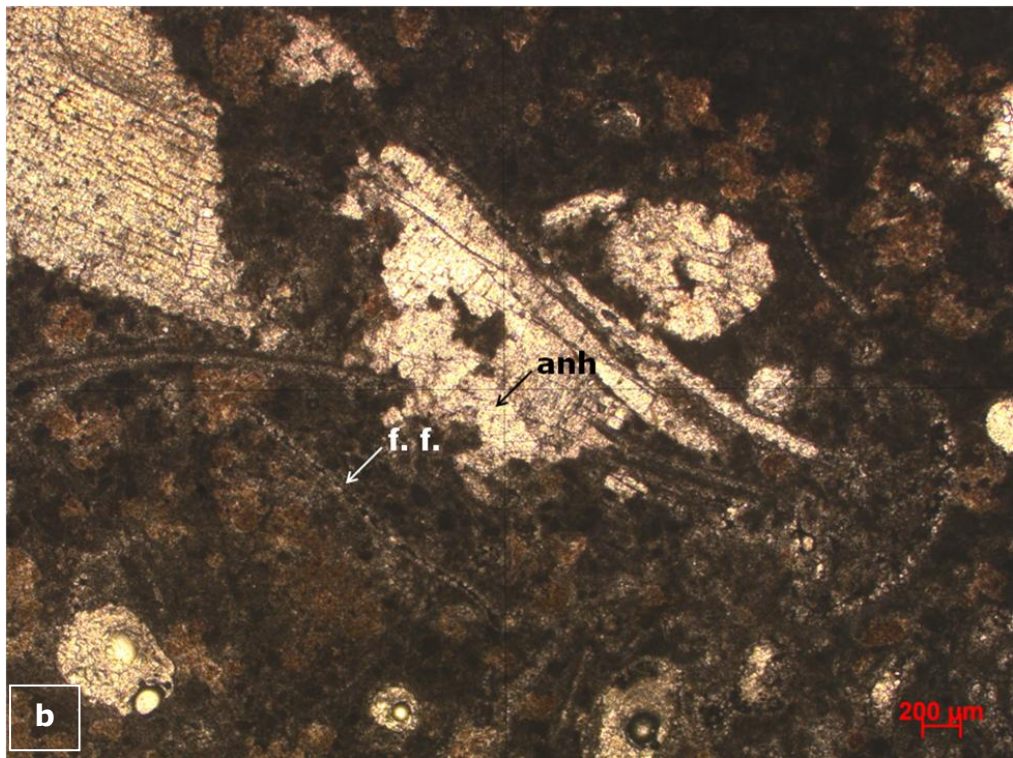
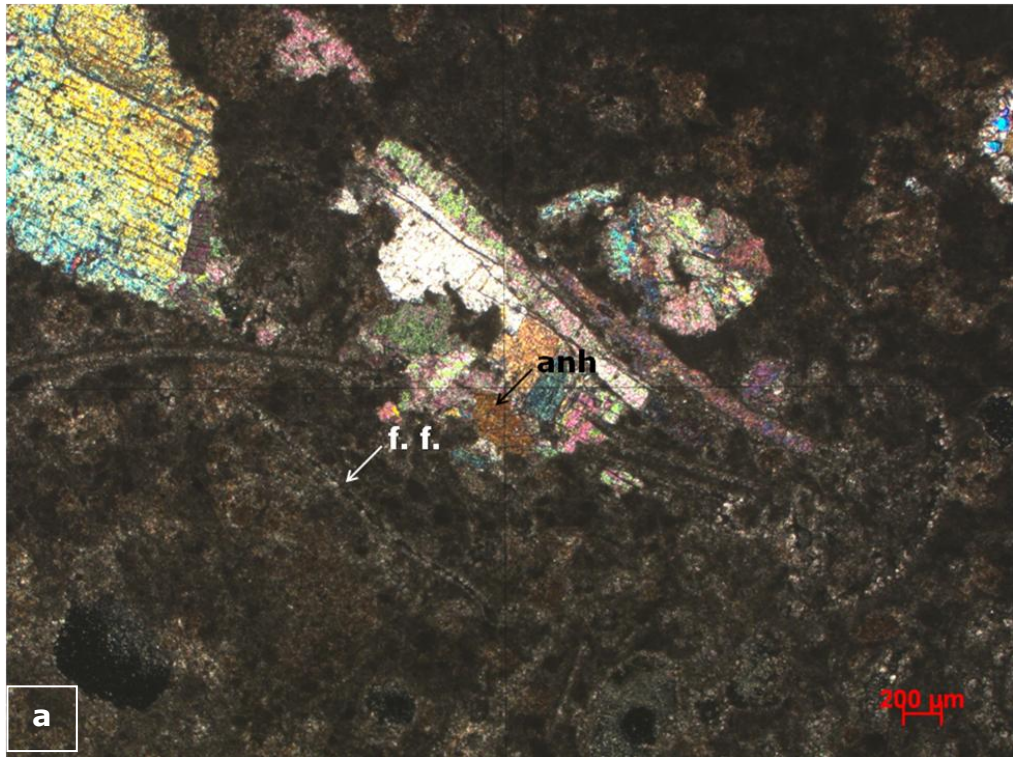


Figure 11. Photomicrograph of thin section no: 257618 belonging to South Dincer-1 Well's Çamurlu Formation (anh: anhydrite and f. f.: fossil fragment), a) Cross nicols, b) Single nicol.

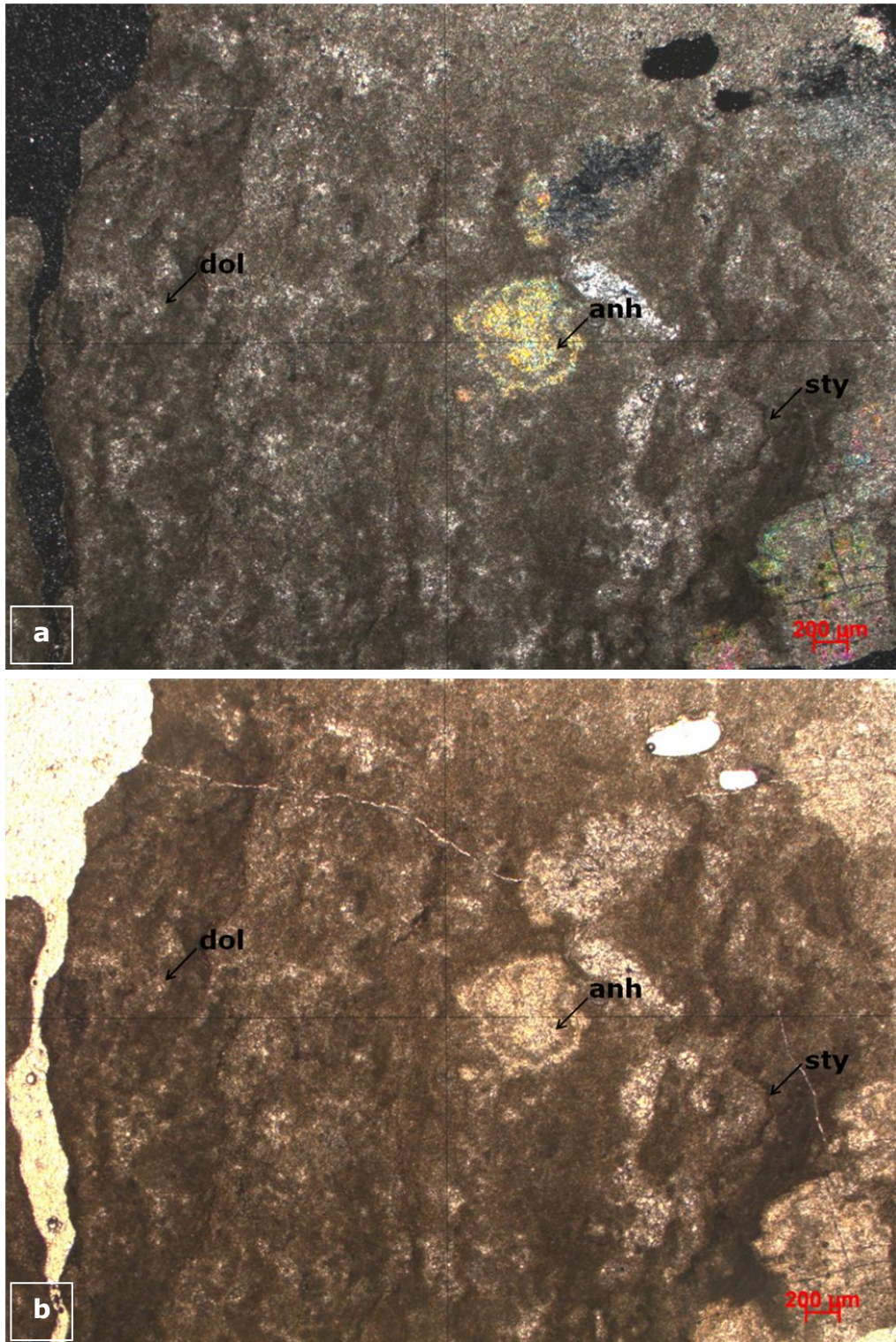


Figure 12. Photomicrograph of thin section no: 257624 belonging to South Dincer-1 Well's Bakük Formation (dol: dolomite, anh: anhydrite and sty: stylolite), a) Cross nicols, b) Single nicol.

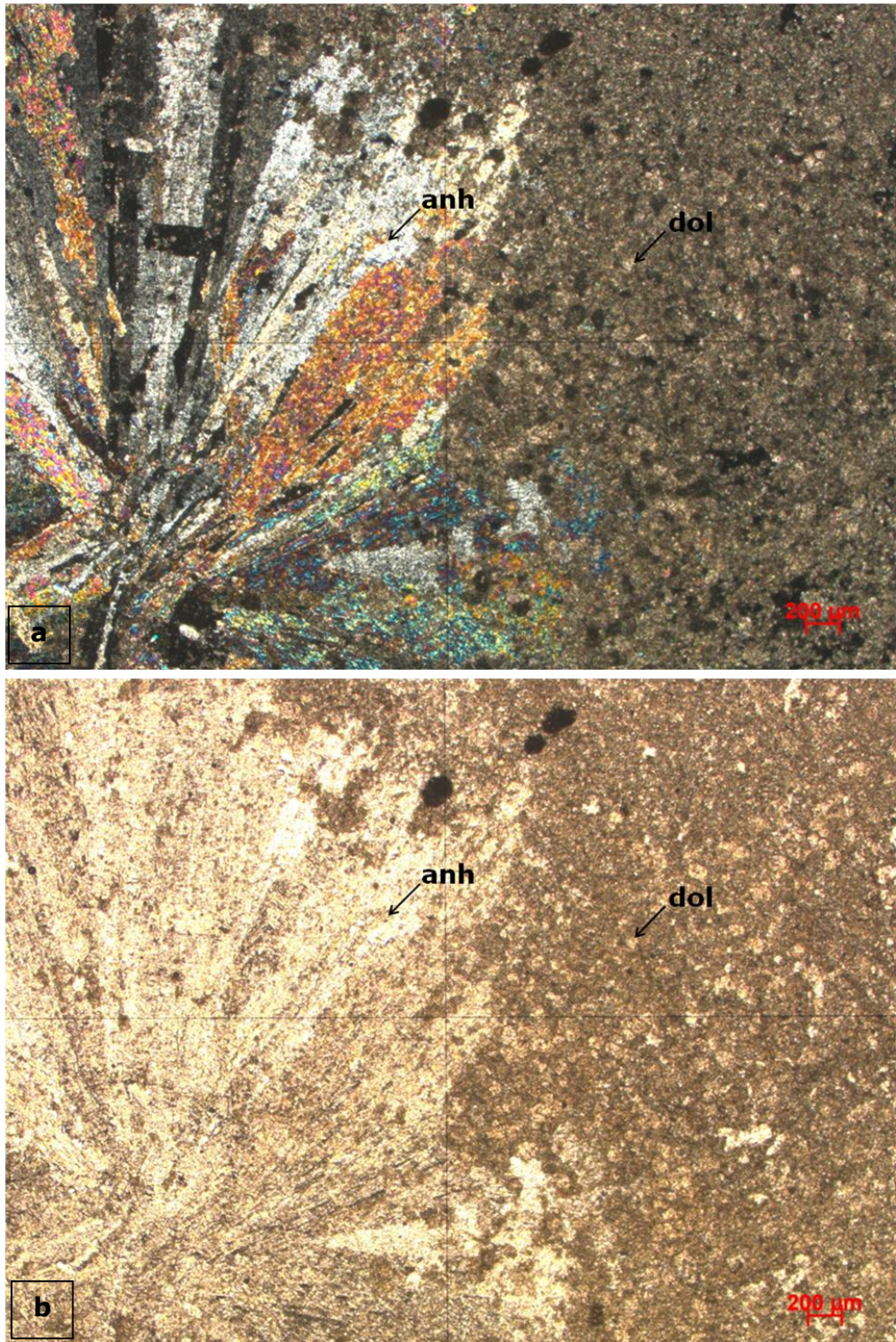


Figure 13. Photomicrograph of thin section no: 257639 belonging to South Dincer-1 Well's Bakük Formation (dol: dolomite and anh: anhydrite), a) Cross nicols, b) Single nicol.

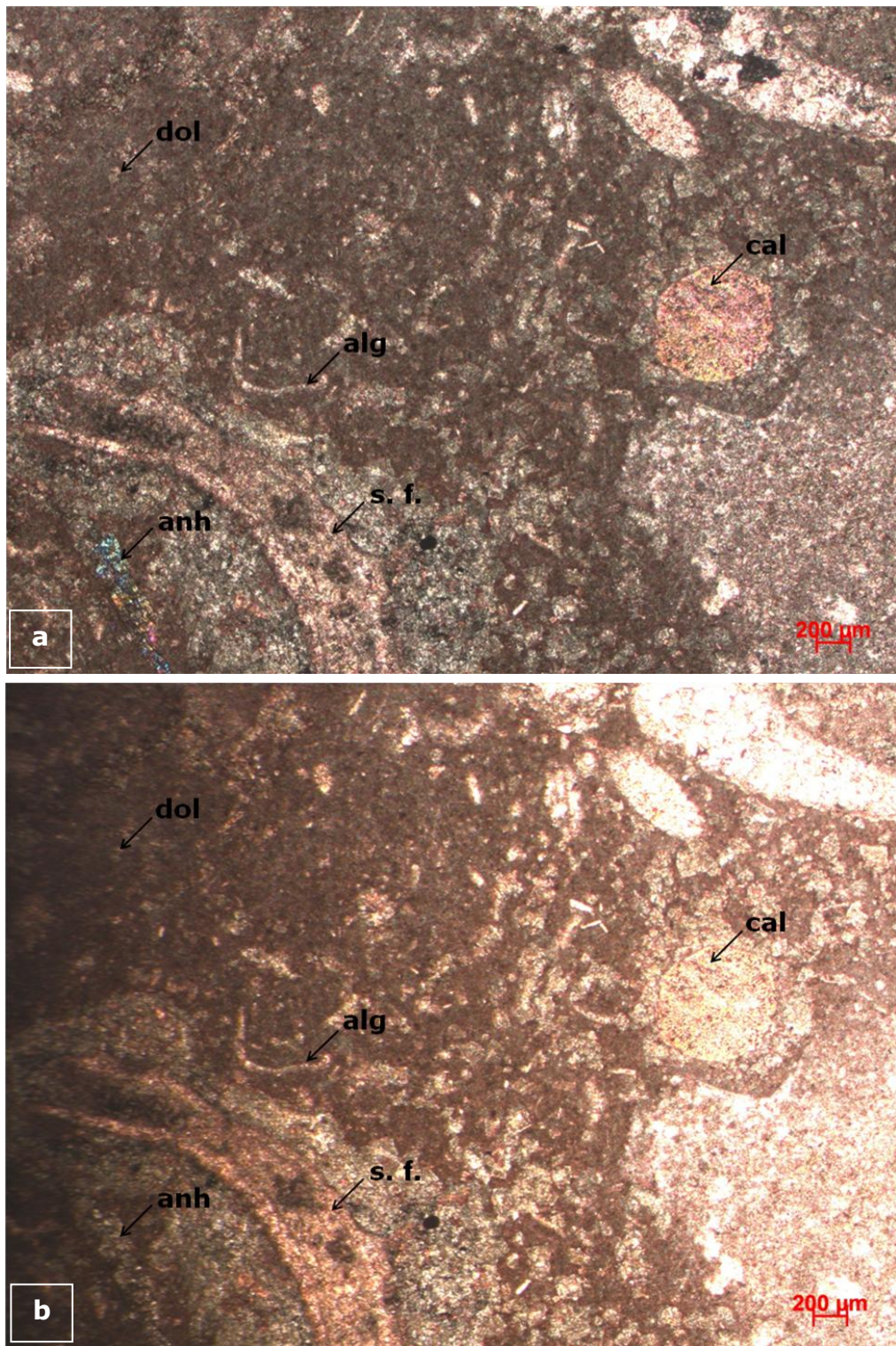


Figure 14. Photomicrograph of thin section no: 43440 belonging to Dinger-1 Well's Bakük Formation (cal: calcite, dol: dolomite, anh: anhydrite, alg: algal structures and s. f.:shell fragment), a) Cross nicols, b) Single nicol.

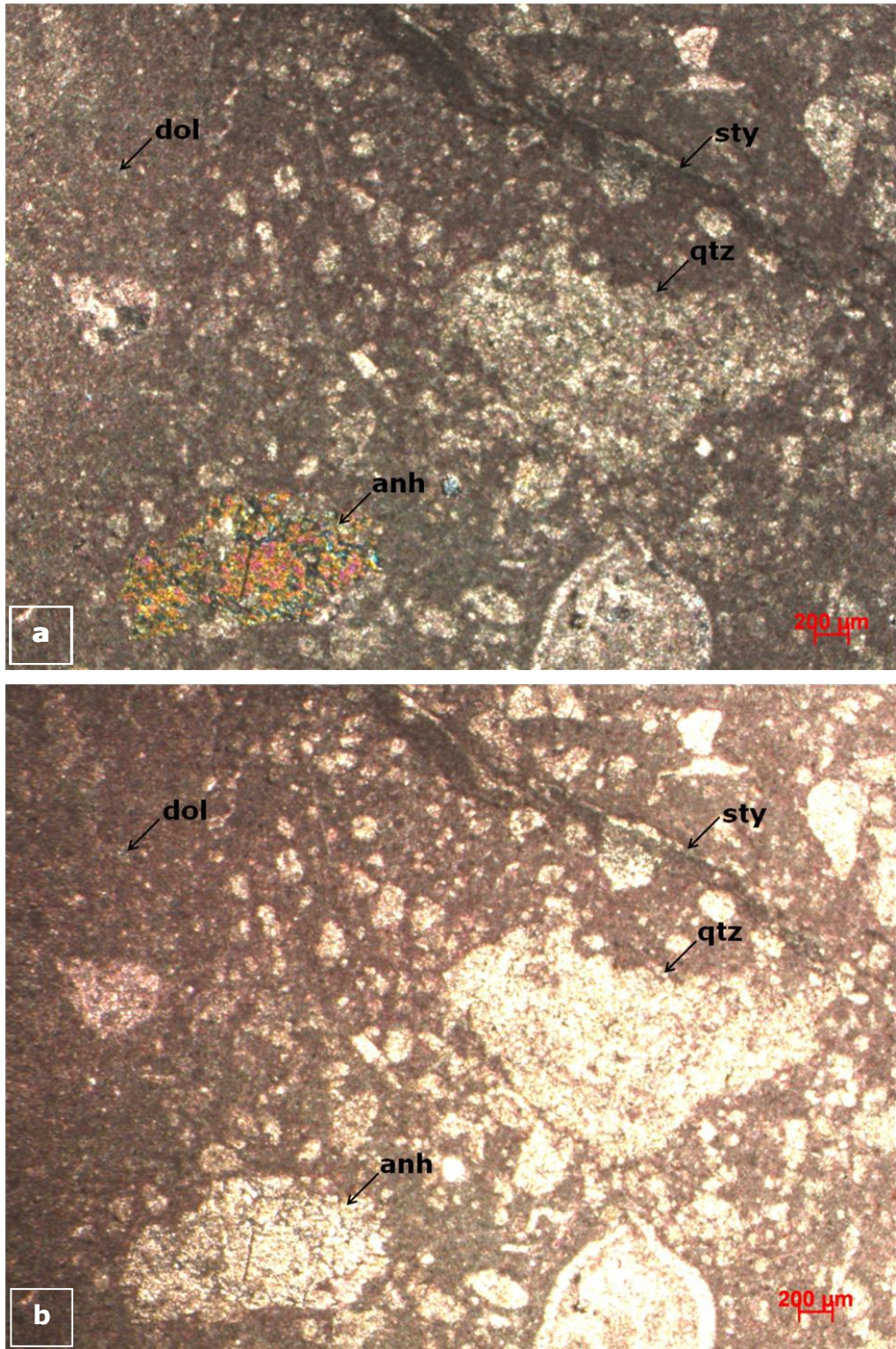


Figure 15. Photomicrograph of thin section no: 43443 belonging to Dincer-1 Well's Bakük Formation (qtz: quartz, dol: dolomite, anh: anhydrite and sty: stylolite), a) Cross nicols, b) Single nicol.

Calcite (CaCO_3) crystals within carbonate group have hexagonal system and they mainly show perfect rhombohedral cleavage. Crystal structures are usually crystalline, granular and rhombohedral. Their birefringence is extreme ($n_w-n_e=0.172$) (Kerr, 1977).

Dolomite ($\text{Ca}(\text{Mg,Fe})(\text{CO}_3)_2$) crystals within carbonate group, as described earlier in Section 3.1, have hexagonal system and they mainly show perfect rhombohedral cleavage. Crystal structures are usually tabular, often with curved faces, also columnar, granular and massive. Their birefringence is extreme ($n_w-n_e=0.180-0.190$) (Kerr, 1977).

Quartz (SiO_2) crystals within silica group have hexagonal system and they mainly show imperfect rhombohedral cleavage. Crystal structures are usually 6-sided prism ending in 6-sided pyramid (typical), drusy, fine-grained to microcrystalline and massive. Their birefringence is rather weak ($n_e-n_w=0.009$) (Kerr, 1977).

Anhydrite (CaSO_4) crystals within sulfates have orthorhombic system and they mainly show perfect cleavage resulting in pseudocubic fragments. Crystal structures are rare tabular and prismatic. They usually occur as fibrous, parallel veins that break off into cleavage fragments. They also occur as grainy, massive, or nodular masses. Their birefringence is strong ($n_\gamma-n_\alpha=0.044$) (Kerr, 1977).

Stylolites can also be found in some of the photomicrographs of Dincer-1 Well's Bakük formation.

The detailed explanation on algal structures can be found within Chapter 3.

2.2 Results of X-Ray Powder Diffraction Analyses

Following the interpretation of the thin sections of the selected cores, whole rock mineral analyses by XRD were accomplished at TPAO laboratories.

2.2.1 Qualitative Analyses of the Whole Rock Samples

For the XRD Analyses, a total of 10 samples from Dincer-1 and 14 samples from South Dincer-1 exploration wells were chosen belonging to Cudi and Çiğlı group formations. In this section, Cudi Group will be described according to its units, towards deeper depth intervals, including its bottom neighbor Uludere Formation of Çiğlı Group. The XRD samples of the two wells were not arranged separately as well wise, but arranged stratigraphically so that each formation in Cudi Group can be evaluated within itself.

Studied sequence's Telhasan Formation, the uppermost studied unit of the group, is observed between Dincer-1 Well's XRD

samples D-AK-1 and 6 in addition to South Dinger-1 Well's XRD samples GD-AK-1 and 6.

In the first XRD sample of Dinger-1 Well (XRD sample no: D-AK-1), from 2495.97 meters, dolomite is the dominant mineral (Figure 16) but towards 2.32 meters deeper (XRD sample no: D-AK-2), dolomite takes place along with another dominant mineral anhydrite (Figure 17).

3.71 meters deeper from the second sample of Dinger-1 Well, D-AK-3 numbered XRD sample exists and inside this sample, dolomite becomes the main mineral again with anhydrite as the minor mineral (Figure 18).

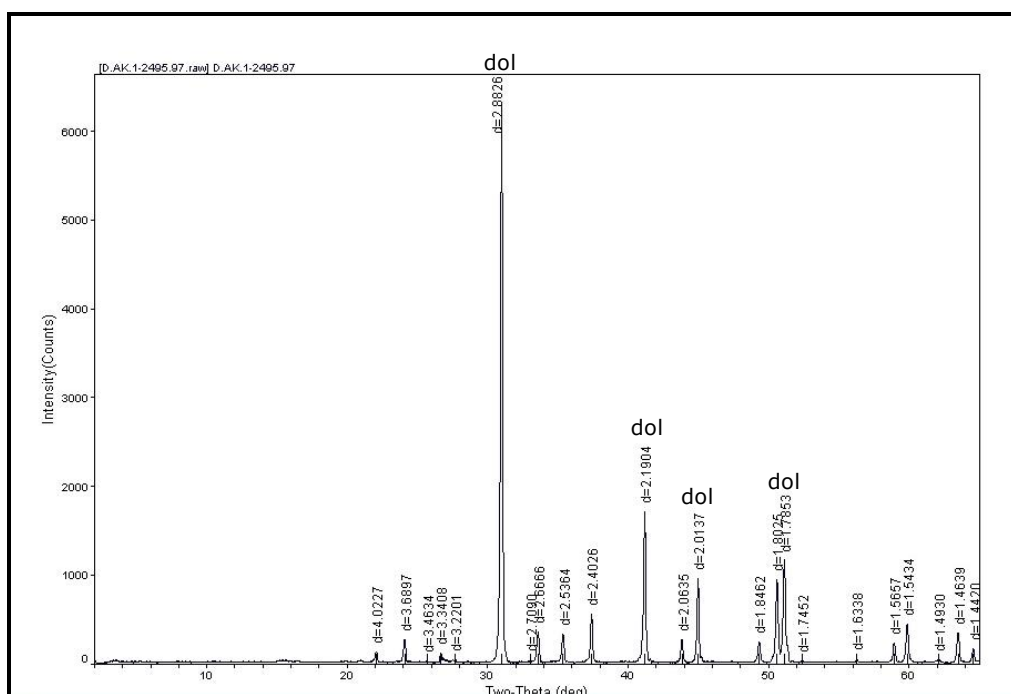


Figure 16. XRD diffractogram of bulk sample D-AK-1 belonging to Cudi Group's Telhasan Formation.

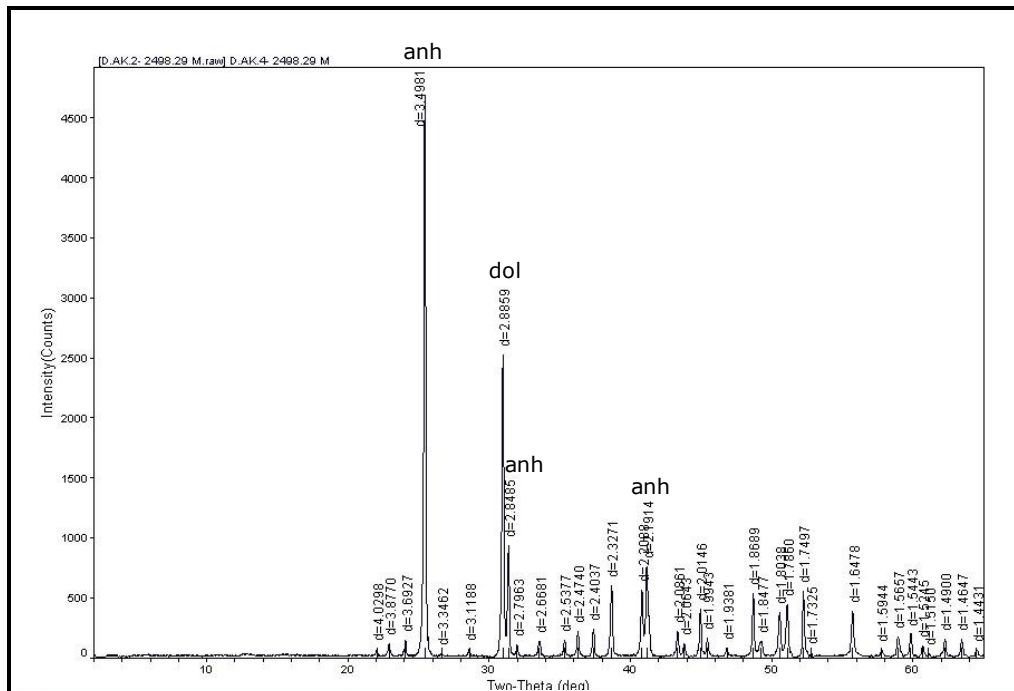


Figure 17. XRD diffractogram of bulk sample D-AK-2 belonging to Cudi Group's Telhasan Formation.

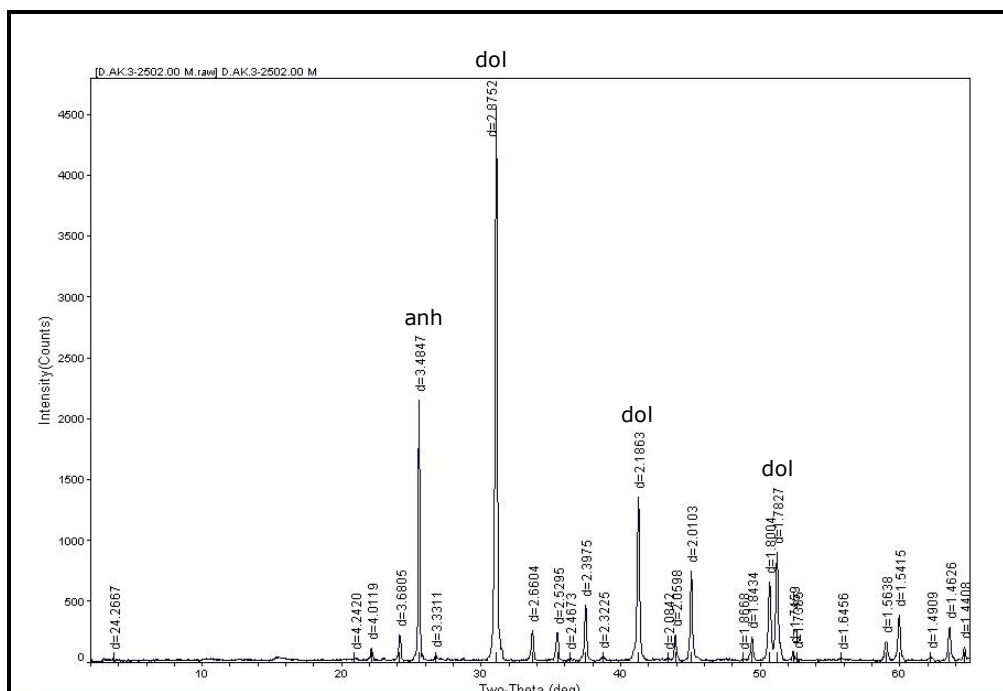


Figure 18. XRD diffractogram of bulk sample D-AK-3 belonging to Cudi Group's Telhasan Formation.

After a slight depth difference of 0.30 meters (XRD sample no: D-AK-4), again anhydrite is observed to be dominant with no other appreciable mineral (Figure 19).

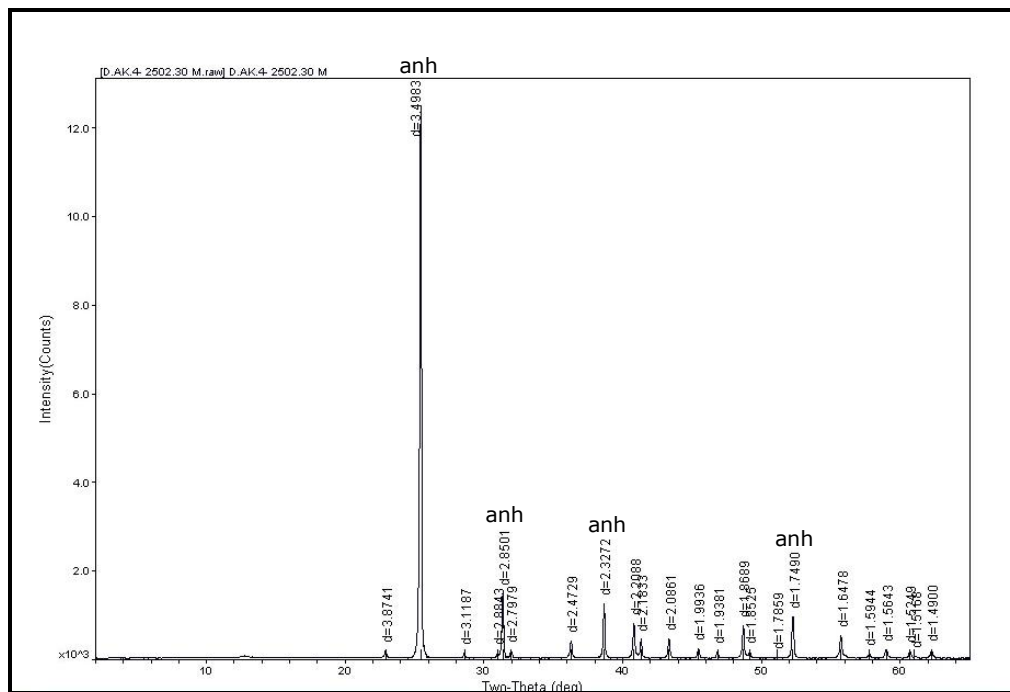


Figure 19. XRD diffractogram of bulk sample D-AK-4 belonging to Cudi Group’s Telhasan Formation.

Dinçer-1 Well’s following two samples (XRD samples no: D-AK-5 and D-AK-6) which are 3 and 3.5 meters deeper than the fourth sample, shows the same features (Figures 20 and 21).

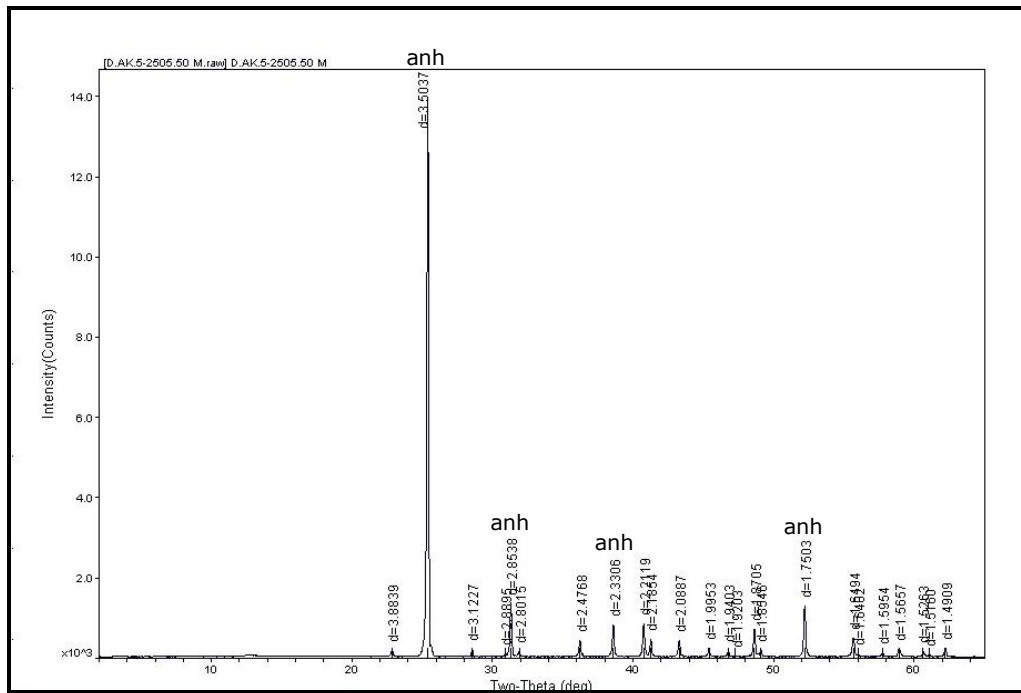


Figure 20. XRD diffractogram of bulk sample D-AK-5 belonging to Cudi Group's Telhasan Formation.

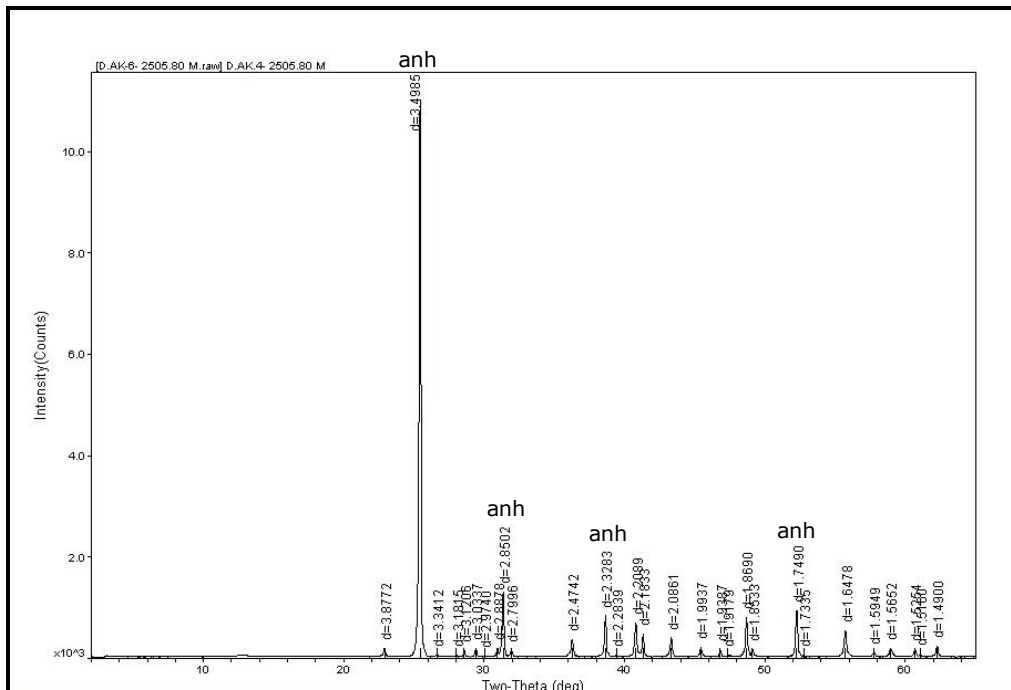


Figure 21. XRD diffractogram of bulk sample D-AK-6 belonging to Cudi Group's Telhasan Formation.

GD-AK-1 numbered XRD sample, the first sample of South Dinger-1 Well's Telhasan Formation representing 2430.80 meters, has anhydrite as the dominant mineral in similar with Dinger-1 Well's final samples belonging to Telhasan Formation (Figure 22).

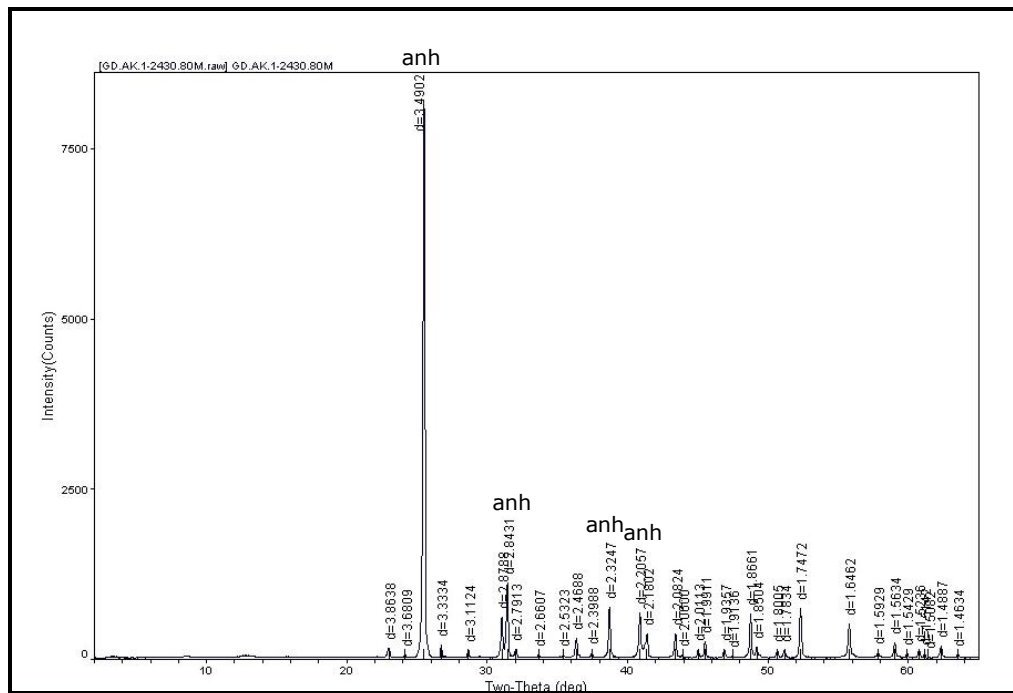


Figure 22. XRD diffractogram of bulk sample GD-AK-1 belonging to Cudi Group's Telhasan Formation.

Towards 76.65 and 79.25 meters deeper from the first sample of South Dinger-1 Well, at the following two samples (XRD samples no: GD-AK-2 and GD-AK-3) anhydrite mineral again is pointed out to be the major mineral (Figures 23 and 24).

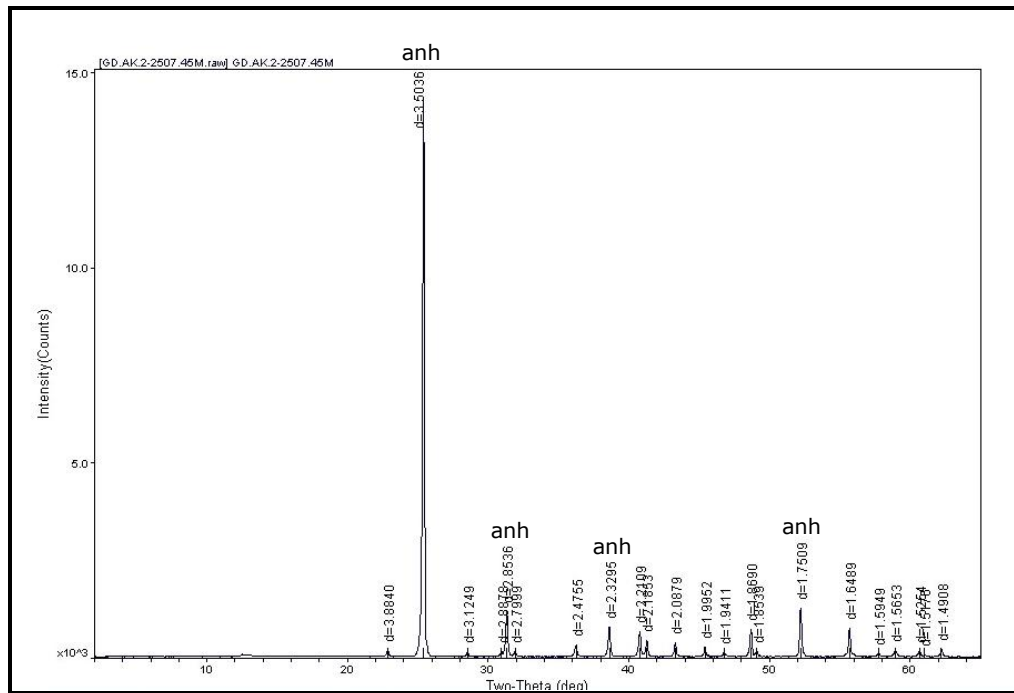


Figure 23. XRD diffractogram of bulk sample GD-AK-2 belonging to Cudi Group's Telhasan Formation.

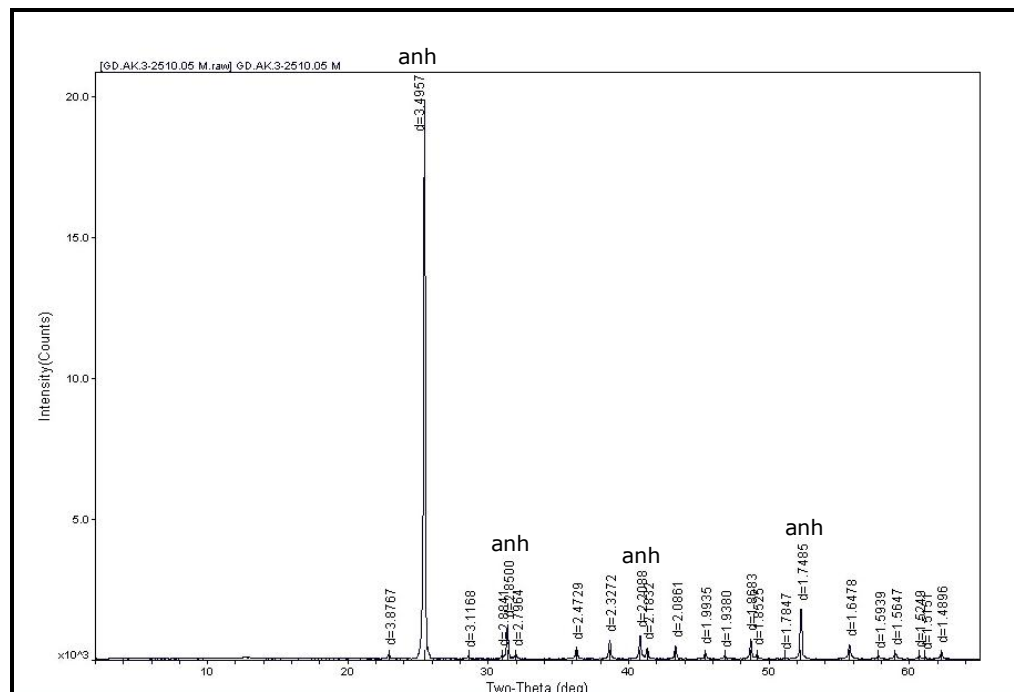


Figure 24. XRD diffractogram of bulk sample GD-AK-3 belonging to Cudi Group's Telhasan Formation.

After 89.5 meters lower from the first sample of South Dinger-1 Well, dolomite is included to the unit, leaving anhydrite to be the dominant mineral in GD-AK-4 numbered XRD sample (Figure 25). Dolomite replaces with anhydrite, in GD-AK-5 numbered XRD sample, 2.35 meters after the previous one (Figure 26). However, this situation becomes reversed after 2.45 meters deeper, in GD-AK-6 numbered XRD sample (Figure 27).

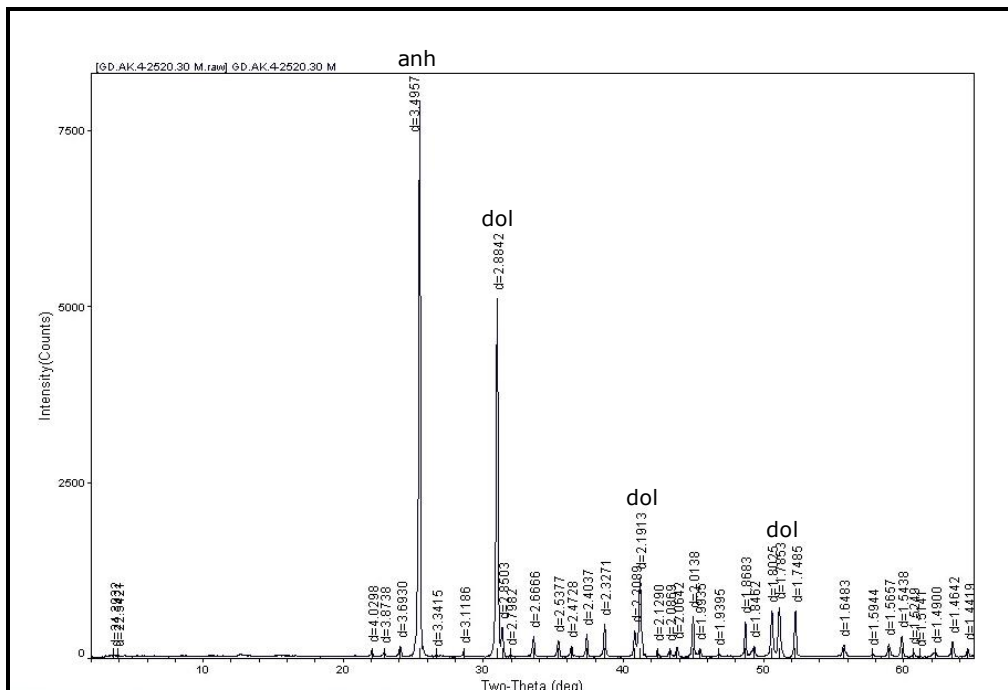


Figure 25. XRD diffractogram of bulk sample GD-AK-4 belonging to Cudi Group’s Telhasan Formation.

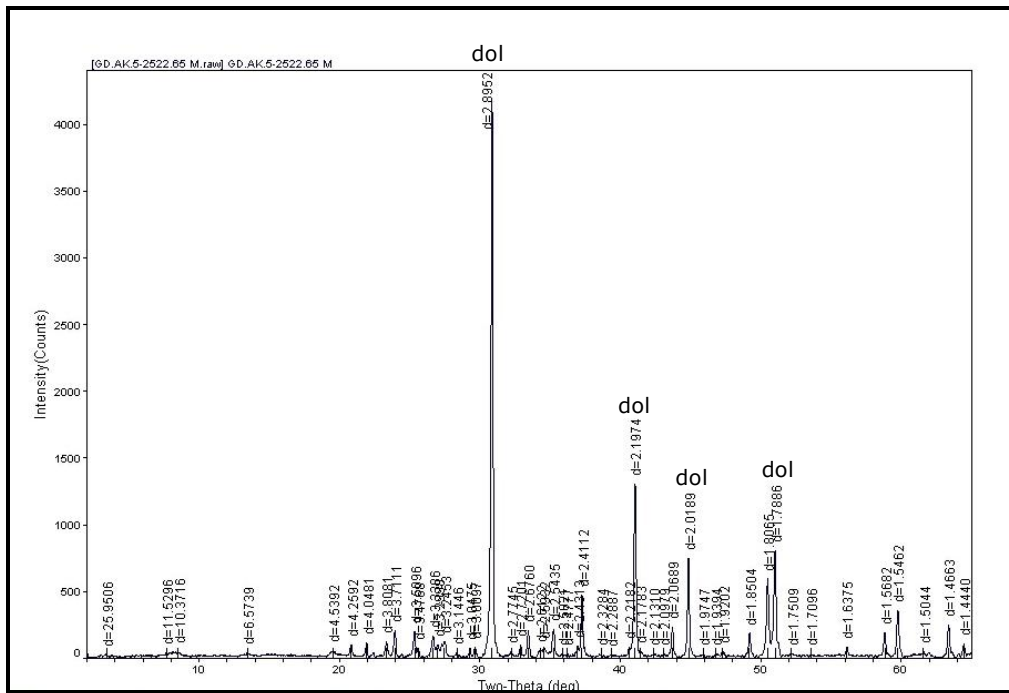


Figure 26. XRD diffractogram of bulk sample GD-AK-5 belonging to Cudi Group’s Telhasan Formation.

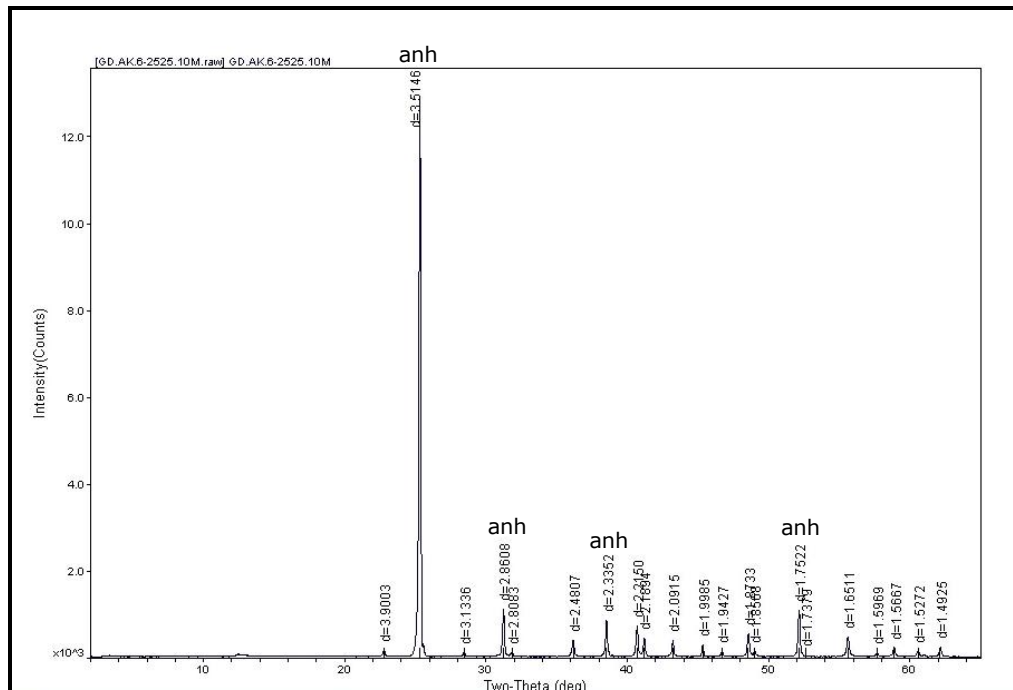


Figure 27. XRD diffractogram of bulk sample GD-AK-6 belonging to Cudi Group’s Telhasan Formation.

Çamurlu Formation, the bottom unit of Telhasan Formation, is examined only between South Dinger-1 Well's GD-AK-7 and 9 numbered XRD samples.

Within South Dinger-1 Well's seventh sample (XRD sample no: GD-AK-7) and after 13.9 meters from the previous sample, dolomite is observed to be the major mineral (Figure 28). Dolomite being the dominant mineral does not change after 10.65 and 11.15 metered thicknesses, in the following two samples (XRD samples no: GD-AK-8 and 9) (Figures 29 and 30).

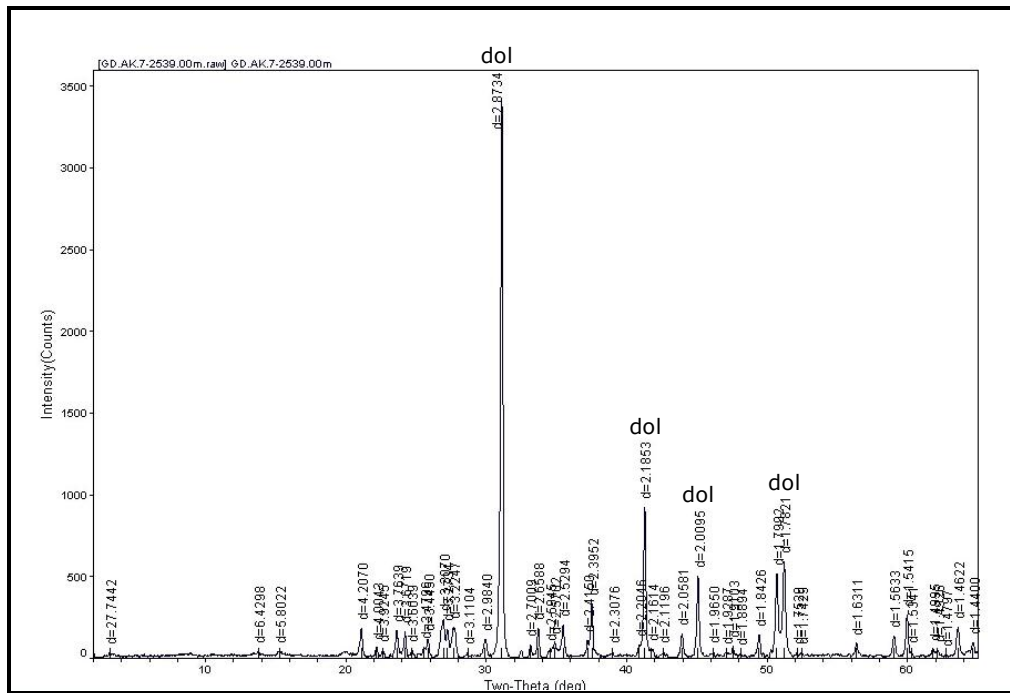


Figure 28. XRD diffractogram of bulk sample GD-AK-7 belonging to Cudi Group's Çamurlu Formation.

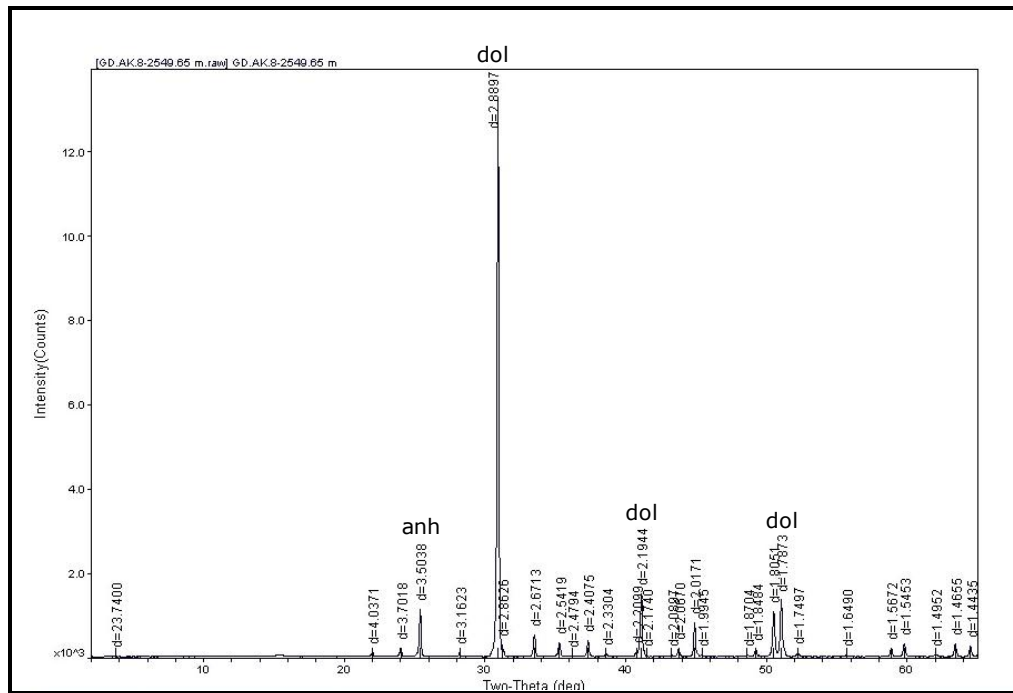


Figure 29. XRD diffractogram of bulk sample GD-AK-8 belonging to Cudi Group's Çamurlu Formation.

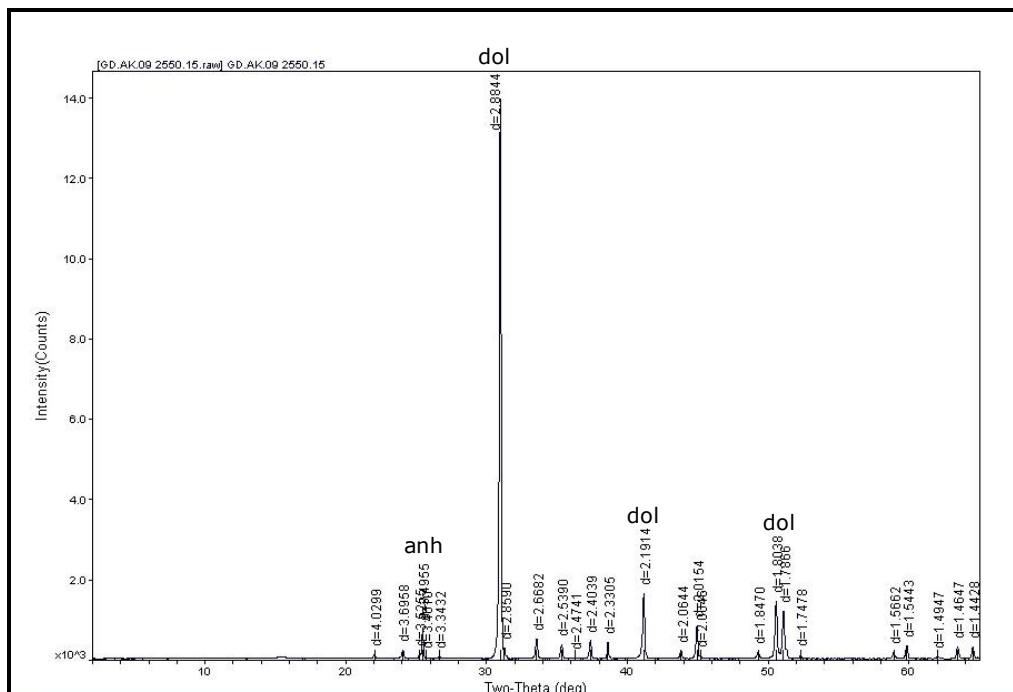


Figure 30. XRD diffractogram of bulk sample GD-AK-9 belonging to Cudi Group's Çamurlu Formation.

The lowermost unit of the examined group is the Bakük Formation. This unit is observed between Dincer-1 Well's D-AK-7 and 9 numbered XRD samples and between South Dincer-1 Well's GD-AK-10 and 12 numbered XRD samples.

Dincer-1 Well's D-AK-7 numbered XRD sample, representing 3171.95 metered depth, demonstrates a dominant new mineral, calcite. Dolomite takes place as the minor mineral (Figure 31). After one meter, the same minerals have the same characters in D-AK-8 numbered XRD sample (Figure 32). However, after 2.05 meters from the same sample (D-AK-7), quartz takes place as the dominant mineral and dolomite, as well as mica group mineral (probably illite?) is observed to be the trace mineral in D-AK-9 (Figure 33).

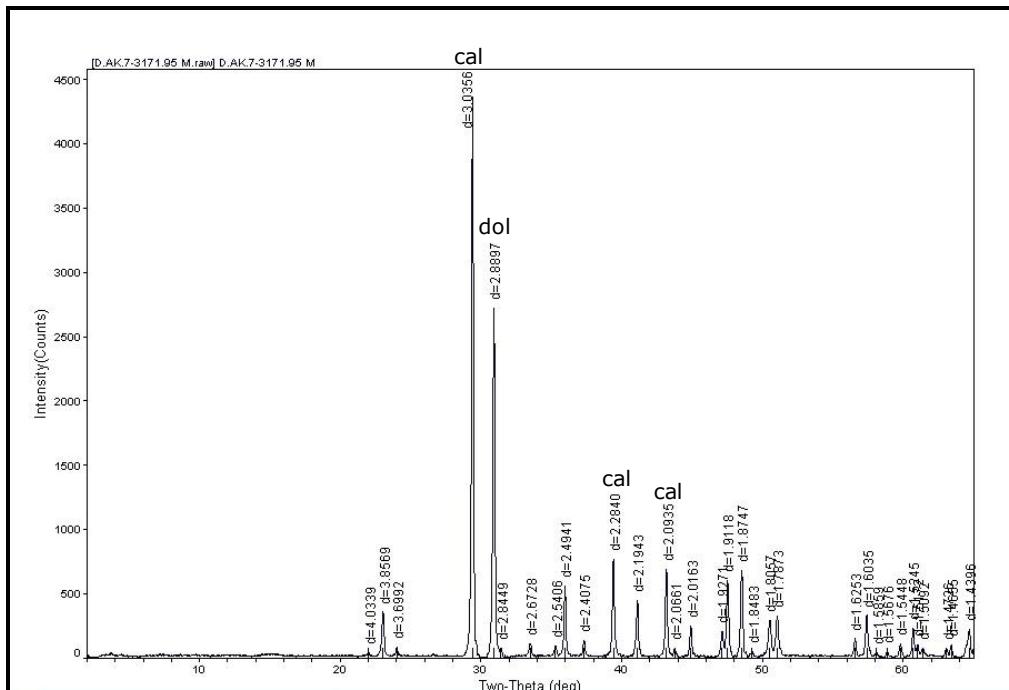


Figure 31. XRD diffractogram of bulk sample D-AK-7 belonging to Cudi Group's Bakük Formation.

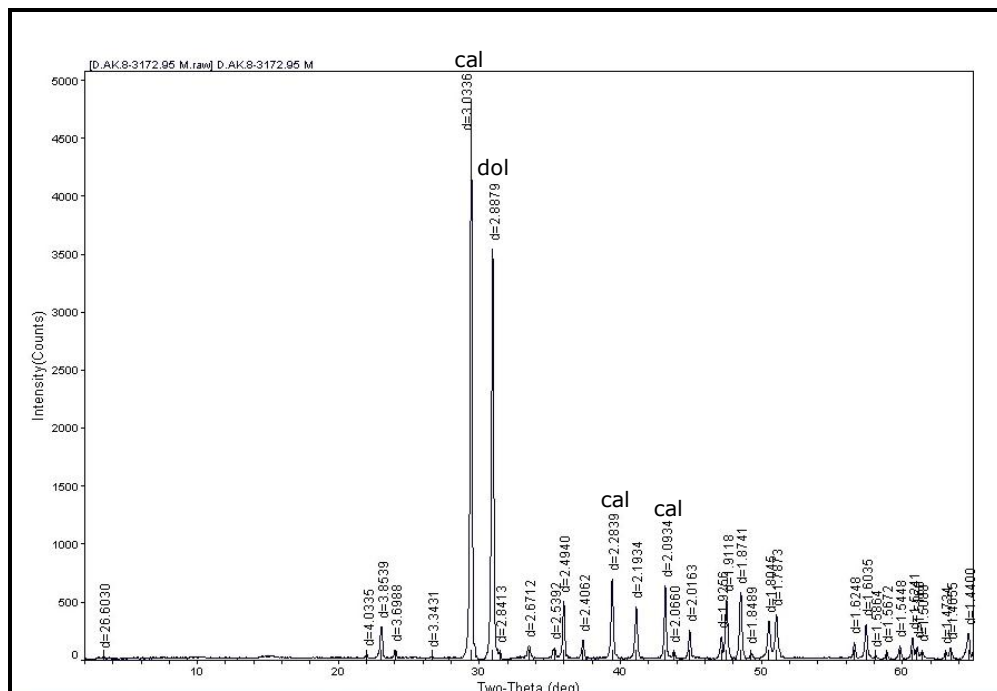


Figure 32. XRD diffractogram of bulk sample D-AK-8 belonging to Cudi Group's Bakük Formation.

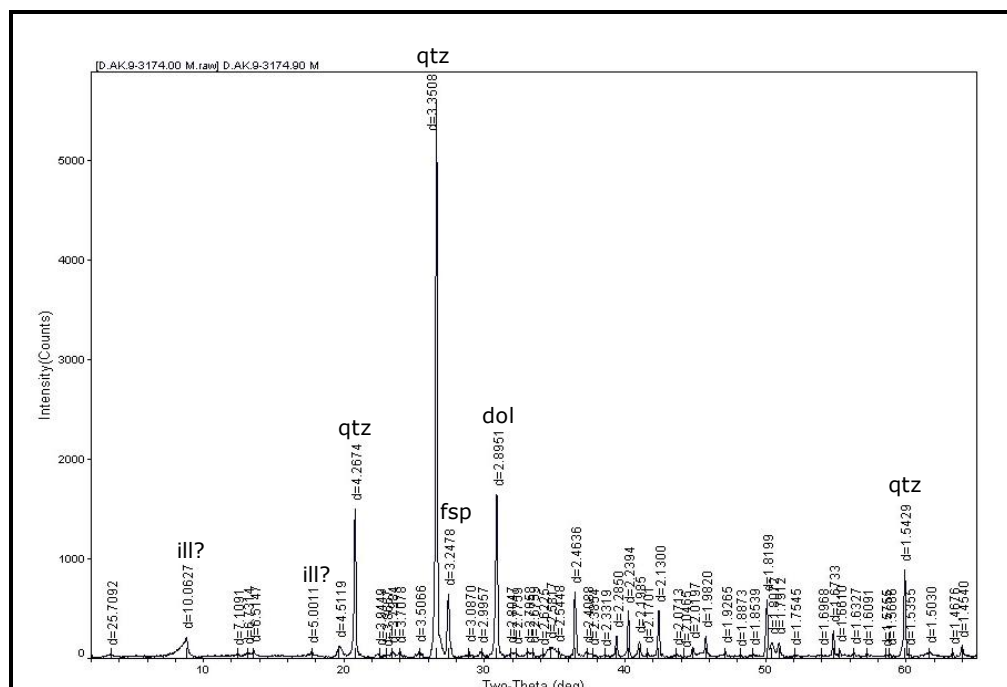


Figure 33. XRD diffractogram of bulk sample D-AK-9 belonging to Cudi Group's Bakük Formation.

The same formation examined in South Dinger-1 Well's GD-AK-10 numbered XRD sample, has dolomite as the major mineral and anhydrite as the minor mineral (Figure 34). This changes after 1.5 meters, in GD-AK-11 numbered XRD sample and anhydrite replaces dolomite to become the major whereas dolomite replaces with anhydrite to become the minor mineral (Figure 35). The same replacements are observed after a relatively thicker depth difference of 35.15 meters, in GD-AK-12 numbered XRD sample (Figure 36).

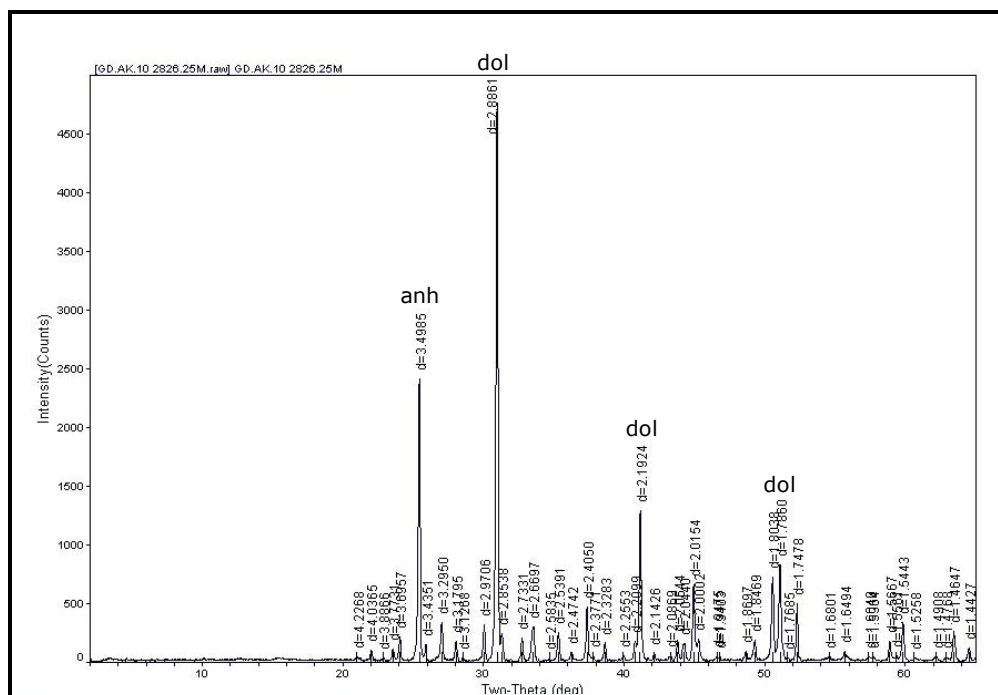


Figure 34. XRD diffractogram of bulk sample GD-AK-10 belonging to Cudi Group's Bakük Formation.

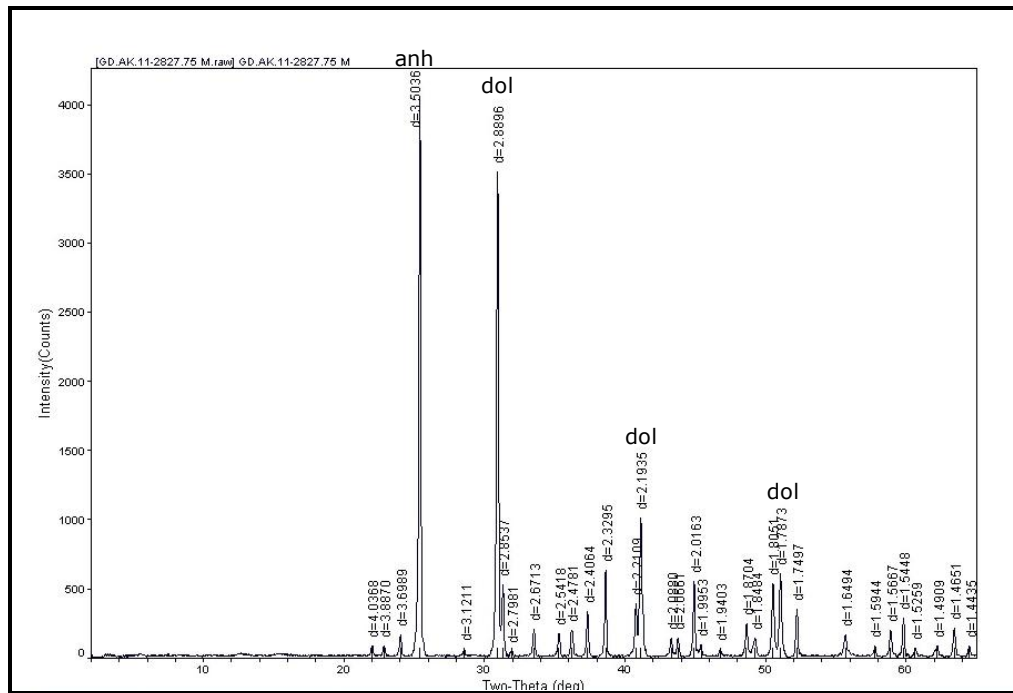


Figure 35. XRD diffractogram of bulk sample GD-AK-11 belonging to Cudi Group's Bakük Formation.

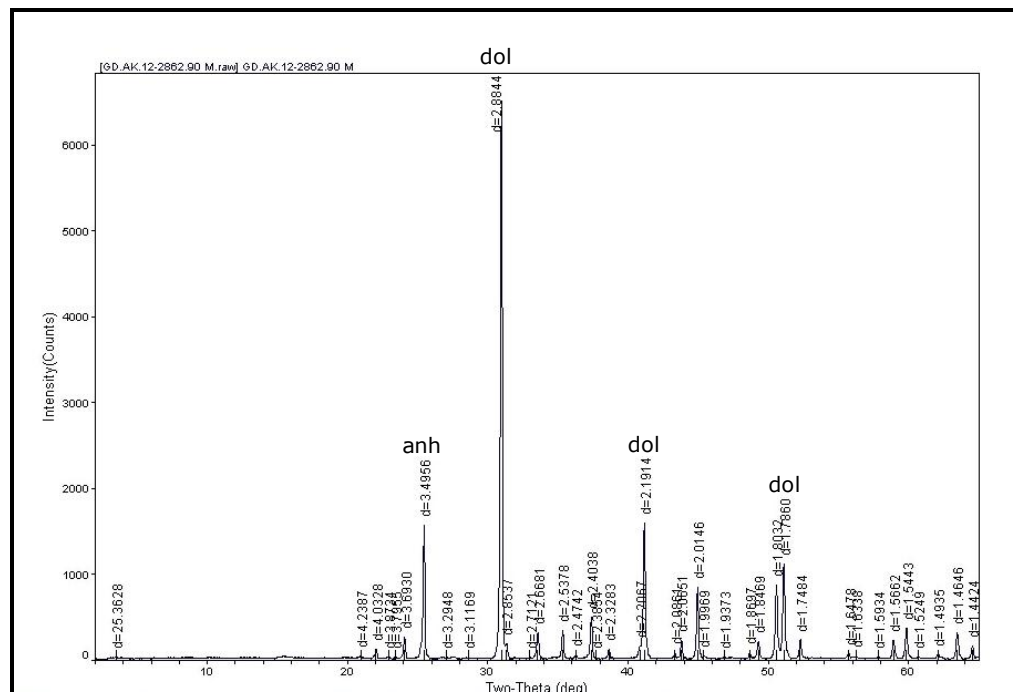


Figure 36. XRD diffractogram of bulk sample GD-AK-12 belonging to Cudi Group's Bakük Formation.

After going over the three important units of the Cudi Group by their XRD diffractograms, the Uludere Formation's XRD analyses for both wells were also done for further interpretations.

Following 129.15 meters from the last XRD sample of Dincer-1 Well (XRD sample no: D-AK-9), one sample (XRD sample no: D-AK-10) within the Uludere Formation of the well was examined where quartz was observed as the major mineral with dolomite as the minor and mica group mineral (probably illite?) as the trace mineral (Figure 37).

South Dincer-1 Well's Uludere Formation was inspected in XRD samples GD-AK-13 and GD-AK-14, at 427.00 and 428.10 meters deeper depths from the last studied XRD sample (GD-AK-12) respectively. The same mineralogical character described above for D-AK-10 numbered XRD sample was observed, quartz as major, dolomite and mica group mineral-illite? as minor minerals (Figures 38 and 39).

By surveying the last XRD sample of Dincer-1 and South Dincer-1 wells, the study regarding the X-ray powder diffraction analyses was completed. The summary of the X-ray powder diffraction analyses per well is given in Tables 4 and 5.

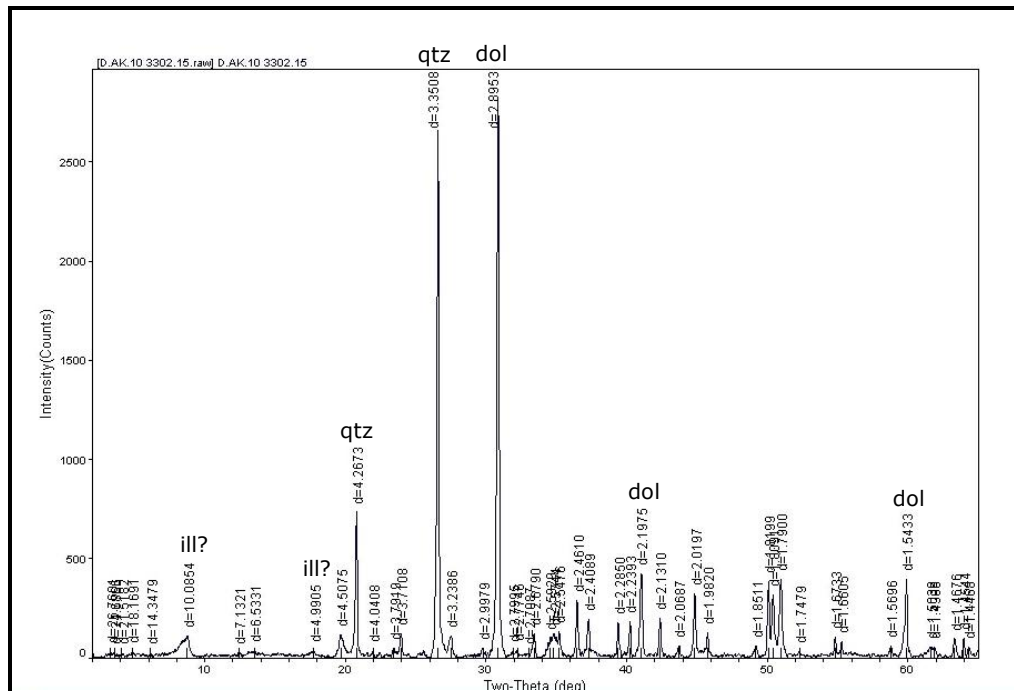


Figure 37. XRD diffractogram of bulk sample D-AK-10 belonging to Çiğlı Group's Uludere Formation.

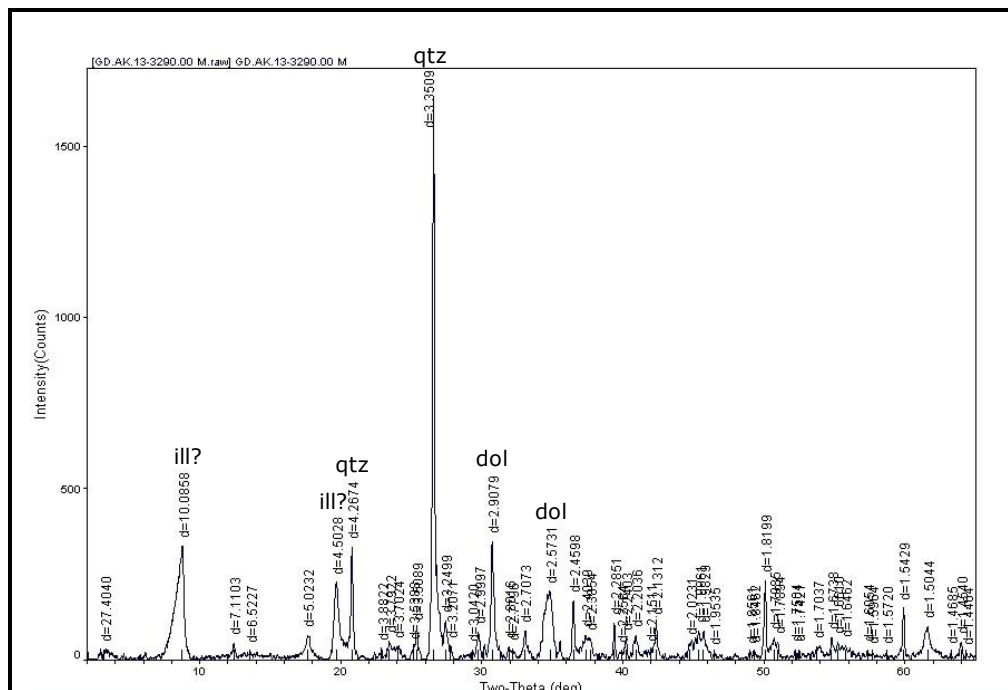


Figure 38. XRD diffractogram of bulk sample GD-AK-13 belonging to Çiğlı Group's Uludere Formation.

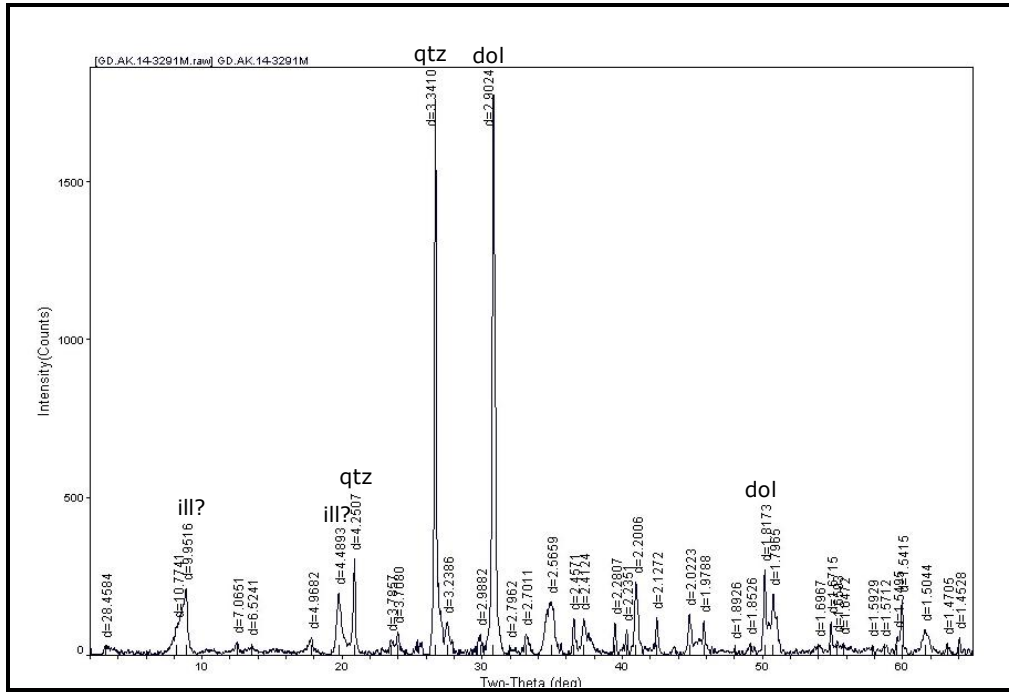


Figure 39. XRD diffractogram of bulk sample GD-AK-14 belonging to Çiğlı Group's Uludere Formation.

Table 4. Mineral facies for Dinger-1 Exploration Well.

Sample No	Thin Section No	Depth (m)	Group	Formation	Mineral Facies (in decreasing order)
D-AK-1	40940	2495.97	Cudi	Telhasan	Dol
D-AK-2	40943	2498.29	Cudi	Telhasan	Anh+Dol
D-AK-3	40945	2502.00	Cudi	Telhasan	Anh+Dol
D-AK-4	40946	2502.30	Cudi	Telhasan	Anh
D-AK-5	40947	2505.50	Cudi	Telhasan	Anh
D-AK-6	40948	2505.80	Cudi	Telhasan	Anh
D-AK-7	43439	3171.95	Cudi	Bakük	Cal+Dol
D-AK-8	43440	3172.95	Cudi	Bakük	Cal+Dol
D-AK-9	43443	3174.00	Cudi	Bakük	Qtz+Dol+Ill+Fsp
D-AK-10	43446	3302.15	Çiğli	Uludere	Qtz+Dol+Ill

Dol: Dolomite
 Anh: Anhydrite
 Cal: Calcite
 Qtz: Quartz
 Ill : Illite
 Fsp: Feldspar

Table 5. Mineral facies for South Dinger-1 Exploration Well (see Table 4 for explanations on abbreviations).

Sample ID	Thin Section No	Depth (m)	Group	Formation	Mineral Facies (in decreasing order)
GD-AK-1	257563	2430.80	Cudi	Telhasan	Anh
GD-AK-2	257582	2507.45	Cudi	Telhasan	Anh
GD-AK-3	257587	2510.05	Cudi	Telhasan	Anh
GD-AK-4	257596	2520.30	Cudi	Telhasan	Anh+Dol
GD-AK-5	257598	2522.65	Cudi	Telhasan	Dol
GD-AK-6	257602	2525.10	Cudi	Telhasan	Anh
GD-AK-7	257609	2539.00	Cudi	Çamurlu	Dol
GD-AK-8	257616	2549.65	Cudi	Çamurlu	Dol+Anh
GD-AK-9	257618	2550.15	Cudi	Çamurlu	Dol+Anh
GD-AK-10	257624	2826.25	Cudi	Bakük	Dol+Anh
GD-AK-11	257628	2827.75	Cudi	Bakük	Anh+Dol
GD-AK-12	257639	2862.90	Cudi	Bakük	Dol+Anh
GD-AK-13	-	3290.00	Çiğli	Uludere	Qtz+Dol+Ill?
GD-AK-14	-	3291.00	Çiğli	Uludere	Qtz+Dol+Ill?

2.2.2 Quantitative Analyses of the Whole Rock Samples

The whole rock analyses were carried out for all of the samples (sample numbers between D-AK-1 and 10, GD-AK-1 and 14) belonging to Dincer-1 and South Dincer-1 exploration wells. These interpretations were conducted at TPAO's Research Center laboratories.

The entire numerical information about the whole rock mineral composition of Dincer-1 Exploration Well is given Table 6, as percentages (volume %).

The XRD analyses regarding the whole rock mineral composition indicates that Dincer-1 Exploration Well's first XRD sample (XRD sample no: D-AK-1), belonging to Telhasan Formation, is composed of dolomite with trace amounts of quartz. So, this sample can be noted a dolostone. The second sample (XRD sample no: D-AK-2) is mainly composed of anhydrite (68%) with a secondary mineral dolomite (32%) and trace amounts of quartz. At the third sample (XRD sample no: D-AK-3), the amount of anhydrite mineral again decreases and becomes 35%. Here, dolomite is the dominant mineral with a 65%. Quartz, similarly takes place as the trace mineral. The fourth sample (XRD sample no: D-AK-4) is completely composed of anhydrite mineral with trace amounts of dolomite.

Table 6. Whole rock mineral composition after XRD analyses for Dincer-1 Exploration Well.

Sample ID	Sample Depth (m)	Whole Rock Mineral Composition (volume %)						
		Feldspar Group		Anhydrite	Quartz	Calcite	Dolomite	Clay+Mica
		Plagioclase	K-Feldspar					
D-AK-1	2495.97	-	-	-	trace	-	100	-
D-AK-2	2498.29	-	-	68	trace	-	32	-
D-AK-3	2502.00	-	-	35	trace	-	65	-
D-AK-4	2502.30	-	-	100	-	-	trace	-
D-AK-5	2505.50	-	-	100	-	-	trace	-
D-AK-6	2505.80	-	-	100	-	trace	trace	-
D-AK-7	3171.95	-	-	-	-	58	42	-
D-AK-8	3172.95	-	-	-	trace	54	46	-
D-AK-9	3174.00	-	18	-	35	-	29	18
D-AK-10	3302.15	-	3	-	18	-	54	25

The following two samples (XRD sample no: D-AK-5 and 6) have the same mineral composition with the D-AK-4 except the D-AK-6 also contains some trace amounts of calcite. These XRD samples were the last samples representing the Telhasan Formation of Dincer-1 Well. With this sample, calcite mineral appears within the well and further on, starts to be one of the major minerals in Bakük Formation.

In the first XRD sample of the Bakük Formation (XRD sample no: D-AK-7), 58% of calcite mineral is observed along with 42% of

dolomite. This proportion does not very much change in the next sample (XRD sample no: D-AK-8); only 4% of calcite mineral replaces with dolomite mineral in addition to trace amounts of quartz mineral.

However, the whole relative mineral character seen in Bakük Formation changes at the last XRD sample of the same formation (XRD sample no: D-AK-9). In this sample, 18% of K-feldspar is observed for the first time. Additionally, calcite takes place as the dominant mineral with 35% of amount. Dolomite mineral and clay mineral+mica are indicated as 29% and 18% respectively.

With the ninth sample, the examination of the Cudi Group formations regarding Dincer-1 Well's whole rock analyses was completed. At the very last XRD sample of Dincer-1 Well (XRD sample no: D-AK-10), belonging to Çiğlı Group's Uludere Formation, K-feldspar amount decreases to a total of 3% and quartz mineral to 18%. In contrast, the dolomite and clay mineral+mica amount increases to 54% and 25% respectively.

Mica group is a sub group of silicates which usually have pseudo-hexagonal system and they show highly perfect basal cleavage. Their sheet like structure is the most prominent characteristic of mica group. The group mainly consists of muscovite, illite (hydromuscovite), lepidolite, phlogopite and biotite. Group's birefringence ranges from moderate to strong ($n_{\gamma}-n_{\alpha}=0.0047-0.059$) (Kerr, 1977).

Illite minerals, $(K,H_3O)(Al,Mg,Fe)_2(Si,Al)_4O_{10}[(OH)_2,(H_2O)]$, within silicates, are clay-sized micaceous minerals. These crystals are phyllosilicates or layered alumino-silicates. They are non-expandable and their structure is formed by the repetition of tetrahedron–octahedron–tetrahedron (TOT) layers. They mainly show perfect cleavage. Crystal structures are monoclinic and prismatic. Poorly hydrated potassium cations which cause the swelling absence, covers the interlayer space of illite crystals (Kerr, 1977).

The details of the whole rock mineral composition of South Dincer-1 Exploration Well can be seen at Table 7, in terms of volume %.

The first XRD sample of South Dincer-1 Exploration Well's Telhasan Formation (XRD sample no: GD-AK-1), subjected to XRD whole rock mineralogical analyses, shows anhydrite mineral as the main (97%) and dolomite mineral as the minor mineral (3%). It also contains trace amounts of quartz mineral. In the second and the third XRD sample (XRD samples no: GD-AK-2 and 3), dolomite replaces with quartz to become the trace mineral. In addition, the sample is observed to be composed 100% of anhydrite. The amount of this mineral decrease to 65% in the following XRD sample (XRD sample no: GD-AK-4). The remaining percentage of volume belongs to dolomite with trace amounts of quartz. K-feldspar appears within the XRD samples of South Dincer-1 Well for the first time with GD-AK-5 numbered sample. Here, dolomite is the dominant mineral with 82% of volume and it is observed with clay+mica (8%) and anhydrite (5%). The next XRD sample (XRD

sample no: GD-AK-6) shows the same mineralogical character with the second and third samples except that it does not contain any trace minerals.

Table 7. Whole rock mineral composition after XRD analyses for South Dinger-1 Exploration Well.

Sample ID	Sample Depth (m)	Whole Rock Mineral Composition (volume %)						
		Feldspar Group		Anhydrite	Quartz	Calcite	Dolomite	Clay+Mica
		Plagioclase	K-Feldspar					
GD-AK-1	2430.80	-	-	97	trace	-	3	-
GD-AK-2	2507.45	-	-	100	-	-	trace	-
GD-AK-3	2510.05	-	-	100	-	-	trace	-
GD-AK-4	2520.30	-	-	65	trace	-	35	-
GD-AK-5	2522.65	-	5	5	-	-	82	8
GD-AK-6	2525.10	-	-	100	-	-	-	-
GD-AK-7	2539.00	-	8	-	-	-	85	7
GD-AK-8	2549.65	-	-	9	-	-	91	-
GD-AK-9	2550.15	-	-	5	-	-	95	-
GD-AK-10	2826.25	-	-	35	-	5	60	-
GD-AK-11	2827.75	-	-	57	-	-	43	-
GD-AK-12	2862.90	-	-	20	-	-	80	-
GD-AK-13	3290.00	trace	5	-	33	-	8	54
GD-AK-14	3291.00	-	3	-	24	-	28	45

Çamurlu Formation's XRD samples are inspected starting with the seventh sample (XRD sample no: GD-AK-7) of South Dinger-1 Well.

K-feldspar is again observed in the well, this time with 8% of volume. The major mineral is dolomite with 85% of volume in addition to 7% of clay+mica. The following two XRD samples (XRD samples no: 8 and 9) shows the same mineralogical character with 91% of dolomite, 9% of anhydrite and 95% of dolomite, 5% of anhydrite respectively.

The volume percentage of dolomite mineral decreases as the studied unit changes from Cudi Group's Çamurlu Formation to Bakük Formation. GD-AK-10 numbered XRD sample is mainly composed of dolomite (60%), anhydrite (35%) and calcite (5%) minerals. The following two samples (GD-AK-11 and 12) have similar compositions except that they do not contain any calcite mineral. Their mineralogical volume percentages are as follows; 57% of anhydrite, 43% of dolomite and 80% of dolomite, 20% of anhydrite, respectively. With these samples, the indication of the whole rock mineral volume percentages of Cudi Group units is completed.

The last two XRD samples of South Dinger-1 Well are from Çiğli Group's Uludere Formation. In GD-AK-13 numbered sample, plagioclase is observed for the first time within the studied well's XRD samples, with trace amounts. This sample also contains 54% of clay+mica, 33% of quartz, 8% of dolomite and 5% of K-feldspar. The very last sample examined with the XRD analyses is GD-AK-14 and it contains 45% of clay+mica chiefly in addition to 28% of dolomite, 24% of quartz and 3% of K-feldspar.

During the XRD analyses of these samples on the low 2theta angle site of diffractograms, peaks around 10Å value were detected. These peaks may belong to mica group mineral or a clay mineral which is illite (Tables 4 and 5). Since the exact identification of the mineral represented by these peaks could not be done in this part of the study, the samples which are selected showing this peak were analyzed for their clay fraction as explained in the following section.

2.3 Results of Clay Fraction Analyses by XRD

Dinçer-1 and South Dinçer-1 Exploration Well's whole rock analyses for the complete 24 XRD samples were evaluated and as a result of this evaluation three samples, belonging to Cudi Group sequence of Dinçer-1 and South Dinçer-1 wells, were chosen according to their observed clay+mica volume percentage for clay fraction analyses by XRD. These selected samples are D-AK-9, GD-AK-5 and GD-AK-7. D-AK-9 numbered sample from Dinçer-1 Well and GD-AK-7 numbered sample from South Dinçer-1 Well will be described in details. The reason for performing this study is to examine the clay mineral properties of Cudi Group which is observed within the studied fields.

The first selected XRD sample for clay analyses is Dinçer-1 Well's ninth sample, from Cudi Group's Bakük Formation, with the D-AK-9 XRD ID number. The details of this sample can be seen at Tables 4 and 6.

A total of 18% of "clay mineral+mica" was observed from the whole rock mineral analyses of D-AK-9 XRD sample (section 4.3.1). As a result of further clay mineral analyses of this sample; these clay minerals were observed to be illite as the dominant mineral, with a trace amount of probable kaolinite mineral (Figure 40). The 10.018Å peak was observed to be the dominant illite mineral whereas the 7.098Å peak as probably the trace kaolinite mineral. The reason for identifying the 7.098Å peak as the kaolinite mineral is that it becomes amorphous at 550°C (D-AK-9 (550) section of Figure 40) and this a known property of the kaolinite mineral.

Kaolinite within clay minerals group has a chemical composition of $\text{Al}_2\text{O}_3 \cdot 2\text{SiO}_2 \cdot 2\text{H}_2\text{O}$ and has triclinic system. They mainly show perfect cleavage in one direction parallel to {001}. Crystal structures are fine mosaic-like masses, in scale-like individuals and in veinlets which replace feldspars along with other minerals. Their birefringence is weak ($n_\gamma - n_\alpha = 0.005$) (Kerr, 1977).

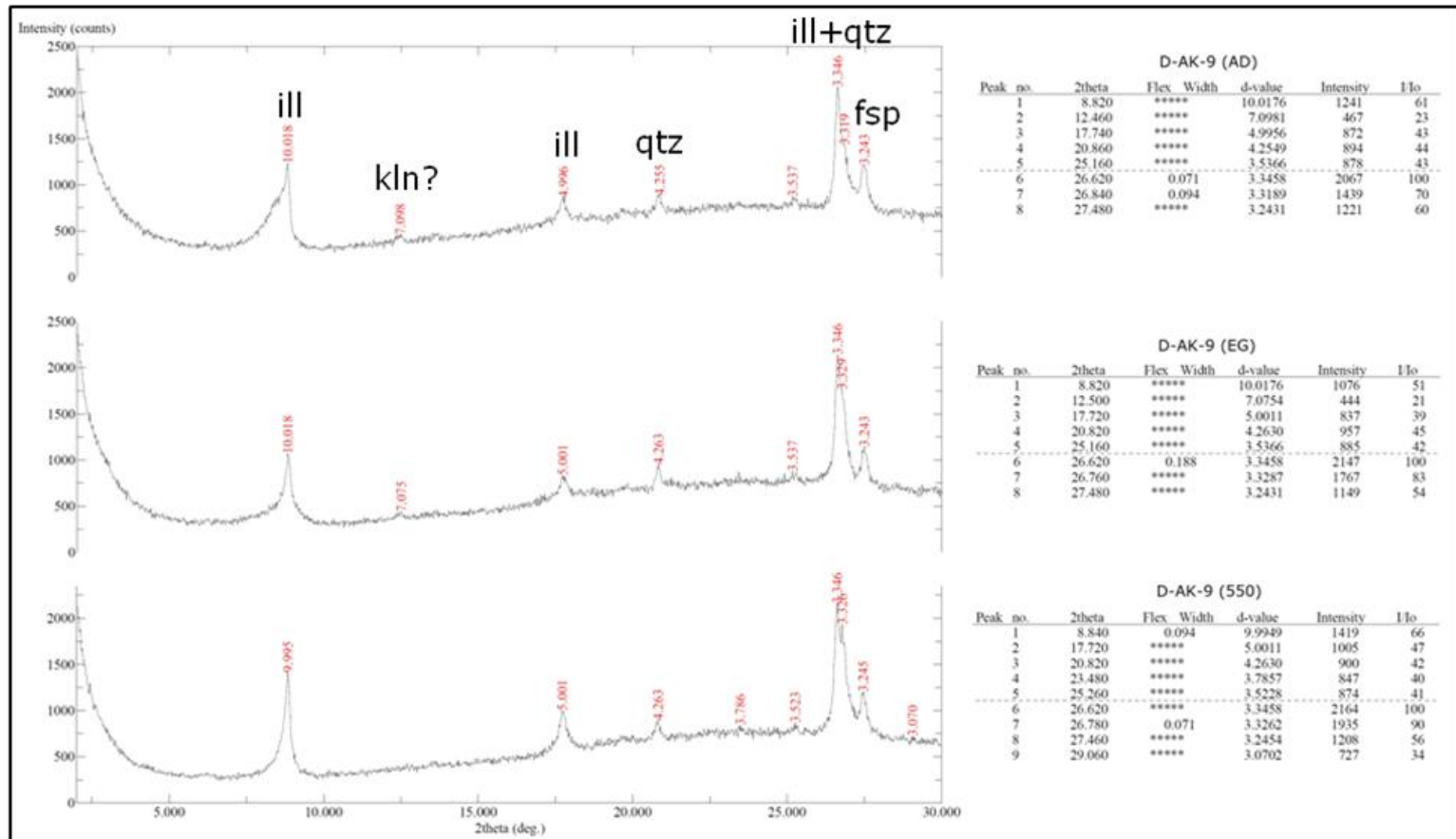


Figure 40. X-ray diffractograms of clay minerals belonging to Dincer-1 Well's D-AK-9 numbered XRD sample (ill: illite, kln: kaolinite, qtz: quartz and fsp: K-feldspar minerals).

The second XRD sample selected for further clay analyses is South Dincer-1 Well's seventh sample with the XRD sample number GD-AK-7, from Cudi Group's Çamurlu Formation. The details of this sample can be seen at Tables 5 and 7.

From the whole rock mineral analyses belonging to GD-AK-7 numbered XRD sample, a total of 7% of "clay mineral+mica" was observed (section 4.3.1). The dominant clay mineral was observed to be illite mineral, as a result of the clay mineral analyses of this sample (Figure 41). The 10.593Å peak was observed to be the dominant illite mineral.

The illite mineral observed from all of three XRD samples, subjected to clay mineral analyses, have a special disordered structure with an asymmetric hump. Because of this reason, one can say that the illite mineral of Cudi Group in the studied wells have a mixed-layer structure.

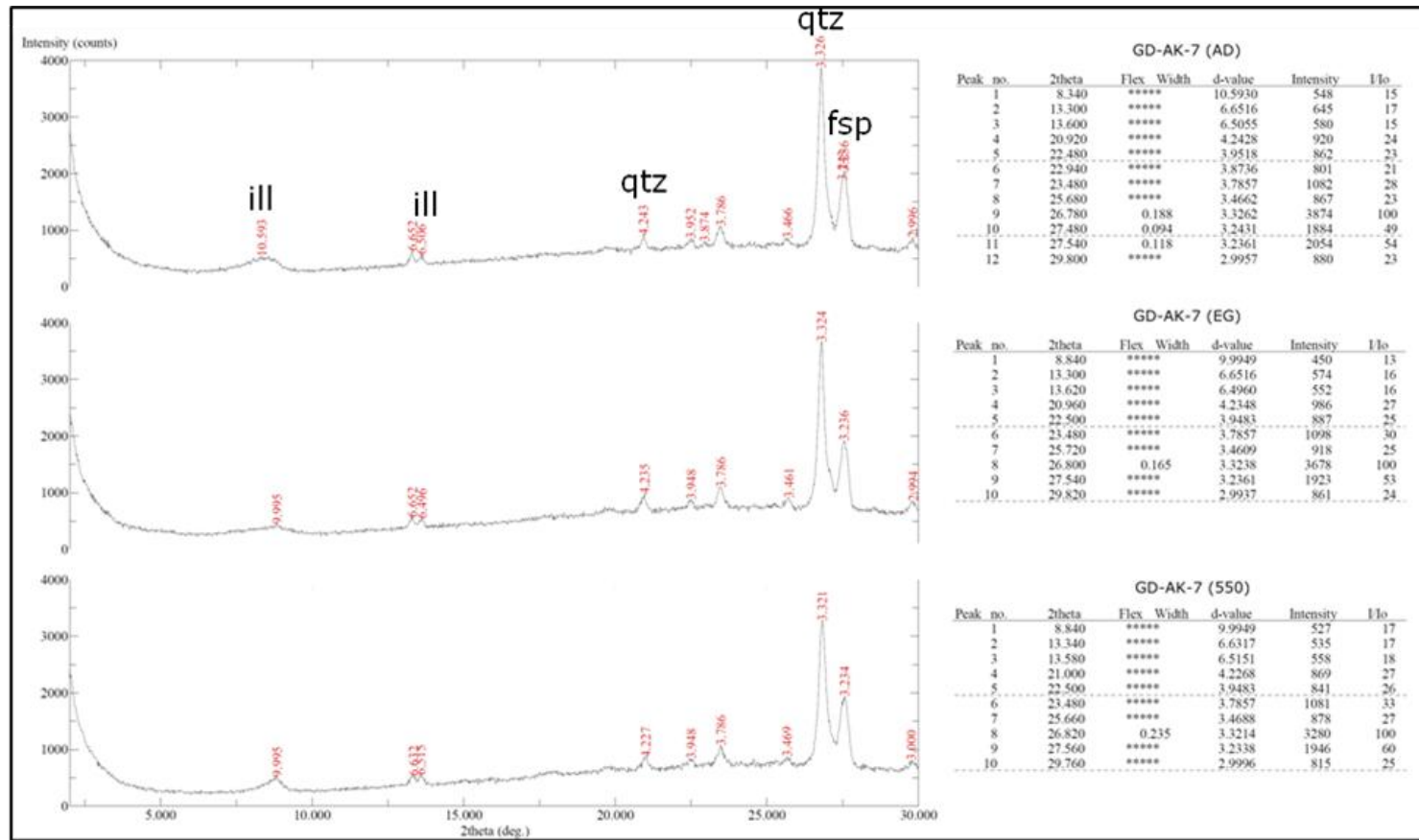


Figure 41. X-ray diffractograms of clay minerals belonging to South Dinger-1 Well' GD-AK-7 numbered XRD sample (ill: illite, qtz: quartz and fsp: K-feldspar minerals).

2.4 Dolomite Stoichiometry

As mentioned in Chapter 3, an ideal dolomite is stoichiometric but in nature it never occurs as such. This regarded character can be used as a tool at examining the geochemistry of dolomite mineral's depositional environment (Süzen and Türkmenoğlu, 2000).

A study related to dolomite mineral's stoichiometry is done for the 7 samples of Dincer-1 Exploration Well and 10 samples of South Dincer-1 Exploration Well, selected due to their composition (the ones with dolomite minerals were selected) (Tables 8 and 9).

The selected XRD samples are composed of varying chemistries which can be observed from their d(104) peak values. The intensity values for all of the sample's d(104) peaks were identified. Following this identification, the Ca excess of the dolomites observed at these samples, were calculated by the formulae given by Lumsden (1979) which can be seen below;

$$N\text{CaCO}_3 = M*d + B.$$

Here, M is a constant equal to 333.33, d is the observed intensity value of the d(104) peak and B is another constant with a value of -911.99. Mg excess of the regarded dolomites was identified by subtracting the Ca excess value from the whole (100%).

From the XRD patterns of these selected samples, the intensity values of d(015) and d(110) values were used in order to identify the degree of ordering (order ratio) which can be used to understand whether the dolomites are primary precipitation products or not. Degree of ordering is the ratio of the intensity value of d(015) peak with the intensity value of d(110) peak (Goldsmith and Graf, 1958a and b).

Following the identification of the related values, the ordering ratio and the CaCO₃ percentage of the studied dolomites were plotted for the two wells in order to make an assumption on the history of the examined dolomites.

The ordering ratio of Dincer-1 Well's dolomites ranges from 0.58 to 0.83 where the CaCO₃% ranges from approximately 46% to 53% (Table 8).

As a result of plotting the degree of ordering vs. CaCO₃% values belonging to Dincer-1 Well's samples, it is observed that the dolomites of D-AK-2 numbered sample of Telhasan Formation shows an ideal stoichiometric character (50% of CaCO₃ volume) (Figure 42). D-AK-1 and 3 numbered samples of the same unit shows a relatively deviated character towards a decreasing CaCO₃%.

Towards deeper depth intervals, D-AK-7 and 8 numbered samples of Bakük Formation again shows a deviation but this time towards an increasing $\text{CaCO}_3\%$ value. The $\text{CaCO}_3\%$ value of D-AK-9 numbered sample from Bakük Formation and D-AK-10 numbered sample from Uludere Formation (Çığlı Group) is very high when comparing with the other sample's $\text{CaCO}_3\%$ values.

Table 8. X-ray diffraction data of studied samples for Dinger-1 Exploration Well.

ID	Depth (m)	Group	Formation	<i>I</i> d(015)	<i>I</i> d(110)	Order Ratio	Å d(104)	CaCO₃%	MgCO₃%
D-AK-1	2495.97	Cudi	Telhasan	309.52	533.33	0.580	2.8826	48.867	51.133
D-AK-2	2498.29	Cudi	Telhasan	133.33	217.54	0.613	2.8859	49.967	50.033
D-AK-3	2502.00	Cudi	Telhasan	220.34	440.68	0.500	2.8752	46.400	53.600
D-AK-7	3171.95	Cudi	Bakük	72.13	124.59	0.579	2.8897	51.234	48.766
D-AK-8	3172.95	Cudi	Bakük	75.00	146.43	0.512	2.8879	50.634	49.366
D-AK-9	3174.00	Cudi	Bakük	41.66	50.00	0.833	2.8951	53.034	46.966
D-AK-10	3302.15	Çiğlı	Uludere	126.32	185.26	0.682	2.8953	53.100	46.900

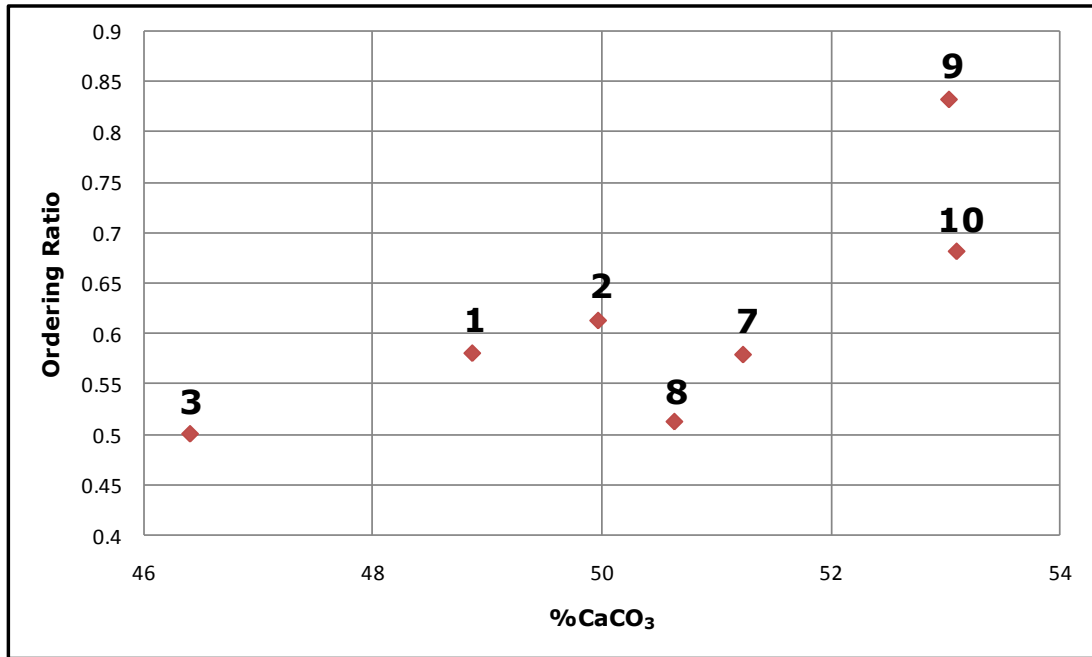


Figure 42. Dincer-1 Exploration Well scattergram showing the relation of ordering ratio with CaCO₃% (Hardy and Tucker, 1988).

So, for Dincer-1 Well, the samples belonging to the same formations, except Bakük Formation's D-AK-9 numbered sample, show the same character regarding their CaCO₃ percentages. One can also say that, for the Uludere Formation as well as one sample from Bakük Formation, ordering ratio increases as the dolomites drift apart from the ideal stoichiometry form.

The ordering ratio of South Dincer-1 Well's dolomites ranges from 0.43 to 3.20 where the CaCO₃% ranges from approximately 45% to 57% (Table 9).

Table 9. X-Ray Diffraction data of studied samples for South Dinger-1 Exploration Well.

ID	Depth (m)	Group	Formation	<i>I</i> d(015)	<i>I</i> d(110)	Order Ratio	Å d(104)	CaCO₃%	MgCO₃%
GD-AK-4	2520.30	Cudi	Telhasan	238.10	297.62	0.800	2.8842	49.400386	50.5996
GD-AK-5	2522.65	Cudi	Telhasan	187.50	437.50	0.429	2.8952	53.067016	46.933
GD-AK-7	2539.00	Cudi	Çamurlu	175.00	325.00	0.538	2.8734	45.800422	54.1996
GD-AK-8	2549.65	Cudi	Çamurlu	300.00	400.00	0.750	2.8897	51.233701	48.7663
GD-AK-9	2550.15	Cudi	Çamurlu	315.79	421.05	0.750	2.8844	49.467052	50.5329
GD-AK-10	2826.25	Cudi	Bakük	250.00	464.29	0.538	2.8861	50.033713	49.9663
GD-AK-11	2827.75	Cudi	Bakük	147.06	294.12	0.500	2.8896	51.200368	48.7996
GD-AK-12	2862.90	Cudi	Bakük	341.46	487.80	0.700	2.8844	49.467052	50.5329
GD-AK-13	3290.00	Çiğli	Uludere	195.12	60.98	3.200	2.9079	57.300307	42.6997
GD-AK-14	3291.00	Çiğli	Uludere	160.00	106.67	1.500	2.9024	55.466992	44.533

A similar study was carried out for the samples belonging to South Dinger-1 Well. Only one GD-AK-7 numbered sample was not plotted due to its relatively low $\text{CaCO}_3\%$ value (Figure 43).

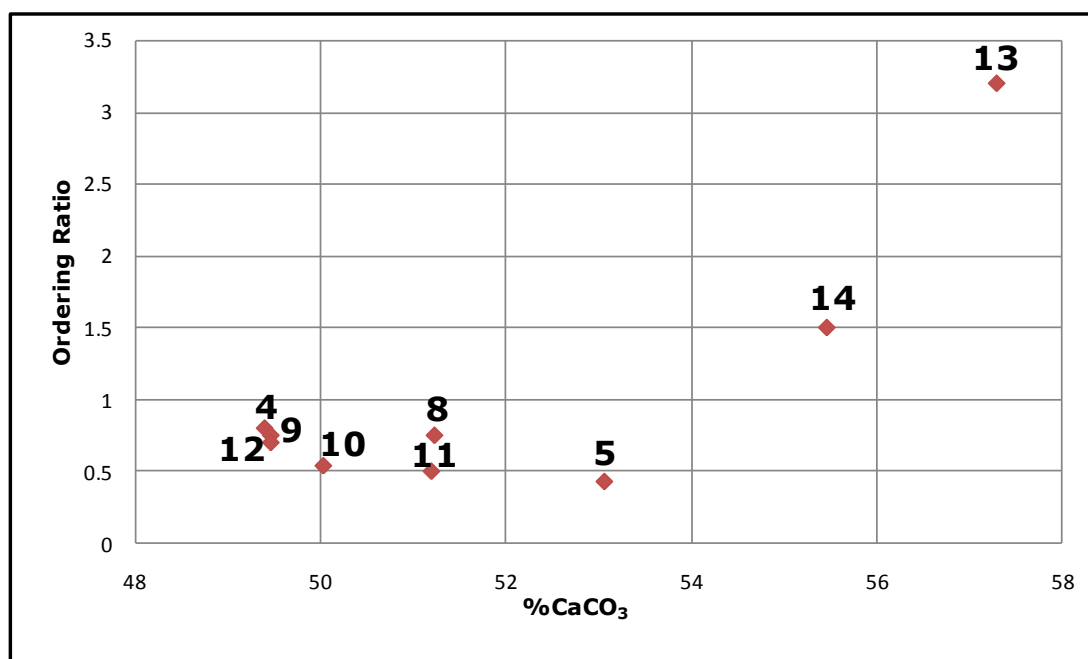


Figure 43. South Dinger-1 Exploration Well scattergram showing the relation of ordering ratio in with $\text{CaCO}_3\%$ (Hardy and Tucker, 1988).

Compared with Dinger-1 Well, South Dinger-1 Well's samples show a more random scattergram of ordering ratios vs. $\text{CaCO}_3\%$ belonging to Cudi Group formations.

GD-AK-10 numbered sample, belonging to Cudi Group's Bakük Formation, shows an ideal stoichiometry with a 50.03% of CaCO_3 .

Cudi Group formations gather around this value of GD-AK-10 numbered sample randomly. However, the samples belonging to ıđlı Group's Uludere Formation (GD-AK-13 and 14) shows the same character of Diņer-1 Well's D-AK-9 and 10 numbered samples. Their CaCO₃ percentage increases as the ordering ratio increases. GD-AK-13 numbered sample, belonging to Uludere Formation, has the highest CaCO₃% and ordering ratio with 57.30% and 3.20 respectively. On the other hand, Diņer-1 Well's D-AK-9 numbered sample belonging to the Bakük Formation has the highest CaCO₃% and ordering ratio with 53.03% and 0.68 respectively.

CHAPTER 3

DISCUSSION OF THE RESULTS

In this chapter the major results of the study will be discussed and the conclusions gained will be explained. The discussions can be separated into two subgroups which are as mentioned below.

3.1 Depositional Environment of Cudi Group Sequence as Indicated by their Petrographic and Mineralogical Characteristics

As supported by Salem (1984), the lithology of the Cudi Group formations is defined as mainly dolostones and evaporates with anhydrites. The sequence also contains relatively less amounts of limestones, shales and sandstones. The formation of the Cudi Group sequence was described as the repetition of the deposition of shallow water carbonates, dolomites and evaporates.

The studied Dincer-1 and South Dincer-1 exploration wells have penetrated a similar sequence of Cudi Group, since they are located at the same field and the distance between the two wells is 1.6 km. As a result, the mineralogical association of the regarded

sequence shows a parallelism. This similarity can be seen at Tables 4 and 5. Cudi Group's Telhasan Formation belonging to Dınçer-1 and South Dınçer-1 wells is mainly composed of dolomite and/or anhydrite as the dominant minerals.

The first sample of Dınçer-1 Well (D-AK-1), belonging to Telhasan Formation, is observed to be dolostone with trace amounts of anhydrite mineral (Table 6). The second and the third samples (D-AK-2 and 3) have both dolomite and anhydrite minerals together. The next three samples (D-AK-4, 5 and 6) are observed to be evaporates with 100% of anhydrite mineral and trace amounts of dolomite along with calcite minerals. Similarly, the first three and the sixth samples of South Dınçer-1 Well (GD-AK-1, 2, 3 and 6) is defined as evaporate with 100% of anhydrite mineral and trace amounts of dolomite along with quartz minerals (Table 7). The fourth and the fifth samples (GD-AK-4 and 5) have anhydrite and dolomite minerals as dominant mineral respectively (65% and 82%) with trace amounts of quartz, K-feldspar, anhydrite and illite minerals. The illite mineral is defined to have 8% of volume within the whole rock and has a disordered structure.

Towards deeper intervals, Çamurlu Formation takes place but only samples from South Dınçer-1 Well belonging to this unit could be studied since core samples belonging to Dınçer-1 Well's regarded formation do not exist. The first sample of Çamurlu Formation belonging to South Dınçer-1 Exploration Well (GD-AK-7) is similarly composed of dolomite as the dominant mineral (85%) with illite (7%) and K-feldspar (8%) as the trace minerals. The next two

samples (GD-AK-8 and 9) are mainly observed to be dolostones with 9% and 5% of anhydrite minerals respectively.

Samples from Cudi Group's Bakük Formation were observed from both of the wells. One of the three samples belonging to this formation of Dinger-1 Well was observed to be completely different from the other two samples. The first two samples of Bakük Formation (D-AK-7 and 8), belonging to Dinger-1 Well, contains calcite mineral as major (58% and 54% respectively) and dolomite mineral as minor (42% and 46% respectively) mineral. However, the third sample of the same unit (D-AK-9) contains quartz as the dominant mineral (35%) with dolomite (29%), K-feldspar (18%) and illite (18%) as less common minerals. Along with illite mineral, kaolinite probably takes place within this sample because its characteristic peaks disappear at 550°C. This mineral composition is observed to be almost the same with the next sample (D-AK-10) belonging to Çiğli Group's Uludere Formation, containing 54% dolomite, 25% illite, 18% quartz and 3% K-feldspar minerals. As a result, the D-AK-9 numbered sample of Dinger-1 Well which was named as Bakük Formation in previous years was observed to be Çiğli Group's Uludere Formation. This finding can be supported by the samples belonging to South Dinger-1 Well's Bakük and Uludere Formations. The samples of the Bakük Formation belonging to this well (GD-AK-10, 11 and 12) contains 60%, 43% and 80% dolomite mineral in addition to 35%, 57% and 20% of anhydrite mineral respectively. Similar to Dinger-1 Well's D-AK-9 and 10 numbered samples, the samples belonging to Uludere Formation (GD-AK-13 and 14), mainly consists of illite (54%, 45%), quartz (33%, 24%)

and K-feldspar (5%, 3%) respectively. Furthermore, GD-AK-14 numbered sample contains 28% of dolomite mineral and plagioclase is seen for the first time within the well with the GD-AK-13 numbered sample.

The depositional environment of the Cudi Group units is relatively quieter than Çiğlı Group's Uludere Formation which is located at the deeper intervals (older than Cudi Group formations). In contrast, the depositional environment of Uludere Formation is more energetic, containing illite mineral with an important proportion.

Algal structures are also observed within the thin sections of Dınçer-1 Well's D-AK-1 and South Dınçer-1 Wells GD-AK-5 numbered samples. These structures are indicated as decomposed fragments. The missing of these structures can be related with the petrographic evidence of a diagenetic process. Because of this process, the fossil structures of these algae have disappeared.

Stylolites (mostly filled with hydrocarbon) are also observed within some samples of the wells (Dınçer-1 Well's D-AK-2 and South Dınçer-1 Well's GD-AK-3, 5, 7, 8 and 10 numbered samples). The existence of these stylolites also due to the diagenetic processes affected these formations during their burial history.

3.2 Dolomite Stoichiometry and Dolomitization

In the studies carried out for understanding the geochemistry of the depositional environment belonging to dolomite minerals, dolomite stoichiometry can be used (Süzen and Türkmenođlu, 2000).

The samples which contain dolomite minerals within their whole rock volume were selected regarding the mentioned study. A total of 7 samples from Dınđer-1 Exploration Well and 10 samples from South Dınđer-1 Exploration Well were selected due to their composition. These selected samples and the results of the calculations related to dolomite stoichiometry of the samples are given in Tables 8 and 9.

From the results of this study, for Uludere Formation of ıđlı Group, it is observed that ordering ratio generally increases as the samples diverts from the stoichiometry field where the volume of CaCO₃ is equal to 50%. In contrast, it is the opposite for Cudi Group formations (Figures 42 and 43).

Both Dınđer-1 and South Dınđer-1 well samples, belonging to Uludere Formation, show the same behavior when the ordering ratio values are plotted against the CaCO₃%. They have relatively high CaCO₃% in addition to high ordering ratios, with respect to Cudi Group formations. Dınđer-1 Well's D-AK-9 numbered sample, which was identified as Bakük Formation of Cudi Group before,

again shows the same behavior with Uludere Formation which can be seen in Figure 47.

Most modern dolomites show poor ordering reflections when compared with the ancient dolomites (Süzen and Türkmenođlu, 2000).

It is observed that the dolomites of the samples belonging to Cudi Group formations are modern dolomites and they are relatively younger formations which are subjected to longer period diagenetic affects in comparison with Uludere Formation's dolomites. The samples belonging to Uludere Formation of ıđlı Group are relatively old and are observed to be ancient dolomites.

CHAPTER 4

CONCLUSIONS

The following conclusions are obtained based on the results of this study.

1. The stylolites and algal fragments observed from thin section studies of 8 samples belonging to Dincer-1 and South Dincer-1 exploration well's Cudi Group formations, indicates the dolomitization process due to the unclarities/deformations of algal structures.
2. As a result of the petrographic analyses, it is observed that Uludere Formation of Çiğli Group, the lowermost unit of the studied sequence, relatively consists of a whole rock composition with more silts and clays compared with Cudi Group formations.
3. Following the qualitative analyses of the whole rock samples belonging to 2 samples of Dincer-1 and 2 samples of South Dincer-1 wells, the unidentified mineral which could be either illite or mica, was proved to be illite, from the clay fraction analyses carried out for those samples.

4. Within Dincer-1 Well's Telhasan Formation, dolomite and anhydrite minerals obtain the dominant character place to place along with trace amounts of quartz and calcite minerals. Towards deeper intervals to Bakük Formation, dolomite is observed with calcite mineral along with quartz as the trace mineral. However, at Çiğlı Group's Uludere Formation, the whole structure changes and quartz, dolomite, illite and K-feldspar minerals share the composition.
5. Within South Dincer-1 Well's Telhasan Formation, mainly anhydrite is the dominant mineral but in a few samples, dolomite replaces with anhydrite to be the dominant mineral. Additionally, illite, quartz and K-feldspar minerals are observed. Samples belonging to the well's Çamurlu Formation were also examined for the first time. This unit contains dolomite as the major, anhydrite, K-feldspar and illite mineral as the minor minerals. Bakük Formation of the well, similar to the same unit of Dincer-1 Well, contains dolomite but this time with anhydrite mineral. The remaining samples belonging to Uludere Formation, mainly consists of quartz, dolomite, illite with trace amounts of K-feldspar and plagioclase minerals as Dincer-1 Well's Uludere Formation (except only the plagioclase mineral).
6. Dincer-1 Exploration Well's D-AK-9 numbered sample, which was previously named as Cudi Group's Bakük Formation, is observed to be Çiğlı Group's Uludere

Formation. The reason for this is that the sample contains the same minerals with Uludere Formations which are quartz (35%) as major mineral and dolomite (29%), illite (18%) and K-feldspar (%18) as other minerals (Table 6) rather than the minerals observed within the Cudi Group formations.

7. D-AK-9 numbered sample belonging to Dincer-1 Exploration Well was also subjected to dolomite stoichiometry studies with the rest of the samples containing the dolomite mineral. From this study, the results given above were supported since the sample shows exactly the same behavior of Uludere Formation's samples.
8. Both Dincer-1 and South Dincer-1 wells contain illite mineral whereas Dincer-1 Well contains kaolinite mineral as well. The broad peaks of the reflections belonging to the illite mineral (Figures 40 and 41) shows detritic behaviors rather than characters representing a diagenetic origin.
9. Obtained results from this study showed that the dolomitization as diagenetic process plays an important role in oil and gas formations within Cudi Group by increasing the secondary porosity.

10. It is observed that the dolomites of the samples belonging to Cudi Group formations are modern dolomites since they show poor ordering reflections. They are also relatively younger formations which are subjected to longer periods of diagenetic affects in comparison with Uludere Formation's dolomites. The samples belonging to Uludere Formation of Çiğli Group are relatively old and are observed to be ancient dolomites because of their good ordering reflections.

Based on the results of the study, dolomitization can be studied regionally regarding more wells located at the studied fields in accordance with the structure of the basin. Since Cudi Group formations are important related to oil-gas production fields around the study area and diagenesis is one of the major events affecting oil-gas developments, the examination of this sequence is suggested for further studies.

REFERENCES

- Açıkbaş, D. and Akalın, T., 1968, Dinçer-1 Well Reports, TPAO Exploration Department Well Archive no. 515 (unpublished).
- Ala, M. A. and Moss, B. J., 1979, Comparative Petroleum Geology of Southeast Turkey and Northeast Syria, *Journal of Petroleum Geology*, V. 1, p. 3-27.
- Altınlı, İ. E., 1952, Siirt Güneydoğusunun Jeolojik İncelemesi, MTA Derleme no. 1977, 95 p.
- Bambach, R. K., Scotese, C. R. and Ziegler, A. M., 1980, Before Pangaea: The Paleozoic World, *American Journal of Science*, v. 68, p. 26-38.
- Bathurst, R. G. C., 1976, Carbonate Sediments and Their Diagenesis, *Developments in Sedimentology*, 12, Second Enlarged Edition, Netherlands, Elsevier Scientific Publishing Company, 658 p.

Berry, L. G., 1972, Powder Diffraction File, Sets: 6-10 and 11-15 (revised), Inorganic Volume, no. PDIS-15 i RB, Joint Committee on Powder Diffraction Standards, Pennsylvania, 701 and 1081 p.

Blatt, H., 1982, Sedimentary Petrology, W. H. Freeman and Company, USA, 564 p.

Boggs, S., Jr., 1995, Principles of Sedimentology and Stratigraphy, 2nd Edition, Prentice Hall, USA, 774 p.

Bordenave, M. L. and Hegre, J. A., 2010, Current Distribution of Oil and Gas Fields in the Zagros Fold Belt of Iran and Contiguous Offshore as the Result of the Petroleum Systems, Geological Society, London, Special Publications, v. 330; p. 291-353.

Bozdoğan, N. and Erten, T., 1990, The Age and Effects of the Mardin High, SE Anatolia, 8th Petroleum Congress of Turkey, Ankara, Turkish Association of Petroleum Geologists, UCTEA Chamber of Petroleum Engineers, p. 207-227.

Bozdoğan, N. and Erten, T., 1991, Mardin Yükseliminin Yaşı ve Etkileri, G. D. Anadolu, TPAO Exploration Department Archive no. 662, 27 p (unpublished).

Brindley, G. W. and Brown, G., 1980, *Crystal Structures of Clay Minerals and their X-Ray Identification*, Mineralogical Society, London, 595 p.

Burke K. and Dewey, J. F., 1973, Plume-Generated Triple Junctions: Key Indicators in Applying Plate Tectonics to Old Rocks, *Journal of Geology*, v. 81, p. 406-433.

Chen, P. Y., 1977, *Table of Key Lines in X-Ray Powder Diffraction Patterns of Minerals in Clays and Associated Rocks*, Department of Natural Resources Geological Survey Occasional Paper, 21, Bloomington, Indiana, 67 p.

Chilingar, G. V., Bissell, H. J. and Wolf, K. H., 1979a, Diagenesis of Carbonate Sediments and Epigenesis (or Catagenesis) of Limestones, *Developments in Sedimentology, Diagenesis in Sediments and Sedimentary Rocks*, Amsterdam, Elsevier Scientific Publishing Company, v. 25A, p. 247-422.

Chilingar, G. V., Zenger, D. H., Bissell, H. J. and Wolf, K. H., 1979b, Dolomites and Dolomitization, *Developments in Sedimentology, Diagenesis in Sediments and Sedimentary Rocks*, Amsterdam, Elsevier Scientific Publishing Company, v. 25A, p. 423-525.

Demicco, R. V. and Hardie, L. A., 1994, Sedimentary Structures and Early Diagenetic Features of Shallow Marine Carbonate Deposits, USA, SEPM Atlas Series, no. 1, 265 p.

Dolomieu, D. G. de, 1791, Sur un Genre des Pierres Calcaires Très-Peu Effervescentes Avec les Acides & Phosphorescentes par la Collision, Journal Physique, v.39, p. 3-10.

Emery, K. O., Tracey, J. J., Jr. and Ladd, H. S., 1954, Geology of Bikini and Nearby Atolls: Part I, U.S. Geological Survey Professional Paper, 260-A, 262 p.

Erođlu, A., 1984, Güney Dincer Sahasının Yeraltı Jeolojisi ve Petrol Olanakları, Yüksek Lisans Tezi, Ankara Üniversitesi, TPAO Exploration Department Archive no. 3331, 43 p (unpublished).

Folk, R. L. and Land, L. S., 1975, Mg/Ca Ratio and Salinity: Two Controls over Crystallization of Dolomite, The American Association of Petroleum Geologists Bulletin, v. 59, no. 1, p. 60-68.

Folk, R. L., Roberts, H. H. and Moore, C. H., 1973, Black Phytokarst from Hell, Cayman Islands, British West Indies, Bulletin of the Geological Society of America, v. 84, p. 2351-2360.

Folk, R. L. and Siedlecka, A., 1974, The "Schizohaline" Environment: Its Sedimentary and Diagenetic Fabrics as Exemplified by Late Paleozoic Rocks of Bear Island, Svalbard, *Sedimentary Geology*, v. 11, issue 1, p. 1-15.

Garrels, R. M. and Mackenzie, F. T., 1971, *Evolution of Sedimentary Rocks*, W. W. Norton & Co., New York, Norton, 397 p.

Goldsmith, J. R. and Graf, D. L., 1958a, Relation Between Lattice Constants and Composition of Ca-Mg Carbonates, *American Mineralogist*, v. 43, p. 84-101.

Goldsmith, J. R. and Graf, D. L., 1958b, Structural and Compositional Variations in Some Natural Dolomites, *Journal of Geology*, v. 66, p. 678-693.

Görür, N., Çelikdemir, E. and Dülger, S., 1991, Carbonate Platforms Developed on Passive Continental Margins: Cretaceous Mardin Carbonates in Southeast Anatolia as an Example, *Bull. Tech. Univ., Istanbul*, v. 44, p. 301-324.

Gribble, C. D. and Hall, A. J., 1992, *Optical Mineralogy, Principles & practice*, Great Britain, UCL Press.

Güven, A., Dincer, A., Tuna, E. M. and Çoruh, T., 1991, Güneydoğu Anadolu Kampaniyen Paleosen Otokton İstifinin Stratigrafisi, TPAO Exploration Department Archive no. 2828, 133 p (unpublished).

Ham, W. E. and Pray, L. C., 1961, Modern Concepts and Classifications of Carbonate Rocks, Classifications of Carbonate Rocks-A Symposium, AAPG Memoir One, Michigan, Edward Brothers Inc., p. 2-19.

Hardie, L. A., 1987, Dolomitization; A Critical View of Some Current Views, Journal of Sedimentary Research, v. 57; no. 1, p. 166-183.

Hardy, R. and Tucker, M., 1988, X-Ray Powder Diffraction of Sediments, in Techniques in Sedimentology, M. Tucker, Ed., Blackwell Scientific Publications Co., Oxford, p. 191-228.

Horbury, A. and Robinson, A., 1993, Diagenesis, Basin Development, and Porosity Prediction in Exploration-An Introduction, Diagenesis and Basin Development, AAPG Studies in Geology, USA, no. 36, p. 1-4.

James, G. A. and Wynd, J. G., 1965, Stratigraphic Nomenclature of Iranian Oil Consortium Agreement Area, AAPG Bulletin, no. 49, p. 2182-2245.

Kerr, P. F., 1977, *Optical Mineralogy*, 4th Edition, McGraw-Hill, New York, 492 p.

Land, L. S., 1985, The Origin of Massive Dolomite, *Journal of Geological Education*, v. 33, p. 112-125.

Landes, K. K., 1946, Porosity through Dolomitization, *Carbonate Rocks II: Porosity and Classification of Reservoir Rocks*, AAPG Bulletin, Reprint Series, no. 5, p. 27-40.

Lang, B. and Mimran, Y., 1985, An Early Cretaceous Volcanic Succession in Central Israel and its Significance to the Absolute Date of the Cretaceous, *Journal of Geology*, v. 93, p. 179-184.

Larsen, G. and Chilingar, G. V., 1979, *Diagenesis of Sediments and Rocks*, *Developments in Sedimentology, Diagenesis in Sediments and Sedimentary Rocks*, Amsterdam, Elsevier Scientific Publishing Company, v. 25A, p. 1-29.

Lumsden, D. N., 1979, Discrepancy Between Thin Sections and X-Ray Estimates of Dolomite in Limestone, *Journal of Sedimentary Petrology*, v. 49, p. 429-436.

Machel, H. G. and Mountjoy, E. W., 1986, Chemistry and Environments of Dolomitization-A Re-appraisal, *Earth Science Reviews*, v. 23, p. 175-222.

Machel, H. G., 2004, Concepts and Models of Dolomitization: A Critical Reappraisal, *Geological Society London, Special Publications*; v. 235; p. 7-63.

Perinçek, D., Duran, O., Bozdoğan, N. and Çoruh, T., 1992, Stratigraphy and Paleogeographical Evolution of the Autochthonous Sedimentary Rocks in the SE Turkey, *Ozan Sungurlu Symposium Proceedings*, v. 1, p. 274-305.

Read, J. F. and Horbury, A. D., 1993, Eustatic and Tectonic Controls on Porosity Evolution Beneath Sequence-Bounding Unconformities and Parasequence Disconformities on Carbonate Platforms, *Diagenesis and Basin Development, AAPG Studies in Geology, USA*, no. 36, p. 155-197.

Roberts, W. L., Campbell, T. J. and Rapp, G. R., Jr., 1990, *Encyclopedia of Minerals, 2nd Edition*, Chapman & Hall, London, 979 p.

Salem, R., 1984, Geologic and Hydrocarbon Evaluation of the Cudi Group Sequence (Triassic-Jurassic) in Southeast Turkey, Part 1 and 2, Fort Worth, Texas U.S.A., Salem Enterprises, TPAO Exploration Department Archive no. 1968/1, 76 p (unpublished).

Sass, E. and Bein, A., 1980, The Cretaceous Carbonate Platform in Israel, Cretaceous Research, v. 3, p. 135-144.

SE Anatolia District Geologists of TPAO, 1979, Geology and Petroleum Possibilities of Southeast Turkey, TPAO Exploration Department Archive no. 1410, 31 p (unpublished).

Schmidt, G. C., 1964, A Review of Permian and Mesozoic Formations Exposed near the Turkey/Iraq Border at Harbol, Mobil Exploration Mediterranean, Inc., Ankara, 20 p (unpublished).

Sungurlu, O., 1974, VI. Bölge Kuzey Sahalarının Jeolojisi, Türkiye İkinci Petrol Kongresi, Tebliğler, p. 85-107.

Sungurlu, O. and Arpat, E., 1978, Türkiye Doğu Kesiminin Jeolojisi ve Beklenir Kabuk Yapısı, TPAO Exploration Department Archive no. 1204, 8 p (unpublished).

Süzen, M. L. and Türkmenoğlu, A. G., 2000, Lacustrine Mineral Facies and Implications for Estimation of Paleoenvironmental Parameters: Neogene Intervolcanic Pelitçik Basin (Galatean Volcanic Province), Turkey, *Clay Minerals*, v. 35, p. 461-475.

Temple, P. G. and Perry, L. J., 1962, Geology and Oil Occurrence, Southeast Turkey, *AAPG*, no. 46, p. 1596-1612.

Ulu, M and Karahanoğlu, N., 1998, Characterization of the Karababa-C Reservoir in the South Karakuş Oilfield, Southeast Turkey, *Marine and Petroleum Geology*, no. 15, p. 803-820.

Wilson, J. L., 1990, Basement Structural Controls on Mesozoic Carbonate Facies in Northeastern Mexico-A Review, *Carbonate Platforms: Facies, Sequences and Evolution*, Special Publication of the International Association of Sedimentologists, 9, Blackwell Scientific Publications, Great Britain, William Clowes Ltd, p. 235-255.

Whitaker, F. F., Smart, P. L. and Jones G. D., 2004, Dolomitization: from Conceptual to Numerical Models, Geological Society, London, *Special Publications*, v. 235; p. 99-139.

Yılmaz, E. and Duran, O., 1997, Güneydoğu Anadolu Bölgesi Otokton ve Allohton Birimler Stratigrafi Adlama Sözlüğü "Lexicon", Ankara, TPAO Araştırma Merkezi Grubu Başkanlığı Eğitim Yayınları, no. 31, 460 p.